PERFORMANCE ANALYSIS OF HYPERSONIC SPACECRAFT

A Thesis Submitted in Partial Fulfillment of the Requirements for the Degree of

BACHELOR OF TECHNOLOGY
(AEROSPACE ENGINEERING)

By
Khyati Nandchahal
(R290209031)

Prateek Gupta
(R290209044)

Gaurav Maithani
(R290209024)

Under the Guidance of

Dr. Ugur Guven

Professor of Aerospace Engineering (Ph.D.)
[Nuclear Science & Technology Engineer (M.Sc.)]

Mr. Sudhir Joshi

Assistant Professor of Aerospace Engineering

Mr. V K Patidar

Assistant Professor of Aerospace Engineering

College of Engineering
University of Petroleum and Energy Studies,

Dehradun

April, 2013

Abstract

The project entails about the different aspects of hypersonic flow regime. It involves study of various aspects of aerodynamics, performance and structural analysis of 2-D geometry of nose of hypersonic vehicles. The primary focus of the project will be to compare the various results of 2-D profiles such as wedge, flat-plate, curved flat plate, curved flat plate with spikes and cavity etc. The result for various geometries will be compared to see the flow changes around the geometries and to understand the basic aspects of spacecraft nose design. The base model will be a curved flat plate and its result will be compared with modified flat plate with spikes and cavity. The analysis will be done in Gambit and Fluent.

Declaration

This is to certify that work contained in this thesis titled **"Performance Analysis of Hypersnic Spacecraft"** has been carried out by **Khyati Nandchahal, Prateek Gupta, Gaurav Maithani** under my supervision and has not been submitted elsewhere for a degree.

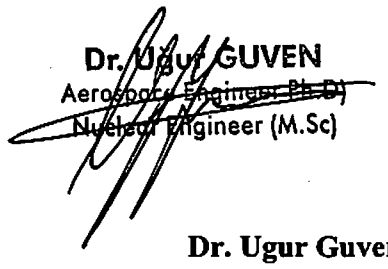

Dr. Ugur Guven

Professor of Aerospace Engineering (Ph.D.)

[Nuclear Science & Technology Engineer, (M.Sc.)]

(April 4, 2013)

Acknowledgement

We would like to express my sincere gratitude to number of people whose contribution to this project has been decisive. We would like to extend my sincere thanks to our mentor who provided us with this golden opportunity to learn the practical aspects of the hypersonic flow and expand our horizon of knowledge. We would like to thank Mr. Sudhir Joshi and Mr. V.K. Patidar for their constant encouragement.

We would also like to express our gratitude to Mr. Rajesh Yadav and Mr. Karthik Sunderraj and Mr. Sourabh Bhatt whose constant support had been instrumental in the completion of our project

Aim and Objectives

Aim

The project involves study and C.F.D. analysis of a previously designed Space tourism vehicle. The vehicle will be undergoing a suborbital flight course and will experience hypersonic speeds throughout its ascent and Re-entry path. The project involves analysis of the shock waves, temperature and pressure profiles on the surface of the vehicle considering efficiency and safety. The softwares being used are GAMBIT 2.2.30 and FLUENT 6.2.16.

Objectives

In order to achieve the aim of this project certain objectives had to be set and completed.

- Learn the CFD analysis software Fluent and Gambit.
- Apply these software on a 2-D flat plate, flat plate with cavity, wedge, flat plate with spikes etc.
- Since the nose of a hypersonic plane resembles a flat plate, such geometry is used. At different altitudes and at different Mach numbers, the flow around the bodies is analyzed for obtaining variation in parameters like entropy, total temperature, static temperature, static pressure, coefficient of lift and drag, wall fluxes, skin friction drag etc.
- Learn the basic aerodynamics, structural and performance aspects of the hypersonic flow regime, the shock equations and other related theories.

Table of Contents **Pages**

List of Figures: **PAGE**

List of Plots: **PAGE**

Literature Review

Mark J Lewis in his article the promise of hypersonic flight has stated about the need of Hypersonic Flight for military as well as for Space Explorations. For this purpose he suggested the development of Hypersonic Spaceplanes. These techniques include air breathing engines which can be a major part of its propulsion technique. He also compared the functioning of a Ramjet engine with a Scramjet one.

In the technical paper propulsion system for hypersonic Spaceplanes the scientists have discussed about the propulsion system for Hypersonic Spaceplanes. Spaceplanes have a simple construction and low weight, so combined rocket, ramjet, pulse-jet engines, or detonation engines instead of turbojets, were taken into consideration as propulsion for hypersonic aircraft by them. Suchiya in his paper optimal design of two stage to orbit Spaceplanes with air breathing engines has suggested to apply an optimization method for conceptual designs of two-stage-to-orbit Spaceplanes with air breathing engines on the first stage boosters and to obtain necessary vehicle sizes and their optimal flight trajectories. It also provides information about the advantage of air breathing engines over rocket engines.

Mc. Clinton in his report on high speed/hypersonic aircraft propulsion technology development tells us that how high speed propulsion system works & what type of aerospace systems will be benefitted with those systems. They have also discussed about the accomplishments of the X-43 scramjet-powered aircraft and in present what needs to be done next to complete this technology development. Segal in his paper propulsion system for hypersonic flight has discussed about the structural aspect of space-planes during high speed flights. This report tells us how the rocket's specific impulse is considerably lower than the other propulsion system but it offers operation capabilities from sea-level static to beyond the atmosphere which no other propulsion system mentioned here can do.

Chapter 1

Introduction to Space Tourism

1.1 Space planes:

The soul motive of a space plane is to go to space and perform tasks or complete missions and thereby safely returning back for being reused as a spaceplane later. There is a need to eliminate the requirement of constructing specialized launch platforms as required in the case of the vertically launched space vehicles and that could be done by using a spaceplane which can be launched from regular airports around the world. In order to do this the spaceplane must be able to take off conventionally.

Within the broad range of aero-thermodynamic conditions, as the need for the hypersonic plane, will be experienced by a scramjet equipped plane being capable of operating with the combined effects of other propulsion modes. As the speed of flight enhances the plane aerodynamic characteristics and the engine performance; the plane forefront becomes the part of engine intake and the plane aft becomes part of the engine nozzle; thereby the engine throttling changes the pressure distribution on the lower part of the fuselage to a significant degree of change.

1.2 Need of space planes:

Since the orbital speeds of the LEO are quite high thus Hypersonic Spaceplane is needed to complete the mission profile. Within the broad range of aero-thermodynamic conditions, as the need for the hypersonic plane, will be experienced by a scramjet equipped plane being capable of operating with the combined effects of other propulsion modes. The current generation of Evolved Expendable Launch Vehicles (EELV) does not meet the needs, but reusable launch vehicles (RLVs) have the potential to greatly surpass the abilities of expendable launch vehicles. RLVs are more responsive since they can be designed for aircraft-like operations from existing airports and air force bases, especially if propelled by air-breathing engines.

1.3 Commercial application of sub orbital space tourism:

Space tourism is space travel for recreational, leisure or business purposes. A number of starts up companies have sprung up in recent years hoping to create a space tourism industry. Space adventure remains the only company to sent paying passengers to space. In conjunction with the Federal Space Agency of Russian Federation and Rocket and Space corporation Energia , space adventure facilitated the flights for all the world's first private explorers . The first three participant s paid in excess of $ 20 million (USD) each for their visit to the ISS.

This could happen in 2015, paving way for the flight of new spaceflight participants . The name of the British singer Sarah Brightman has been mentioned for such an assignment. In the absence of serious distruption to world economic growth, by 2030 the space tourism industry could be carrying some 5-10 million passengers to low earth.

1.4 Sub orbital space flight:

A suborbital space flight is one in which the spacecraft reaches space but its trajectory intersect with atmosphere, so that is doesn't complete an orbital revolution. For example the path of object launched from earth that reaches 100 km from sea level, and then falls back to earth is considered as suborbital flight.

1.5 Mission planning architecture:

Suborbital space flight mission planning with zero g experience and picturesque observation of earth's surface . the mission planning architecture will undergo in the following manner:

- Launch vehicle selection
- Launch vehicle propulsion systems
- Mission profile

1.6 Launch vehicle dynamics:

For launching the vehicle in space for suborbital flight we require rocket equation. Let's consider a rocket vehicle of mass M, ejecting combustion projects at a rate m with a constant exaust velocity of v_e. Due to the thrust F developed by the exaust, the rocket accelerates in the thrust direction.

The thrust developed by the exaust is given by Newtons's third law:

$F=m*v_e$, Where $m = dm/dt$.....(1.1)

The acceleration of the rocket is given by second law of Newton,

$dv/dt=F/M$.....(1.2)

$dv/dt=-V_e*(dm/dt)*1/m$.....(1.3)

$dV=-V_e*dm/m$.....(1.4)

$V=-V_e \log_e *m_o/m$.....(1.5)

1.7 Conceptual high altitude flight:

Regions on the surface of Earth (or in its atmosphere) that are high above mean sea level are referred to as high altitude. High altitude is sometimes defined to begin at 2,400 meters (8,000 ft) above sea level.At high altitude, atmospheric pressure is lower than that at sea level. This is due to two competing physical effects: Gravity, which causes the air to be as close as possible to the ground and the Heat Content of the air, which causes the molecules to bounce off each other and expand.

High-altitude aircraft provides the opportunity to experience various aspects of space for example, passengers in a flight to 60,000 feet and above would see the curvature of the earth below and the dark sky of space above. They would see expansive views of whatever region they were flying over.

1.7.1 Some high-altitude aircraft with their description:

SR-71, this Lockheed creation is the highest-performance aircraft ever built. It holds both altitude and speed records. As an example of its performance, the Blackbird cruises above Mach 3 (three times the speed of sound). It has set numerous speed and altitude records. For a passenger, both the speed and the altitude would provide a considerable and unique thrill. The top speed of an aircraft was in excess of 2,193 miles per hour at an altitude of over 85,000 feet.

1.8 Example of economic failure:

1.8.1 Concorde flight: Since the Concorde is viewed as an economic failure, in the sense that it does not pay its full costs (the French and British governments absorbed the development and manufacturing costs), but only the direct operating costs, that this means that there is no money to be made in a high-altitude tourism venture. This argument flawed on at least two grounds:

The Concorde experience was not exactly what would be provided in a high-altitude joy ride-the windows, for the seats that have them, were rather small, most of the flight was over the ocean, and fifty-thousand feet may not be sufficiently high to offer the full experience. Since the view is the main attraction of the activity proposed here, one cannot draw any conclusions about the demand for such an activity from Concorde flights.

1.9 Orbital flight :

Orbital space flight is a flight in which the spacecraft remains in the trajectory where it remain in space for at least in one orbit. To do this around earth, it must be in an free trajectory which has an altitude in perigee above 100 km. to remain in an orbit it has an orbital speed of 7.8km/s. orbital speed is slower for higher orbits, but attaining them require higher delta –v.

1.10 Orbital launch:

Orbital space flights from earth is only achieved by launch vehicles that use rocket engines for propulsion. To reach the orbit the rocket must impart to a payload of delta-v of about 9.3-10km/s. this is only for horizontal acceleration needed to reach orbital speed, but allows for atmospheric drag , gravity loses and gaining altitude.

The main proven techniques involves for launching vehicles nearly vertically for few kilometres while performing a gravity turn, and then progressively flattening a trajectory out an altitude of 170 km and accelerating on horizontal trajectory for 5-8 minutes burn until orbital velocity is achieved. Most launches are by expendable launch system.

1.11 Stability:

An object in an orbit in an altitude of less than of 200 km is consider as unstable due to atmospheric drag. For a satellite to be in stable orbit 350 km is standard altitude for low earth orbital. However the exact behaviour of objects in orbit depends on altitude, their ballistic coefficient, and details of space weather which can affect the height of upper atmosphere.

1.12 Orbits : There are three main 'bands' of orbit around the Earth: low Earth orbit (LEO), medium Earth orbit (MEO) and geostationary orbit (GEO).

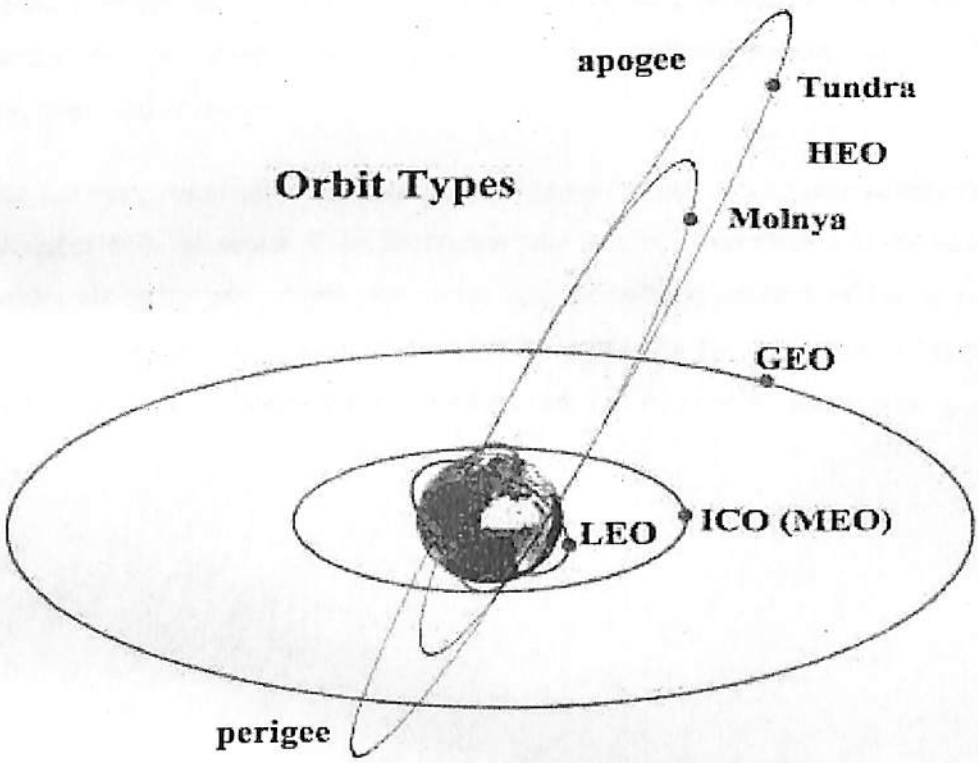

Figure 1.1: Types Of Orbits

1.12.1 Low earth orbit: A low Earth orbit (LEO) is generally defined as an orbit below an altitude of 2,000 kilo meters (1,200 mi). Given the rapid orbital decay of objects below approximately 200 kilo meters (120 mi), the commonly accepted definition for LEO is between 160 kilo meters (99 mi) and 2,000 kilo meters (1,200 mi) above the Earth's surface.

1.12.2 Medium Earth Orbit: Medium Earth orbit (MEO), sometimes called intermediate circular orbit (ICO), is the region of space around the Earth above low Earth orbit (altitude of 2,000 kilometers (1,243 mi)) and below geostationary orbit (altitude of 35,786 kilometers (22,236 mi)).The most common use for satellites in this region is for navigation, communication, and geodetic/space environment science.

1.12.3 Geo Stationary Orbit: A geostationary orbit, or Geostationary Earth Orbit (GEO), is a circular orbit 35,786 kilometers (22,236 mi) above the Earth's equator and following the direction of the Earth's rotation. An object in such an orbit has an orbital period equal to the Earth's rotational period (one sidereal day), and thus appears motionless, at a fixed position in the sky, to ground observers.

Due to Orbital mechanics orbits are in a particular, largely fixed plane around the Earth, which coincides with the center of the Earth, and may be tilted with respect to the equator. The Earth rotates about its axis within this orbit, and the relative motion of the spacecraft and the movement of the Earth's surface determines the position that the spacecraft appears in the sky from the ground, and which parts of the Earth are visible from the spacecraft.

Chapter 2

Hypersonic Flight Fundamentals

2.1 Introduction: Hypersonic flight has special traits, some of which are seen in every hypersonic flight. Presence of these particular features during a flight is highly dependent on type of trajectory, configuration etc. In short it is the mission requirement which decides the nature of hypersonic atmosphere encountered by the flight vehicle. Some missions are designed for high deceleration in outer atmosphere during reentry. Hence, those flight vehicles experience longer flight duration at high angle of attacks due to which blunt nosed configuration are generally preferred for such aircrafts.

2.2 Re-entry Vehicles (RV): These vehicles are typically launched using rocket propulsion system. Reentry of these vehicles is controlled by control surfaces. Large angle of attack flight of blunt nosed configurations is the need of these flights. Space shuttle (US), BURAN (Russian), HOPE (Japan) and HERMES (European) are some examples of these kind vehicles.

2.2.1 Cruise and Acceleration Vehicle (CAV): Slender configurations with low angle of attack flights are main features of these flights. These vehicles are prepared for high heating loads with ablative cooling system. Air breathing propulsion system of ram or scramjet type is generally preferred for these vehicles.

2.2.2 Ascent and Reentry Vehicles (ARV): These vehicles have opposing requirements of their design due to dual duty of Ascent, which is dominated by fuel requirements, and reentry by aero-braking. Rocket or air breathing propulsion systems can be preferred for these flights. NASP or National Aerospace Plane of US, Space Plane by Japan and HOTOL are some examples of these vehicles.

2.2.3 Aero assisted Orbit Transfer Vehicle (AOTV): This is one more class in which hypersonic vehicles are classified. Ionisation and hence presence of plasma in the viscinity of the spacecraft is the major concern of these vehicles. Each of these vehicles faces different flight challenges based on their mission and flight configuration. These challenges inclusively termed as hypersonic flow field.

2.3 Definition of hypersonic flow regime: Definition of flow regime is based on the Mach number of the flow. If Mach number is below unity then the flow is called as subsonic. Sonic flow has Mach number exactly equal to one however flow in the narrow range of Mach number between 0.8-1.2 is called as transonic flow. When the flow Mach number exceeds beyond 1 then flow is called as supersonic flow. As per the thumb rules, when flow speed exceeds five times the sound speed, it is treated as hypersonic flow. However hypersonic flow has certain characteristics which when experienced in the flow should then only be termed as hypersonic. These characteristics of hypersonic flow are mentioned below.

2.3.1 Thin Shock Layers: Region between shock and the body (flight vehicle) is named as shock layer. From the relations between shock angle, Mach number and flow deflection angle or wedge angle, it would be clear that, for same flow deflection angle, shock angle decreases with increase in Mach number. Hence the thickness of the shock layer decreases with increase in Mach number for the same flow deflection angle.

2.3.2 Entropy Layer: One of the main properties of the curved shock waves in that, each streamline passing through the shock faces differential entropy rise where stronger portion of shock leads to higher entropy rise than the weaker portion. Therefore, a layer of entropy variation getting formed downstream of the shock is termed as entropy layer.. As it was evident that the shock layer thickness decreases with increase in Mach number and shock comes closer to the sharp leading edge configurations like wedge or cone, it is also obvious that shock detachment distance decreases with increase in Mach number for blunt bodies. Hence the entropy layer exhibits strong gradient of entropy which leads to higher vortices at higher magnitudes of Mach numbers.

2.3.3 Viscous Interaction: Formation of boundary layer takes place near the wall due to no-slip property of the viscous fluid flow. Formation of this boundary layer takes place across enormous loss of kinetic energy at hypersonic speeds. This kinetic energy necessarily gets converted in to thermal energy which leads to increase in temperature of the flow in the vicinity of the wall. This phenomenon is called as viscous dissipation. Viscous dissipation leads to increase in boundary layer thickness due to increase in viscosity coefficient with temperature.

2.4 High temperature flow: As we know, viscous dissipation leads to higher boundary layer thickness and temperature of the boundary layer fluid. Therefore any hypersonic flight experiences presence of high temperature fluid in the vicinity of the flight vehicle. Apart from this, blunt nosed configurations encounter very high temperatures due to normal shock present at the stagnation point. Therefore at these elevated temperature, treatment of fluid as calorically perfect. The dependence of thermodynamic properties on temperature mainly comes from microscopic changes in the fluid due to increase in internal energy of the fluid by the virtue of loss of kinetic energy.

Increased internal energy leads initially to vibrational excitation followed by dissociation and finally ionization according to the extent of increase in internal energy. Some consequences of presence of high temperature reacting fluid or plasma in the vicinity of the flight vehicle include, influence on aerodynamic parameters, aerodynamic heating and communication block-out. Flight parameters like pitch, roll, drag, lift, defection of control surfaces get largely deviated from their usual estimate of calorically perfect gas. Presence of hot fluid near the cold vehicle surface induces heat transfer not only through convection but also through radiation.

2.5 Low-Density Flow: Hypersonic flights at higher altitudes experience very low density flows. The governing non-dimensional parameter for these regimes is called as Knudsen number which is defined as the ratio of mean free path to the characteristic length of the object. Here mean free path is termed as the mean distance traveled by the fluid molecule between two successive collisions with other molecules. Since density of air is very high on the earth's surface, therefore Knudsen number is close to zero for standard dimensions of hypersonic flights.

However if we consider any standard hypersonic flight taking off from earth surface, it becomes clear that, the flight vehicle is going to encounter change in density with increase in altitude. Validation of continuum assumption and in turn the usage of usual governing equations remains intact till the altitude of around 90 km from earth surface where Knudsen number is below 0.3. Above this altitude, till 150 km from earth surface, density becomes lower as a effect of which fluid velocity and temperature at the surface do not remain in equilibrium with the surface. Therefore flow for Knudsen number in range 0.3 to 1 is treated in the transitional regime where slip wall boundary conditions should be used along with the usual governing equations.

2.6 Hypersonic Flow Governing Equations:

2.6.1 The acceleration field of a fluid: The Cartesian vector form of velocity field that varies in space and time is $V(r,t)= iu(x,y,z,t) + jv(x,y,z,t) + kw(x,y,z,t)$. To write Newton's second law for an infinitesimal fluid system, we need to calculate the acceleration vector field of the flow. Since each scalar component (u,v,w) is a function of four variables (x,y,z,t) ,then we can use the chain rule to obtain each scalar time derivative. The term dv/dt is called the local acceleration. The terms in the parentheses are called the convective acceleration, which arise when the particle moves through regions of spatially varying velocity.

2.6.2 The Differential Equation for mass conservation: The flow through each side of the element is approximately one dimensional hence the approximate mass conservation relation is used here

$$\partial/\partial t dV + \Sigma(\rho_i A_i V_i)_{out} - \Sigma(\rho_i A_i V_i)_{out} - \Sigma(\rho_i A_i V_i)_{in} = 0 \quad .....(2.1)$$

This is the desired equation of conservation of mass for an infinitesimal control volume. This is also called continuity equation. Also, the continuity equation can be written in a comparable form:

$$\partial/\partial x(\rho u) + \partial/\partial y(\rho v) + \partial/\partial z(\rho w) = \Delta.(\rho v) \quad .....(2.2)$$

We can also write in the compact form as:

$$\partial/\partial t(\rho) + \Delta.(\rho v) = 0 \quad .....(2.3)$$

2.6.3 The Differential equation of linear momentum:

The equation of linear momentum is as follows

$$\Sigma F = \partial/\partial t(\int V \rho dv)\, dxdydz + \Sigma(m_i V_i)_{out} - \Sigma(m_i V_i)_{in} \quad .....(2.4)$$

Here v is the volume of the elemental control volume.

As the control volume is considered to be so small the integral is reduced to a derivative

$$\partial/\partial t(\int V\rho dv) = \partial/\partial t(V\rho)\, dxdydz \quad \text{.....(2.5)}$$

$$\Sigma F = \partial/\partial t(\, V\rho)\, dxdydz + \Sigma(m_i V_i)_{out} - \Sigma(m_i V_i)_{in} \quad \text{.....(2.6)}$$

Hence the momentum equation (Eq.) reduces to

$$\Sigma F = \rho dV/dt\, dxdydz \quad \text{.....(2.7)}$$

Equation points out that the summation of all the forces acting on the elemental control volume leads to change in momentum of the element. However, these forces are of two types viz. body forces and surface forces. Examples of body forces are gravity, magnetism etc. The only body force we shall be considering in the gravity for demonstration. The gravity force acting on the differential mass ρdxdydz within the control volume is

$$dF_{grav} = \rho g dxdydz \quad \text{.....(2.8)}$$

Body forces acting on the elements are pressure force and shear stress. The tensor for pressure and viscous stress is,

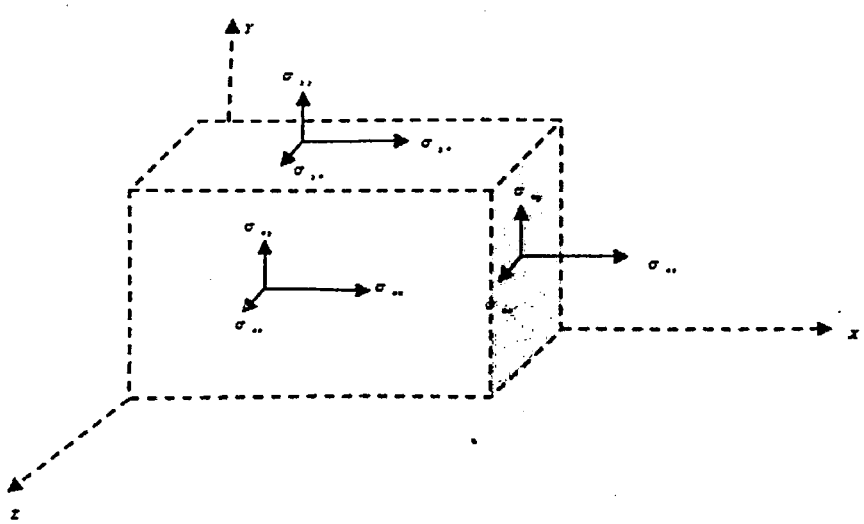

Figure 2.1 Notation For Stresses In Relation With The Control Volume

2.7 Aerodynamic shape configurations: Three concept classes – defined in terms of aerodynamic shape configurations – capsule class, winged-body class or lifting-body class and demo-flight objectives. Regarding the lifting-body class, two sub-classes may be identified: the sphinx derived shape and the slender body shape.

Unique features of hypersonic flight for space access are embedded in the phenomena of rarified gas dynamics, viscous-in-viscid interaction, surface ablation, non-equilibrium thermodynamics and chemical reaction, as well as, radiative heat transfer.

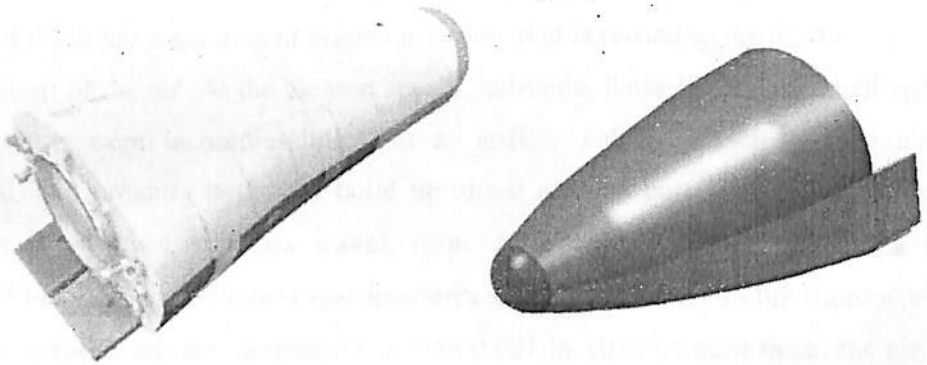

Figure.2.2 Candidates For Aerodynamic Shape

2.8 Hypersonic flight vehicles and shock waves: Hypersonic flight is considered flight at Mach 5 (five times the speed of sound) or greater. The aerodynamic flow and characteristics of a flight vehicle as it accelerates from Mach 4.99 to Mach 5.01 do not markedly change. In contrast, when it accelerates from Mach 0.99 (subsonic) to Mach 1.01 (supersonic), there is a dramatic change in the physics of the flow, including the generation of shock waves at supersonic speeds.

Hypersonic flight may be regarded as that portion of the high-speed flight regime where certain physical phenomena become important that are not so important at lower speeds. At hypersonic speeds, shock waves lie very close to the surface of the vehicle, and there is a major thickening of that portion of the flow immediately adjacent to the surface that is affected by friction (the boundary layer), causing an interaction between the shocks and the boundary layer. Moreover, at

high Mach numbers, the tremendous kinetic energy of the free stream flow ahead of the vehicle is dissipated through the shock waves and in the boundary layers and it is converted into heat which creates high temperatures in the flow around the hypersonic vehicle.

2.9 Shock waves: The characteristics exhibited by air or objects moving at hypersonic speeds are complex. When an aircraft reaches hypersonic speed, the amount of pressure it generates – its dynamic pressure – has increased to 25 times the atmospheric pressure. This permits sustained flight at high altitudes where the atmospheric pressure is extremely low provided the aircraft's speed is high enough. This contrasts with the dynamic pressure of aircraft flying at low speeds, which is small relative to the ambient atmospheric pressure.

High-speed flight has a significant effect on airflow that is related to the elasticity (compression and expansion) of the air. At the slowest speeds, subsonic, these effects are small and the air is treated as if it were incompressible. But as airflow velocities increase, the air becomes compressed, and pressure begins to build up ahead of each part of the aircraft, until finally distinct pressure waves, or shock waves, form. At supersonic speeds, the shock waves are distinct and trail behind any object that interferes with the airstream in the form of a wedge, or cone. While a shock wave is normally less than 0.001 in. (0.0254 mm) thick, the air undergoes large changes in pressure, density, and temperature across this boundary. These effects even extend to the ground in the form of sonic booms.

At speeds approaching the hypersonic range, the shock waves continue to increase in strength and number, and the angle that the shock wave makes with the airflow forms an acute angle. The streamlines that pass through the shock wave are bent as they pass between the shock wave and the surface of the aircraft body. This region of multiple shock waves is called the shock layer, and because it is very small, it can interact with the boundary layer. The body of the aircraft experiences turbulence, and the air around the aircraft becomes a swarming jumble of hot gases whose heat transfers to the aircraft is minimum.

In the hypersonic region, the equations of supersonic flow at this point no longer apply, and many interactions between shock waves and the flow field occur. One major effect is the decrease in lifting effectiveness of the wings and tail surfaces because the shock waves weaken the aerodynamic forces. Even more important, the friction of the air flowing along any surface

raises the air temperature to many times that of the surrounding atmosphere. This shock wave pattern dictates that airplanes travelling at hypersonic speeds have a highly swept, wedge-shaped wing, possibly merged into the fuselage so that the two components form.

2.10 Types of shock waves:

2.10.1 Hypersonic flight vehicles and shock waves: Hypersonic flight is considered flight at Mach 5 (five times the speed of sound) or greater. The aerodynamic flow and characteristics of a flight vehicle as it accelerates from Mach 4.99 to Mach 5.01 do not markedly change. In contrast, when it accelerates from Mach 0.99 (subsonic) to Mach 1.01 (supersonic), there is a dramatic change in the physics of the flow, including the generation of shock waves at supersonic speeds.

Hypersonic flight may be regarded as that portion of the high-speed flight regime where certain physical phenomena become important that are not so important at lower speeds. At hypersonic speeds, shock waves lie very close to the surface of the vehicle, and there is a major thickening of that portion of the flow immediately adjacent to the surface that is affected by friction (the boundary layer), causing an interaction between the shocks and the boundary layer.

Moreover, at high Mach numbers, the tremendous kinetic energy of the free stream flow ahead of the vehicle is dissipated through the shock waves and in the boundary layers, and it is converted into heat which creates high temperatures in the flow around the hypersonic vehicle—temperatures that are frequently high enough to chemically dissociate and ionize the gas in the flow field.

Under these conditions, extreme aerodynamic heating becomes a driving consideration in the design of a hypersonic vehicle. All of this and more comprise the aerodynamic characteristics of hypersonic flight, making it perhaps the most challenging flight regime to conquer. However, the quest to fly faster and higher historically has been a major driving force in the advancement of flight, and hypersonic flight is the next objective in this quest.

2.10.2 Shock waves: The characteristics exhibited by air or objects moving at hypersonic speeds are complex. When an aircraft reaches hypersonic speed, the amount of pressure it generates – its dynamic pressure – has increased to 25 times the atmospheric pressure. This permits sustained flight at high altitudes where the atmospheric pressure is extremely low provided the aircraft's

speed is high enough. This contrasts with the dynamic pressure of aircraft flying at low speeds, which is small relative to the ambient atmospheric pressure. High-speed flight has a significant effect on airflow that is related to the elasticity (compression and expansion) of the air.

At the slowest speeds, subsonic, these effects are small and the air is treated as if it were incompressible. But as airflow velocities increase, the air becomes compressed, and pressure begins to build up ahead of each part of the aircraft, until finally distinct pressure waves, or shock waves, form. At supersonic speeds, the shock waves are distinct and trail behind any object that interferes with the airstream in the form of a wedge, or cone. While a shock wave is normally less than 0.001 in. (0.0254 mm) thick, the air undergoes large changes in pressure, density, and temperature across this boundary. These effects even extend to the ground in the form of sonic booms.

At speeds approaching the hypersonic range, the shock waves continue to increase in strength and number, and the angle that the shock wave makes with the airflow forms an acute angle. The streamlines that pass through the shock wave are bent as they pass between the shock wave and the surface of the aircraft body. This region of multiple shock waves is called the shock layer, and because it is very small, it can interact with the boundary layer. The body of the aircraft experiences turbulence and the air around the aircraft becomes a swarming jumble of hot gases.

These shock waves make testing of hypersonic vehicles difficult, and require the use of special hypersonic wind tunnels. These tunnels need more power to increase air pressure to the necessary point and to heat the temperature of tunnel air in the chamber preceding the nozzles that eject the air into the test area typically to 3,000°F (1,649°C) so that the air in the testing section, chilled to -350°F (-212°C), does not liquefy. Aerodynamicists in the 1950s feared that hypersonic tunnel tests might prove of little value in predicting actual flight conditions. However, the flights with the X-15 research plane in the early 1960s disproved this as predicted wind tunnel data generally agreed with data produced through airplane flight tests.

Test data proved that hypersonic laminar flow conditions did not develop, which led to the recognition that the small surface irregularities that prevented laminar flow at low speeds also prevented its formation at hypersonic speeds. In the hypersonic region, the equations of supersonic flow at this point no longer apply, and many interactions between shock waves and

the flow field occur. One major effect is the decrease in lifting effectiveness of the wings and tail surfaces because the shock waves weaken the aerodynamic forces. Even more important, the friction of the air flowing along any surface raises the air temperature to many times that of the surrounding atmosphere.

This shock wave pattern dictates that airplanes travelling at hypersonic speeds have a highly swept, wedge-shaped wing, possibly merged into the fuselage so that the two components form and between the shock layer and the boundary layer can affect drag and can also cause unusual thermal reactions, contributing significantly to aerodynamic heating, a product of the frictional effect of the high-speed airflow over the vehicle's surface. The flow fields around vehicles travelling at hypersonic speeds actually become so hot that the nitrogen and oxygen molecules in the air dissociate, meaning that the heat destroys the molecular bond between those elements. Individual atoms move in the airflow and various chemical reactions form new compounds, making the behavior of the atmosphere even more complex. When the airflow reaches hypersonic velocities, the science of thermodynamics, by necessity, becomes an additional focus. Aerothermodynamics. Aerodynamicists soon realized that the slender aircraft body suited to supersonic flight was unsuited to hypersonic flight. Rather, they found that a blunt-nose body experienced much less heating than a pointed body, which would burn up before reaching the Earth's surface.

The blunt reentry body, discovered in 1951 by H. Julian Allen, an engineer with the NACA's Ames Research Center, created a stronger shock wave at the nose of the vehicle and dumped a good deal of the reentry heat into the airflow, making less heat available to heat the reentry vehicle itself. This finding was so significant, and so in contrast with intuitive thinking, that it was classified for a while. But by 1958, Allen's work became public, and all successful reentry vehicles since have used the blunt body.

The Space Shuttle is an example of an aircraft that operates at hypersonic speeds, reaching an orbital speed of about 18,000 mph or about 5 miles per second (8 km/s). But since there is practically no atmosphere at the Shuttle's final orbital altitude, ordinary rules of aerodynamics do not apply. It is during reentry that atmospheric hypersonic flight conditions appear. The Shuttle reaches Mach numbers above 10 and surface temperatures of 11,000°F (6,000°C).

The behavior and characteristics of hypersonic airflow are extremely complex and difficult to analyze. While there is some understanding of the pressures and heat input along the wing and the fuselage of an aircraft travelling at hypersonic speeds, the areas where different aircraft structures meet, such as between the wing and fuselage and the tail and fuselage, are areas of "chaotic combinations" of multiple shock waves and interference, especially when an aircraft is travelling at high angles of attack. These areas also experience uneven pressure and heating, resulting in unknown loads and thermal stresses. There is also the challenge of developing power plants to produce the thrust necessary for sustained hypersonic flight; the scramjet (supersonic combustion ramjet) is attempting to meet this challenge.

2.10.3 Types of shock waves:

2.10.4 Normal shock: when the shock wave is normal to the flow, it is called normal shock wave. Shock wave is almost compression process, where the pressure increases almost discontinuously across the wave. In region 1 ahead of the shock, the mach number, flow velocity, pressure, density, temperature, entropy, total pressure and total enthalpy are denoted by $M_1, V_1, p_1, \rho_1, T_1, s_1, p_{0,2}$, and $h_{0,2}$ respectively.

The pressure, temperature ,density and entropy increases across shock whereas total pressure, mach number and velocity decreases, physically the flow across the shock is adiabatic. The total enthalpy is constant across the shock. The flow ahead of shock must be supersonic whereas the flow downstream of the shock is subsonic.

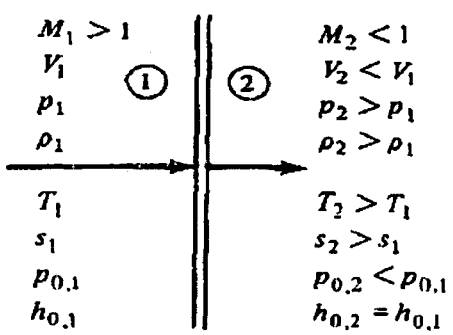

Figure 2.3 Normal Shock Waves

The supersonic flow over a blunt body is shown in figure, here a strong bow shock wave exist in front of the body. Although the wave is curved, the region of the shock closest to the nose is essentially normal to the flow. The stream line that passes through this normal portion of bow shock later impinges on the nose of the body and controls the value of stagnation temperature and pressure at the nose. Since the nose region of high speed blunt bodies is practical interest in calculation of drag and aerodynamic heating, the properties of flow behind the normal portion of shock waves. In the following figure the supersonic flow is established inside the nozzle where the back pressure is high enough to cause normal shock waves to stand inside the nozzle.

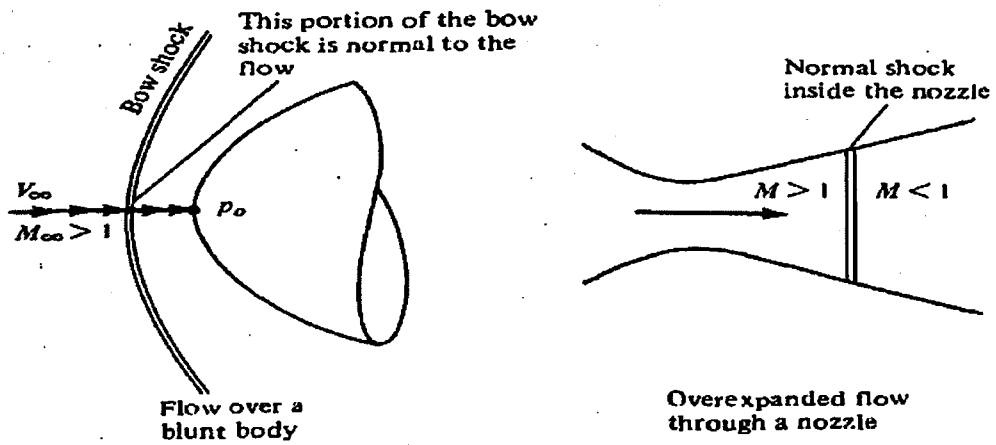

Figure 2.4 Example of Normal Shock

2.10.5 The basic normal shock wave equation: Consider the normal shock wave in figure . region 1 is a uniform flow upstream of the shock and region 2 is different uniform flow downstream of the shock. The pressure, temperature, density, mach number, velocity, total pressure, total enthalpy, total temperature and entropy in region 1 are p_1, ρ_1 , T_1, M_1 ,u_1, $p_{0,1}$, $h_{0,1}$,$T_{0,1}$ and s_1 respectively . the corresponding variable in region 2 is denoted by p_2 ,ρ_2, T_2, M_2 ,u_2 ,$p_{0,2}$,$h_{0.2}$,$T_{0,2}$, and s_2.

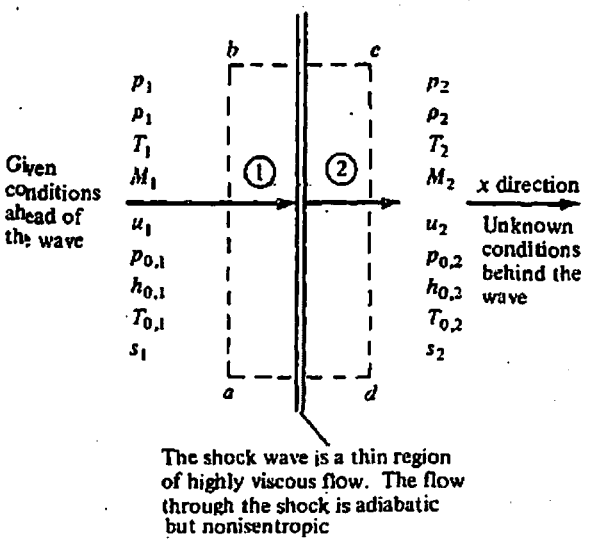

Figure 2.5 Normal Shock Properties

2.10.6 Oblique shocks wave: Oblique shock waves are those shock waves which makes some angle with flow. Ahead of the shock wave there must be a supersonic flow but irrespective to the normal shock here we have supersonic flow downstream of the flow. In oblique shock waves pressure increase discontinuously across the shock waves. Supersonic flow is also characterized by oblique expansion waves, where the pressure decreases across the wave. Let us examine two wave further consider a supersonic flow over a wall with the corner at point A.

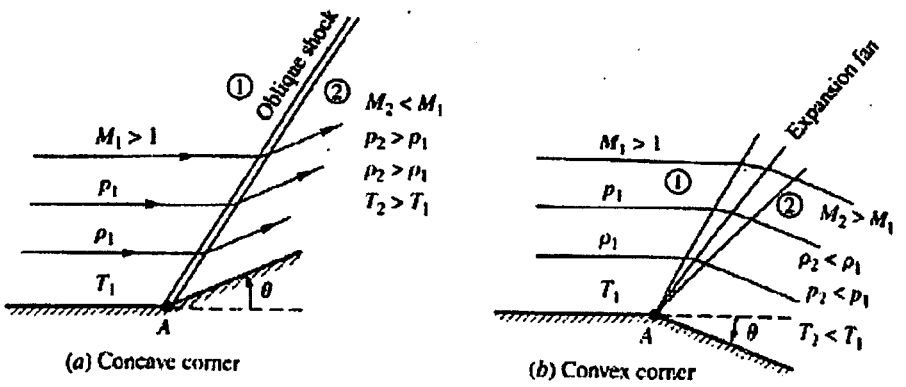

Figure 2.6 Property Changes Around Normal And Oblique Shock

The wall is turned upward at the corner through the deflection angle Θ. That is the corner is concave. The flow at the wall must be tangent to the wall, hence the stream lines are also deflected upward through the angle Θ. The bulk of the gas is above the wall, the stream lines are turned upward into the main bulk of the flow. Whereas the supersonic flow is turned into itself, an oblique shock wave will occur. Across the wave the mach number discontinuously decreases and the pressure, temperature and density discontinuously increases.

In contrast when the wall is turned downwards through the deflection angle Θ. The bulk of the gas is above the wall and the stream lines are turned downwards away from the main bulk of the flow. Whenever there is supersonic flow is turned away from itself an expansion wave will occur. This expansion wave is in the shape of fan centered at the corner.

2.10.7 Shock relations for hypersonic flow: Consider a supersonic flow passing from a compression corner as shown in Figure

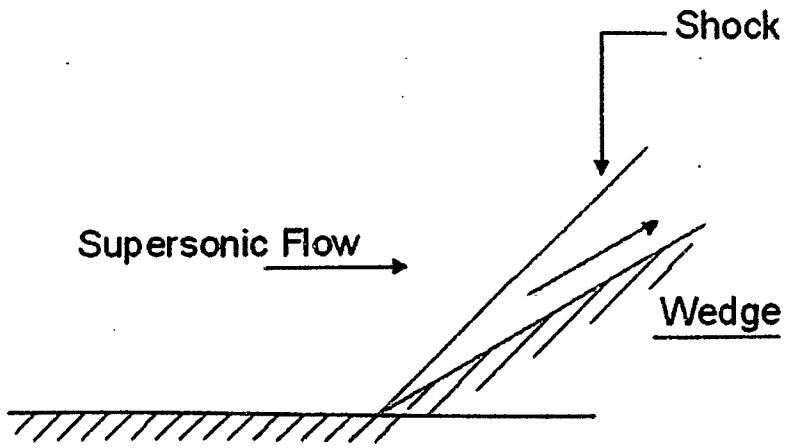

Figure 2.7 Supersonic flow over a compression corner

Since hypersonic flows have very high Mach number we can assume that M 1 >>1. This leads to the modification as, $M^2 \sin^2 ß\text{-}1 \approx M^2 \sin^2 ß$.

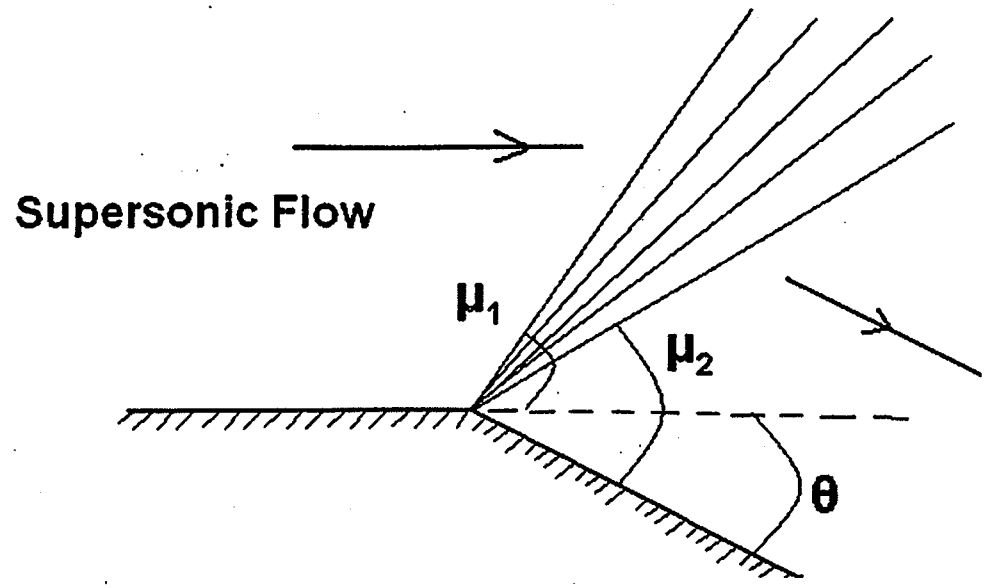

Figure 2.8 Supersonic flow at an expansion corner

2.11 Hypersonic Re-entry: During much of the early re-entry period the space shuttle travels at hypersonic speed which, for the purposes of calculating heat transfer and thermodynamic properties, is distinctly different from supersonic and subsonic speeds. Hypersonic flight differs from supersonic flight in that it has a separate distinct region between the shock wave and the 3boundary layer known as the 4shock layer. In the shock layer kinetic energy is turned into heat so temperature, pressure and or density may change by a factor of 2 or more. This happens when air molecules pass through the shock wave and are excited to higher vibrational and chemical energy modes. As more energy is absorbed by the air molecules the nitrogen and oxygen molecules begin to disassociate creating ionized particles or forming ionized plasma. The major sources of increased heating during supersonic and hypersonic flight are skin and fluid friction as the atmospheric gasses pass over the surface of the aircraft and compression of the gas molecules as they pass through the boundary of the shock wave.

2.11.1Sonic Shock Waves and Boundary Layer Flow:

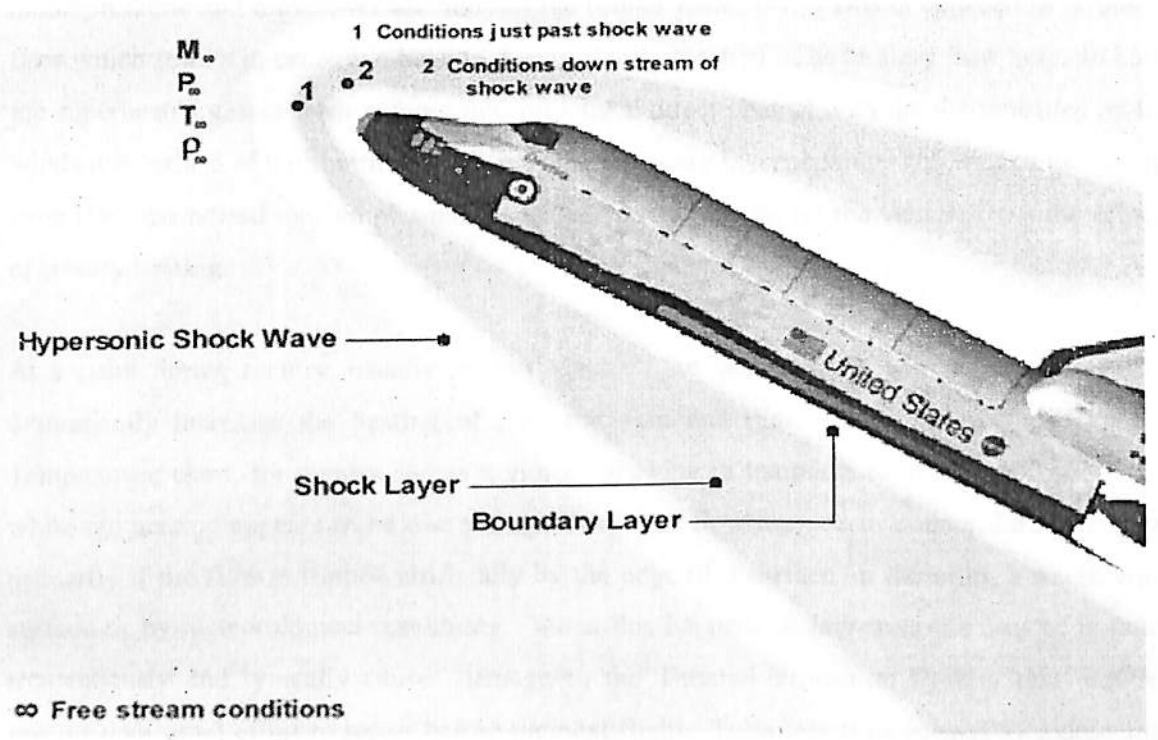

Figure 2.9 Boundary Layer

If it is assumed that the gas is thermally perfect, the following equation can be used :

$P = \rho RT$

$(P_1)/(\rho_1 RT_1) = (P_2)/(\rho_2 RT2)$

P= Pressure, R= Gas constant, T= temperature, ρ=Density

Using the above equation, if some of the free stream conditions are known, many of the properties in the shock layer and boundary layer can be calculated. The temperatures in the shock layer will easily reach 2500 to 3500°F.

2.12 Laminar flow Vs. Turbulent flow: In Laminar flow, the gasses in the boundary layer are incompressible and move over the body of the orbiter with flow. (This is opposed to turbulent flow which results in excessive heating during shuttle reentry). The laminar flow helps to keep the superheated gasses from coming into prolonged direct contact with the thermal tiles on the windward surface of the shuttle. In this way the boundary layer separates the wall of the shuttle from the superheated ionized plasma and actually works to protect the vehicle from the effects of reentry heating.

At a point during reentry, usually around Mach 8, the laminar flow trips to turbulent. This dramatically increases the heating of the orbit skin and tiles. This is why the Time vs. Temperature chart, for reentry shows a violent upswing in temperature at the 1300 sec. mark while the heating appears to be decreasing. Turbulent flow may occur sooner during re-entry primarily if the flow is tripped artificially by the edge of a surface on the orbit, a rough wing surface or by meteorological conditions. When this happens, it increases the heat of re-entry tremendously and typically causes damage to the Thermal Protection System that requires greater than usual effort to repair before the next flight. Turbulent flow caused by a defect on the surface of the orbit will most likely be confined to a small area aft of the surface anomaly that tripped the flow. Excessive turbulent flow has never placed an orbit or crew in danger during re-entry.

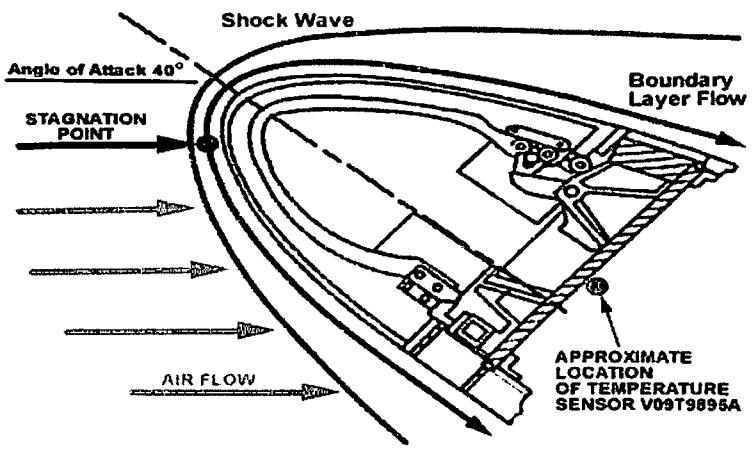

Figure 2.10 Stagnation Heating

2.13 Stagnation heating: The point right at dead center front of the shock wave is called the stagnation point, as shown below. This is where the highest temperatures occur and they are known as stagnation temperatures and or stagnation heating. As long as the orbit is re-entering the atmosphere with the blunt nose forward and the body at the correct Angle of Attack (AOA) the hypersonic shockwave is simply pushed along by the shuttle some distance in front of it. This keeps the hot gasses from coming into direct contact with the shuttles skin and TPS material. If the shuttles attitude changes so that an edge with a shape other than the blunt nose faces forward, such as a wing tip, the shockwave may touch the shuttle subjecting it to stagnation heating and subsequent damage. The areas of the shuttle that have stagnation points are the nose, the leading edges of the wings and the leading edge of the tail.

Angle of attack plays the most significant role in how plasma forms around the shuttle and where heat is concentrated. The shuttle's extreme Angle of Attack of 40° is difficult to maintain but helps to slow the rate of descent more than any other method. Figure below shows how the hypersonic boundary layer affects the shuttle during two different reentry scenarios. One is the standard Angle of Attack while the other shows what would happen without AOA control.

Chapter 3

Hypersonic Flight Structure

3.1 Introduction: Structural design of hypersonic aircraft is severely impacted by the high temperatures and this high temperature lead to high thermal stresses and a significant reduction in material strength and stiffness. This reduction in structural rigidity requires innovative concepts and a stronger focus on aero-elastic deformations in the design and optimization of the aircraft structure. This imposes the need for a closer coupling of the aerodynamic and structural tools. The results indicate that skin buckling is the main driver for the wing structural weight regardless of the number of spars and ribs used. A wing structure with 6 spars and 6 ribs with cross-grid stiffeners leads to the lightest solution, weighing in just under 20 tons Uni-axial stiffened skin concepts are considerably heavier.

3.2 Re-entry from Orbit: The earliest studied and most often encountered hypersonic flows involve the re-entry of a spacecraft from orbit around the earth. NASA's Mercury, Gemini, and Apollo spacecraft experienced hypersonic flows as they safely returned their crews to the earth's surface during the 1960's. The current NASA Space Shuttle, Russian Soyuz, and Chinese Shenzhen must also pass through the hypersonic flow regime.

The mission of a re-entering spacecraft is to slow from 17,500 mph to zero at the surface, the spacecraft is designed to have high drag. During re-entry, the craft is unpowered and strong shock waves generate tremendous heat on the windward side of the vehicle. All of the space "capsules" used ablative heat shields to protect the crew from the heat; the surface of the spacecraft was designed to slowly burn away. The Space Shuttle uses a different mechanism for thermal protection. The bottom of the shuttle is covered with silicon tiles that insulate the aluminium skin from the heat of re-entry.

3.3 Air-breathing Cruiser: There have been several design studies to build air-breathing, hypersonic cruising aircraft. The military has proposed hypersonic cruise missiles, high altitude, high speed reconnaissance vehicles, and piloted global reach vehicles that could deliver cargo or weapons to any location on earth in just a few hours. On the civilian side, the Orient Express was proposed to carry passengers from California to the Pacific Rim in a few hours.

3.4 Air-breathing Accelerator: Besides hypersonic cruise vehicles, there have been several proposed hypersonic accelerator vehicles. The distinction from the cruise vehicle is that the accelerator must continually produce excess thrust, thrust greater than drag, in order to accelerate; the accelerator is never flown in a steady cruise condition.

The accelerator can be used as a single stage to orbit vehicle, like the National Aerospace Plane (NASP) shown on the figure, or as the re-usable first stage of a two stage booster, like the German Sanger configuration. Depending upon the exact mission, the accelerator may employ either TBCC or RBCC engines. The NASP design used an ejector ramjet for low speed operation. Many of the flow problems associated with the cruise vehicle also apply to the accelerator. Although, depending on the exact mission, the accelerator may have to operate over a larger Mach range.

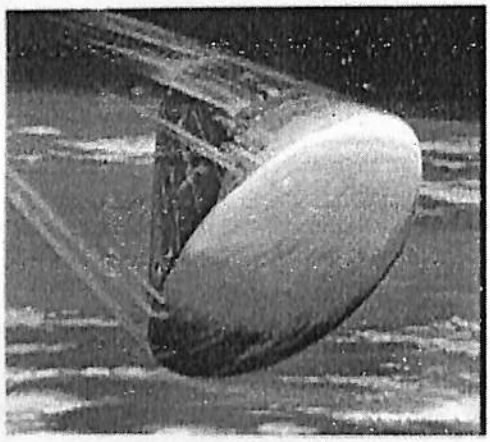

Figure 3.1 Re-entry from Orbit

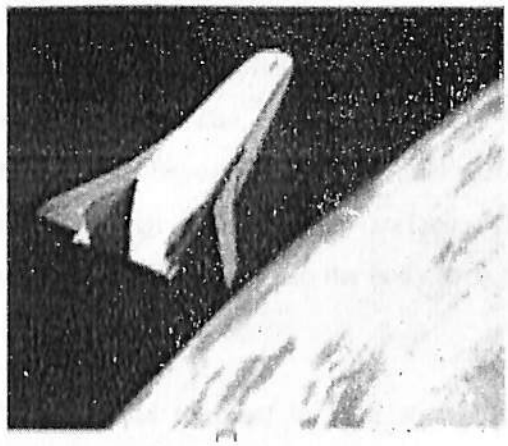

Figure 3.2 Air Breathing Cruiser

3.5 Temperature Variations during Orbit and Re-entry of the Space Shuttle: It is important to determine what the ultimate temperature imparted to these components was. Since the temperature sensors monitoring these components did not register any temperatures high enough to cause damage, it must then be determined what these temperatures were by using heat transfer calculations and engineering methodology. The only mode of heat transfer to and from a spacecraft in orbit is through radiation. Depending the exact mission, the accelerator may employ either TBCC or RBCC engines.

3.6 On Orbit Heating Vs. Cooling: The shuttle orbits the earth upside down and backwards about once every 90 min. with the exact orbit period depending on its altitude. The only mode of heat transfer to and from a spacecraft in orbit is through radiation. When the shuttle is in direct sunlight the black surface on the belly of the shuttle absorbs solar energy while the white surface on the top of the shuttle reflects infrared energy coming from the earth's atmosphere.

When the shuttle is in the earth's shadow all of the shuttles surfaces emit thermal radiation cooling the shuttles tiles and eventually its aluminium skin. It can be assumed that the shuttle typically spends half its time heating and the other half cooling, (45 min. / 45 min.). The shuttle surfaces may not absorb and emit thermal radiation at exactly the same rate so it will have to be determined by calculating the radiation rates for the shuttles surfaces whether or not the shuttle cools completely to absolute 0 K before it begins heating again. This analysis will be done for the black tiles on the orbiteers belly because that is the area of concern.

3.7 Aerodynamic heating: Aerodynamic heating is the heating of a solid body produced by the passage of fluid (such as air) over a body such as a meteor, missile, or airplane. It is a form of forced convection in that the flow field is created by forces beyond those associated with the thermal processes. The heat transfer essentially occurs at the vehicle surface where aerodynamic viscous forces ensures that the flow is at zero speed relative to the body for a very thin layer of molecules at the surface.

When fluid flow slows down its kinetic energy is converted to heat; in high speed flows, tremendous energy is represented by the mean motion of the flow. As the flow is slowed to near zero speed, its temperature increases, the gradient in the speed in a direction normal to the surface allows small scale mass transport effects to dissipate the temperature in the outward direction and thus the temperature at the surface is less than the stagnation temperature; the actual temperature is referred to as the recovery temperature. These viscous dissipative effects to neighbouring sub-layers make the boundary layer slow down via a non-isentropic process. Heat then conducts into the surface material from the higher temperature air. The result is an increase in the temperature of the material and a loss of energy from the flow. The forced convection ensures that other material replenishes the gases that have cooled to continue the process.

The space shuttle orbiter re-enter the earth's atmosphere at an altitude of about 121,920 m (400,000 ft.) and at extremely high velocity (nearly Mach 25 at the time of reentry). In order to protect the shuttle structure from severe reentry aerodynamic heating, the entire shuttle structure is covered with a thermal protection system. The regions of the shuttle surfaces receiving lower heating rates (for example, wing upper surfaces, fuselage side walls, and bay doors) are covered with highly flexible felt reusable surface insulation , and the regions exposed to higher heating rates (for example, wing and fuselage lower surfaces) are covered with TPS tiles.

3.8 Aero-elastic Forces: Aero-elastic is the science which studies the interactions among inertial, elastic and thermodynamic forces. It was defined by Arthur Collar in 1947 as "the study of the mutual interaction that takes place within the triangle of the inertial, elastic, and aerodynamic forces acting on structural members exposed to an airstream, and the influence of this study on design." Aero-elasticity can be divided in two fields of study: steady (static) and dynamic aero-elasticity.

3.9 Steady Aero-elasticity: Steady aero elasticity studies the interaction between aerodynamic and elastic forces on an elastic structure. Mass properties are not significant in the calculations of this type of phenomena.

3.10 Divergence: Divergence occurs when a lifting surface deflects under aerodynamic load so as to increase the applied load, or move the load so that the twisting effect on the structure is increased. The increased load deflects the structure further, which brings the structure to the limit loads (and to failure).

3.11 Control surface reversal: Control surface reversal is the loss (or reversal) of the expected response of a control surface, due to structural deformation of the main lifting surface.

3.12 Dynamic Aero elasticity: Dynamic Aero elasticity studies the interactions among aerodynamic, elastic, and inertial forces. Examples of dynamic aero elastic phenomena are:

3.13 Flutter: Flutter is a self-feeding and potentially destructive vibration where aerodynamic forces on an object couple with a structure's natural mode of vibration to produce rapid periodic motion. Flutter can occur in any object within a strong fluid flow, under the conditions that a positive feedback occurs between the structure's natural vibration and the aerodynamic forces.

That is, that the vibrational movement of the object increases an aerodynamic loads which in turn drives the object to move further. If the energy during the period of aerodynamic excitation is larger than the natural damping of the system, the level of vibration will increase, resulting in self-exciting oscillation. The vibration levels can thus build up and are only limited when the aerodynamic or mechanical damping of the object match the energy input, this often results in large amplitudes and can lead to rapid failure.

At its mildest this can appear as a "buzz" in the aircraft structure, but at its most violent it can develop uncontrollably with great speed and cause serious damage to or the destruction of the aircraft. In some cases, automatic control systems have been demonstrated to help prevent or limit flutter related structural vibration. Flutter can also occur on structures other than aircraft. One famous example of flutter phenomena is the collapse of the original Tacoma Narrows Bridge.

3.14 Dynamic response: Dynamic response or forced response is the response of an object to changes in a fluid flow such as aircraft to gusts and other external atmospheric disturbances. Forced response is a concern in axial compressor and gas turbine design, where one set of airfoils pass through the wakes of the airfoils upstream.

3.15 Buffeting: Buffeting is a high-frequency instability, caused by airflow separation or shock wave oscillations from one object striking another. It is caused by a sudden impulse of load increasing. It is a random forced vibration. Generally it affects the tail unit of the aircraft structure due to air flow downstream of the wing.

3.16 Other fields of study: Other fields of physics may have an influence on aero-elastic phenomena. For example, in aerospace vehicles, stress induced by high temperatures is important. This leads to the study of aero-thermo elasticity. Or, in other situations, the dynamics of the control system may affect aero-elastic phenomena. This is called aeroservoelasticity.

3.17 Prediction and cure: Aero-elasticity involves not just the external aerodynamic loads and the way they change but also the structural, damping and mass characteristics of the aircraft. Prediction involves making a mathematical model of the aircraft as a series of masses connected by springs and dampers which are tuned to represent the dynamic characteristics of the aircraft structure.

3.18 Forces and there variation: The model can be used to predict the flutter margin and, if necessary, test fixes to potential problems. Small carefully-chosen changes to mass distribution and local structural stiffness can be very effective in solving aero-elastic problems.

3.19 Media: These videos detail the Active Aero-elastic Wing two-phase NASA-Air Force flight research program to investigate the potential of aerodynamically twisting flexible wings to improve maneuverability of high-performance aircraft at transonic and supersonic speeds, with traditional control surfaces such as ailerons and leading-edge flaps used to induce the twist.

3.20 Buckling: In science, buckling is a mathematical instability, leading to a failure mode. Theoretically, buckling is caused by a bifurcation in the solution to the equations of static equilibrium. At a certain stage under an increasing load, further load is able to be sustained in one of two states of equilibrium: an un-deformed state or a laterally-deformed state.

In practice, buckling is characterized by a sudden failure of a structural member subjected to high compressive stress, where the actual compressive stress at the point of failure is less than the ultimate compressive stresses that the material is capable of withstanding. For example, during earthquakes, reinforced concrete members may experience lateral deformation of the longitudinal reinforcing bars. This mode of failure is also described as failure due to elastic instability. Mathematical analysis of buckling makes use of an axial load cccentricity that introduces a moment, which does not form part of the primary forces to which the member is subjected. When load is constantly being applied on a member, such as column, it will ultimately become large enough to cause the member to become unstable.

Chapter 4

Aircraft Performance

4.1 Introduction: Performance of the airplane is of two type , one is static performance and other is dynamic performance. Static performance associated with zero acceleration and dynamic performance associated with some acceleration. Under static performance we examines such important aspect as how to calculate maximum velocity of the airplane, how fast it can climb (rate of climb), how high it can fly(maximum altitude), how far it can fly(range), how long it can stay in the air(endurance). Under static performance we examines take-off and landing characteristics, turning flight, and accelerated rate of climb.

4.2 Equation of motion: Consider an aircraft is in air. The flight path(direction of motion of the airplane) is inclined at angle Θ with respect to horizontal.

The four physical forces acting on the airplane :

1. Lift L, which is perpendicular to the flight path direction.
2. Drag D, which is parallel to flight path direction.
3. Weight W, which acts vertically towards the center of earth.
4. Thrust T, which is generally inclined at angle α_T with respect to flight path direction.

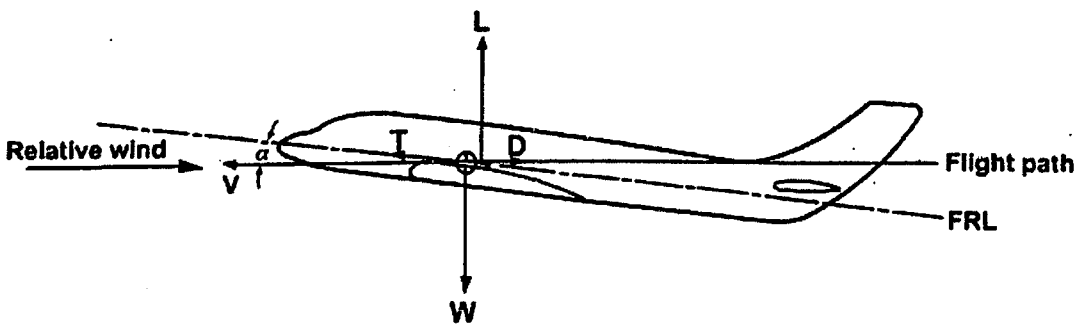

Figure 4.1 Forces on Steady Flight

Since force = mass* acceleration, apply Newton's second law along the flight path gives

$\Sigma F_{\parallel} = m*a = m*dV/dt$ .....(4.1)

Where ΣF is summation of all forces parallel to the flight path.

Now applying Newton's law perpendicular to the flight path,

$\Sigma F_{\perp} = m*V^2/r_c$ .....(4.2)

Where $\Sigma F_{\perp}$ is summation of all forces perpendicular to flight path, the right hand side is nothing but centrifugal force.

Forces parallel to the flight path are-

$\Sigma F_{\parallel} = T\,Cos\alpha_T - D - W\,Sin\Theta$ .....(4.3)

Forces perpendicular to the flight path are-

$\Sigma F_{\perp} = L + T\,sin\alpha_T - W Cos\,\Theta$ .....(4.4)

Combining equation (i) and(iv) –

$T\,Cos\alpha_T - D - W Sin\Theta = m*dV/dt$ .....(4.5)

$L + T\,sin\alpha_T - W Cos\,\Theta = m*V^2/r_c$ .....(4.6)

When $\Theta = 0$, $Sin\alpha_T = 0$, $Cos\alpha_T = 1$,

Then we have,

$T = D$ .....(4.7)

$L = W$.....(4.8)

4.3 Thrust required for level unaccelerated flight: When the Mach number is less than about 0.7, the drag polar is generally independent of Mach number. In this case, C_D / C_L and $C_D / C_L^{3/2}$.

Can be calculated for different values of C_L. The curves shown in Fig. are obtained by plotting C_D / C_L and $C_D / C_L^{3/2}$ as functions of C_L. From these curves it is observed that C_D / C_L is minimum at a certain value of C_L. This C_L is denoted by C_L md as the drag is minimum at this C_L. The power required is minimum when $C_D / C_L^{3/2}$ is minimum. The C_L at which this occurs is denoted by $C_L$mp . Thus in steady level flight:

$T_{min} = W(C_D / C_L)_{min}$

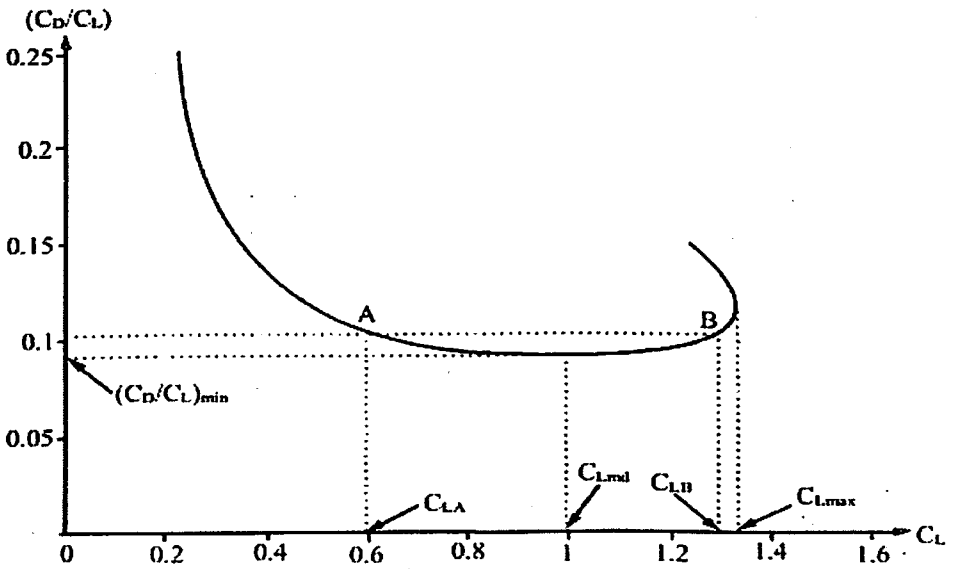

Figure 4.2: C_d/C_l Vs. C_l

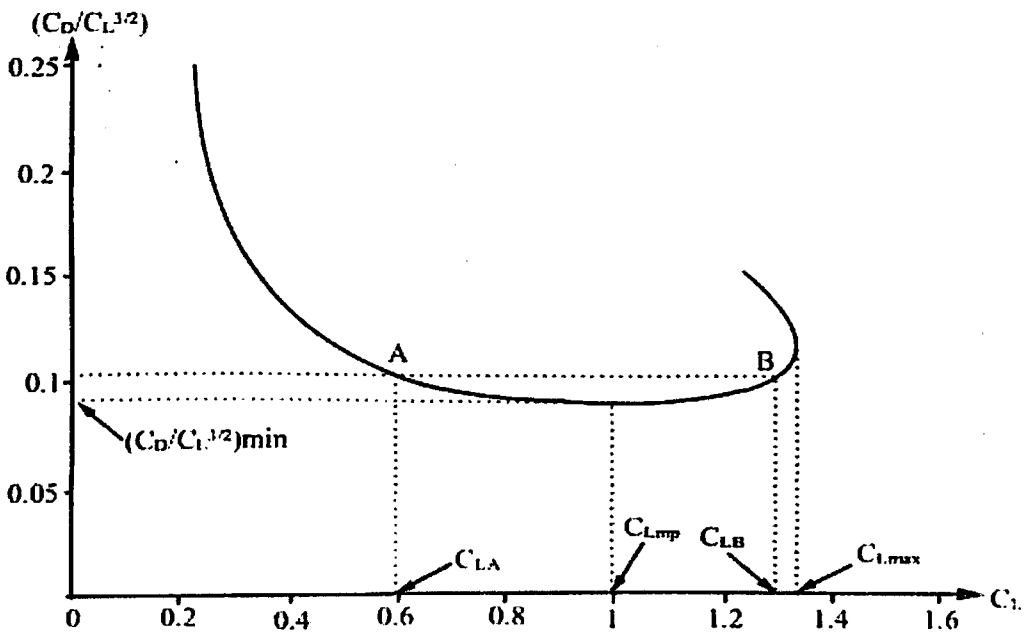

Figure 4.3 $C_d/C_l^{3/2}$ Vs. C_l

4.4 Thrust and power required in steady level flight :

Drag polar equation is given by: $C_D = C_{D0} + KC_L^2$ .....(4.9)

Since an equation is available for the drag polar, it is possible to obtain mathematical expressions for the power required and thrust required. In this section it is assumed that C_{D0} and K are constant with Mach number. Substituting for C_D in expression for thrust required gives:

$Tr = D = (1/2)V^2SC_D = (1/2)\rho V^2S(C_{D0}+KC_L^2)$ .....(4.10)

Substituting for C_L as $W/\{(1/2)PV^2S\}$ in Eq. (b) yields.....(4.11)

$T_r=1/2\rho V^2SC_{DO} + 2KW^2/((\rho V^2S)$ .....(4.12)

In Eq(c). the first term (½) ρ V2 SC_{D0} is called 'Parasite drag'. The second term $2KW^2/(\rho V^2S)$ is called 'Induced drag'. Typical variations of the parasite drag, induced drag and total drag are shown in Fig.(a)

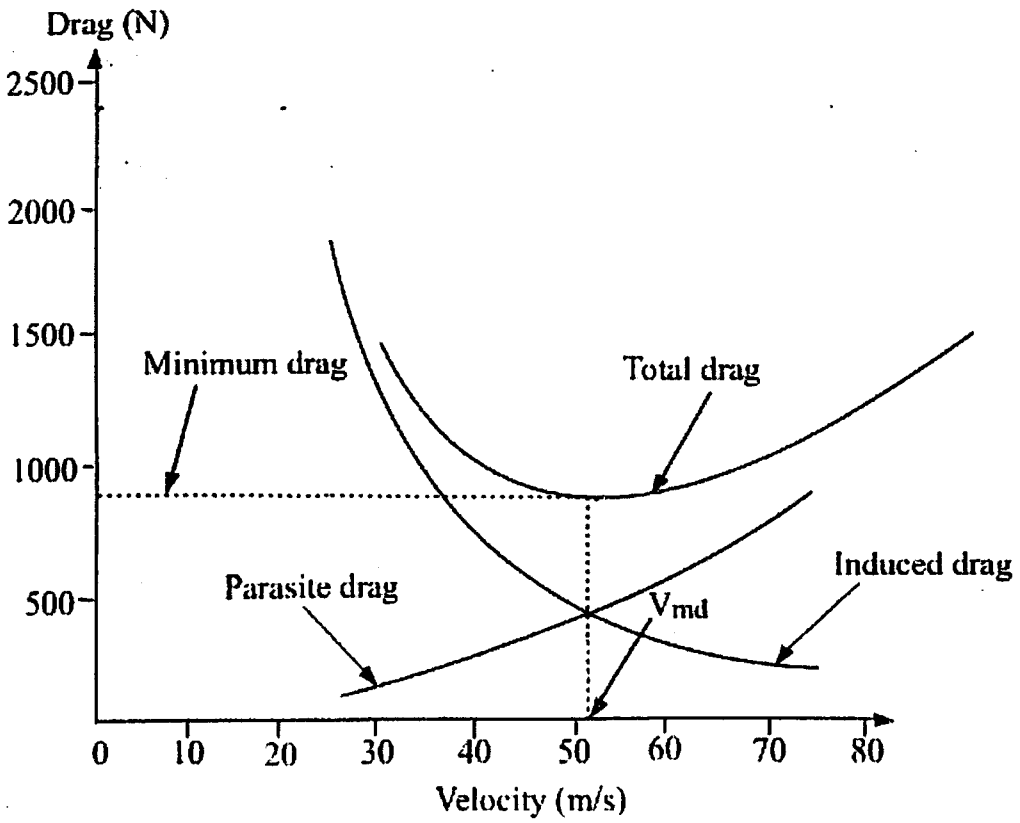

Figure 4.4 Drag Vs. Flight Speed

It is observed that from Fig. that the parasite drag, being proportional to V^2, increases rapidly with speed. The induced drag being proportional to $1/V^2$ is high at low speeds but decreases rapidly as speed increases. The total drag, which is the sum of the induced drag and the parasite drag, is approximately equal to induced drag at low speeds and approaches parasite drag at high speeds. It has a minimum value at a speed (V_{md}) where the parasite drag and induced drag are equal to each other.

Substituting V_{md} in given Eq. (c) gives minimum thrust required i.e.

$T_{rmin} = W (C_{D0} K)1/2+W(C_{D0}K)1/2 = 2W(C_{D0} K)1/2$ .....(4.13)

From given Eq. (e) it is observed that when V equals V_{md}, the parasite drag and

induced drag both are equal to $W (C_{D0}K)1/2$.

Expression for power required in the present case is given by :

Substituting for C_D from given Eq.(a) gives.....(4.14)

$P_r=1/2000(\rho V^3 SC_{DO}) + 1/500(KW^2/\rho VS)$ .....(4.15)

The first term in Eq. is called 'Parasite power'

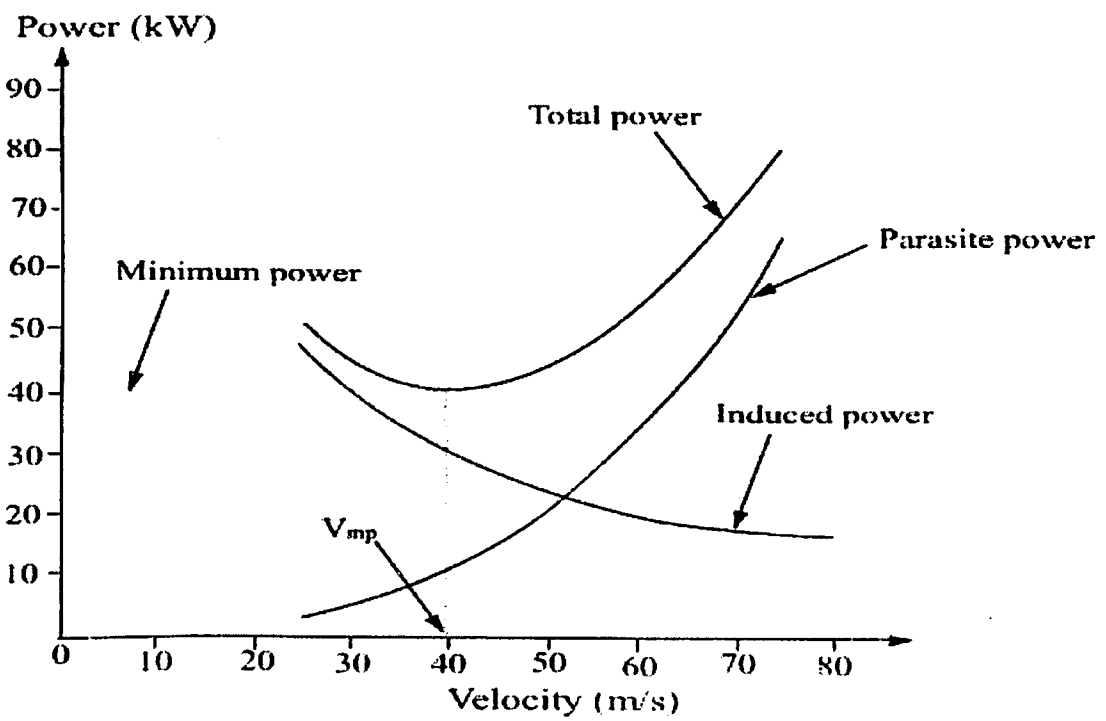

Figure 4.5 Power Vs. Flight Speed

Chapter 5

Real Gas and Aerodynamic Phenomenon

5.1 Introduction: The aerodynamic can also be looked at as a real gas effect and flow phenomenon related to the hypersonic flight. The basic distinction regarding the real gas is the thermally perfect or imperfect gas and calorically imperfect or perfect gas. For a gas to be thermally perfect it must follow-:

$p=\rho RT$ ..... (5.1)

Further for a gas to be calorically perfect it must have constant specific heats c_p and c_v. A gas may be thermally perfect but calorically imperfect but a gas that is thermally imperfect has to be calorically imperfect as well. Such a gas is a real gas.

5.1.1 Vander wall forces: The van der Waals is an important aspect to study the gas effects. Thermally perfect gasses are supposed to have spatial extensions and no intermolecular forces unless there is collision taking place. Again we see for thermally perfect gasses we have

$p=\rho RT$ .....(5.2)

Also, if specific heats c_p and c_v are constant and independent of temperature, the gas is calorically and thermally perfect gas. Van der walls exists if the molecular spacing is comparable to the intermolecular forces. This happens at low temperatures and significantly high densities and pressures. The equation of state then is written as

$p= \rho RTZ(\rho,T)$ ..... (5.3)

Z being the real gas factor, which is a function of "virial coefficient"

$Z(\rho,T)=1+\rho B(T)+ \rho^2C(T)+\rho^3D(T)+.....$ ..... (5.4)

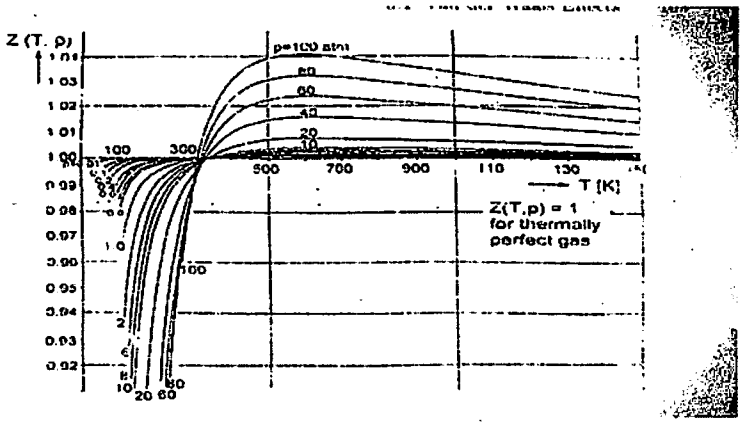

Figure 5.1 Real Gas Factor Z(ρ,T) Of Air

The figure 4.1 shows that especially at temperatures below 300K approximately along with high pressures and densities, van der Waals are effectively applicable. However the real gas effect is close to the value one. This is also applicable at higher temperatures. Also from fig. 5.1 we see that in hypersonic flight the tendencies of pressure/densities and temperature are against the van der walls. In free stream at small temperatures also pressure/density are small whereas in the stagnation areas at large pressure/density also the temperature is large. Thus in general the van der walls can be neglected in flight that is covered by the hypersonic vehicles in the earth's atmosphere .The situation with the ground facilities varies with high reservoir pressures and enthalpies. Here the van der Waals effects can play a role that must be taken into account.

5.2 HIGH-TEMPERATURE REAL-GAS EFFECTS

A gas is considered as calorically imperfect when high temperature real gas effects play in. There are four parts of internal energy

$$e = e_{trans} + e_{rot} + e_{vibr} + e_{el} \quad \ldots\ldots (5.5)$$

where e_{trans} = translational energy, e_{rot} = rotational energy, e_{vibr}= vibrational energy

e_{el}= electronic excitation energy (can be neglected)

The high temperature real gas effects of interest thus are vibrational excitation and dissociation/recombination. Dissociated gases can be considered as mixtures of thermally perfect gasses, whose molecular species are calorically imperfect.

The internal energy and its parts can be illustrated by their degrees of freedom

- Three translational degrees of freedom
- Two rotational degrees of freedom
- Two vibrational degrees of freedom

The internal energies of a mixture of thermally perfect gases in equilibrium is given by-

$E = \sum ni_{=1} \omega_i e_i$ ..... (5.6)

Thus,

$e = e_{trans(i)} + e_{rot(i)} + e_{vibr(i)} + e_{el(i)}$ .....(5.7)

$e_{trans(i)}$ and $e_{rot(i)}$ apply to both molecules and atoms $e_{vibr(i)}$ and $e_{el(i)}$ apply to both molecules only The enthalpy of a gas is defined as-:

$h = e + p/\rho$ .....(5.8)

For thermally perfect gas with constant c_v and c_p and gas constant $R=C_p-C_v$, we have

$dh = C_p dT = (C_v + R)dT$ .....(5.9)

Likewise it holds for the internal energy,

$de = C_v dT$ .....(5.10)

The principle of equi-partition of the energy permits us to formulate the internal energy e, the specific heats C_v, C_p, and their ratio $\Upsilon = C_v/C_p$ of atoms and molecules in terms of the degrees of freedom f, which gives us insight into some basic high-temperature phenomena. Consider excitation of all degrees of freedom. (Neglecting the electronic excitation).

For species with molecular weight M and R_O being universal gas constant

$e=(fR_O/2M)T$; $c_v = fR_O/2M$; $c_p = (f+2)R_O/2M$; $\Upsilon = f+2/f$ ..... (5.11)

Note-: For Atoms (N, O) we take f=3

For Molecules (N_2, O_2, NO) we take f=5,

For Molecules with full vibrational excitation, f=7,

For Molecules with half vibrational excitation f=6.

For Molecules with infinitely large number of degrees of freedom, f=∞

5.3 Dissociation and recombination

Collisions cause the excitation of internal degree of freedom of molecules. If the molecule receives too much energy then it will dissociate. When the atoms recombine, they form the molecule again. Dissociation and recombination are chemical reactions, which alter the composition of the gas, and which bind or release heat. The five species N, O, NO, N_2, O_2 are basically products of three reactions.

5.4 Thermal and chemical rate reaction:

The excitation by collision is of vital importance to be considered to understand the thermal and chemical rate processes. The number of collision per unit time depends on the density and the temperature of the gas. The number of collision at which molecules react is much less than the number of collision they undergo, because only a fraction of the collision involves sufficient energy, and a fraction of molecules collisions with sufficient energies lead actually to some reaction.

Since excitation is a process in time, we have another factor to be considered i.e. T (characteristic excitation or reaction time), which is needed to have the necessary collisions to excite degrees of freedom or to induce reactions. Comparing this time with a characteristic flow time leads to the consideration of the thermal and chemical rate processes.

Chapter 6

Numerical Analysis and Results

6.1 2D Cylinder (Without Cavity)

6.1.1.1 Problem Setup (Angle Of Attack=20 Degree): CFD Analysis of Hypersonic flow over a 2D Cylinder with dimensions 7m in length and 3m in diameter. Free Stream Mach no is 5. Ambient Temperature is 270.68 K.

Step 1: The 2D curved plate of 7m in length and 3m in diameter was created in Ansys ICEM. Farfield was assumed to start 25.5m ahead of the plate and 85m behind the plate. It extended up to a height of 85m above and below the plate as shown in the figure given below.

Step 2: The meshed geometry looked like as shown in the following figure

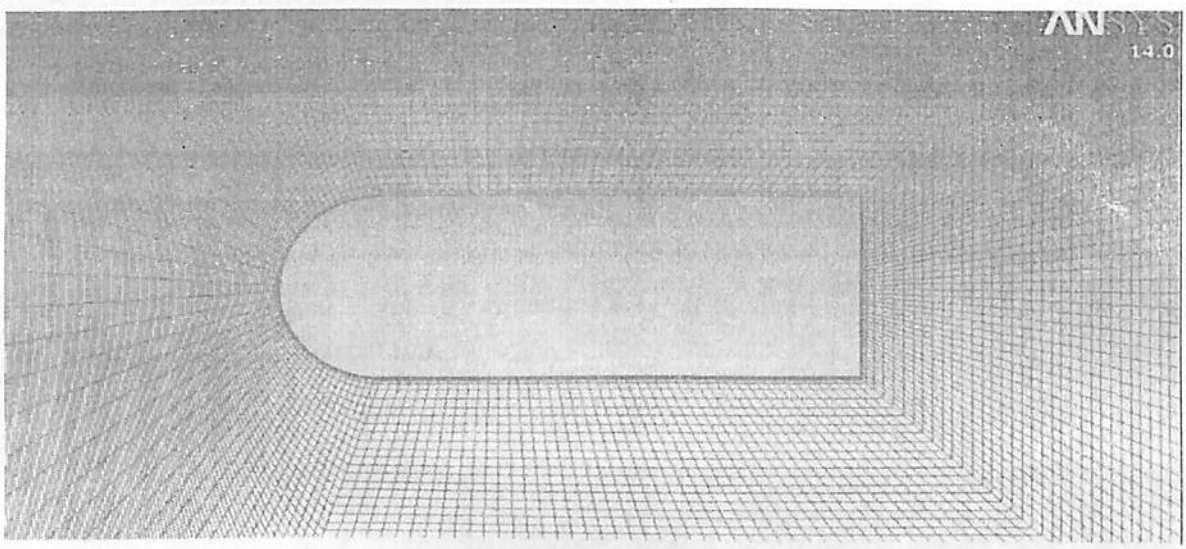

Figure 6.1: Meshed Geometry

Step3: Wall Y+ Estimation:

- Under the conditions specified the Reynolds's number was calculated and the flow turned out to be turbulent.
- Wall Y+ was estimated using an wall Y+ calculator online.
- It was specified as 2.1e-4 and the growth factor (b/a) of 1.2 was taken, with 20 rows.

Step 4: Problem Setup in Ansys Fluent 14:

- In the solver menu Coupled solver was selected and 2D was selected in Space.
- The Viscous model was taken as Spalarat Allmaras (1 eqn).
- Under the materials option the density of air was taken as ideal gas.
- Under the materials option the Cp was taken as piecewise polynomial.
- Viscosity was taken as Sutherland relation.
- The operating pressure was defined 0.
- Farfield values were set as Mach no=5 and gauge pressure was taken as 79.799 pa.
- Temperature was set as 270.69 K.
- Angle of attack was defined as 20 degree in the boundary conditions.
- Monitors of Cd and Cl were also set to compare the various values.
- The solution was initialized and residuals were set to 1e-6.

6.1.1.2 Result Analysis and Plots:

- 10000 initial iterations were given and the solution didn't stabilize early and kept on fluctuating so additional iterations were given.
- The continuity and Energy equations stabilized at 1e-2 but didn't converge below 1e-2.
- The X velocity and Y velocity equations kept on oscillating between 1e-2 and 1e-3 but didn't converged below 1e-6.

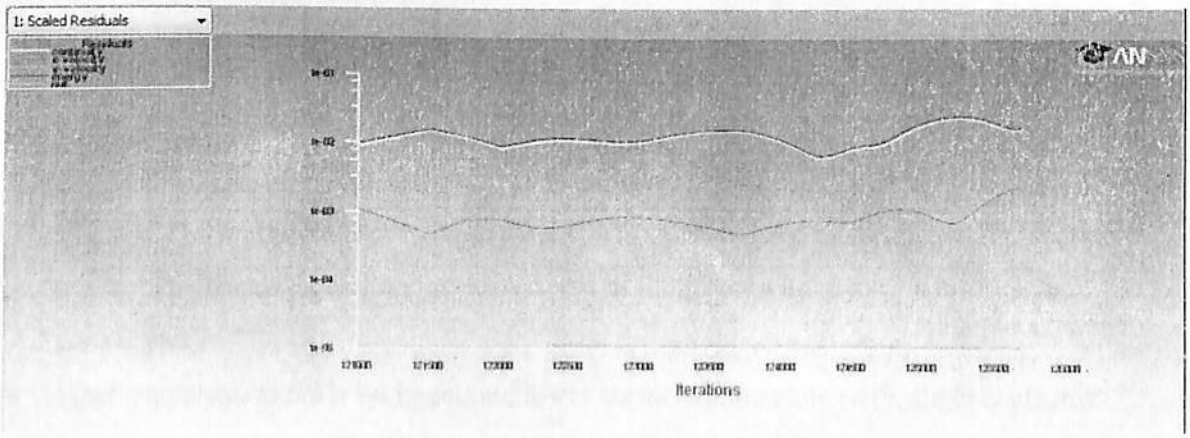

Figure 6.2: Iterations (AOA 20 Degree)

- The mach no decreases substantially behind the Normal shock (<1 just in front of the stagnation point).
- Mach no decreases fairly behind the oblique Shock (>1 in front of curved part).
- There was an expansion wave formation at the end of the plate and sudden decrease in mach no at the end of plate.

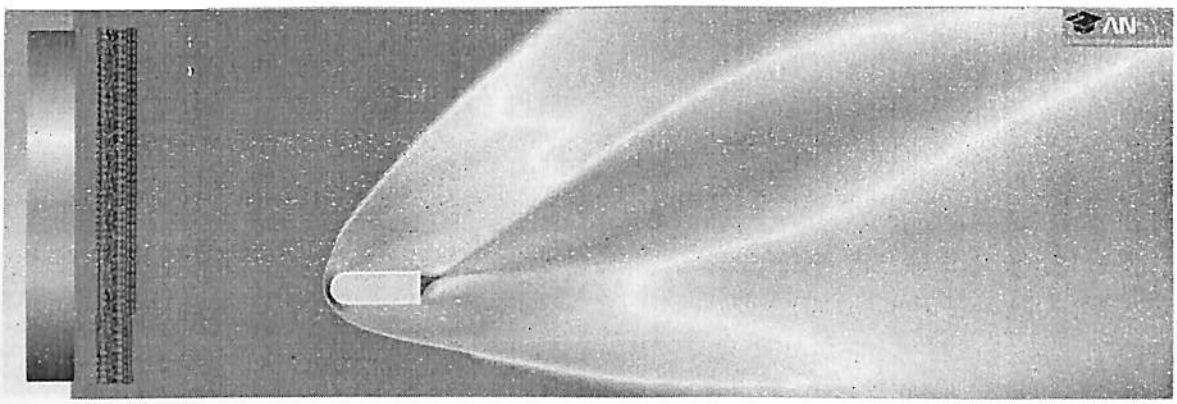

Figure 6.3: Mach No Contour (AOA 20 Degree)

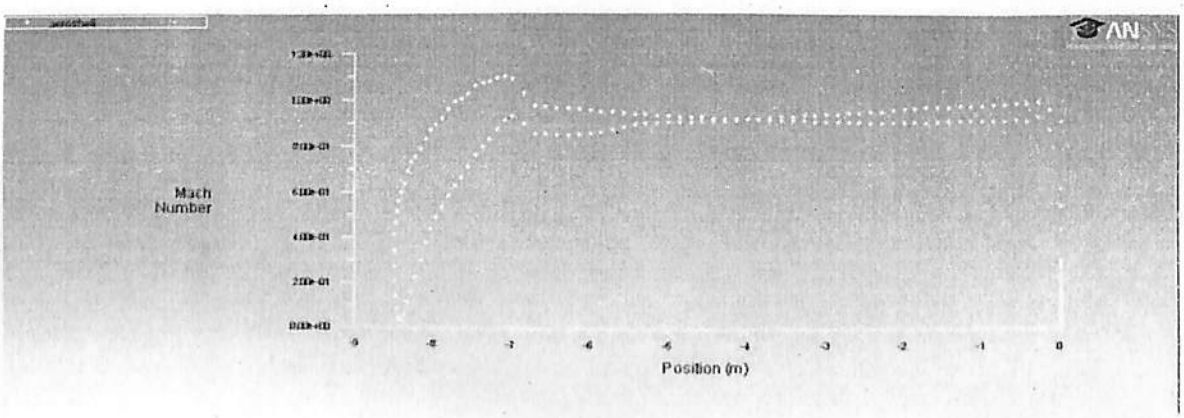

Figure 6.4: Mach No Plot (AOA 20 Degree)

- The mach no on the front part of the plate is 0 because of it being the stagnation point.
- Mach no increases rapidly on the curved part of the plate (with greater rate at upper curved part).
- Mach no increases fairly on upper and lower surface of the plate (with slightly greater rate at upper portion of the plate).

- Static pressure rises substantially behind the Normal shock portion (in front of the stagnation point).
- Static pressure rises fairly behind the oblique shock portion (in front of the curved part).
- Static pressure rises slightly as we move progressively on the lower part of the plate and is roughly constant on the upper edge.

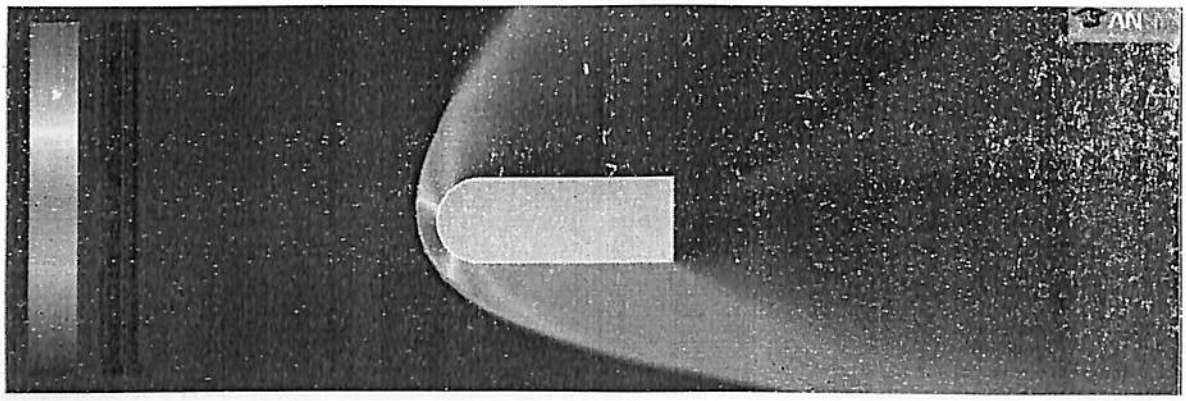

Figure 6.5: Static Pressure Contour (AOA 20 Degree)

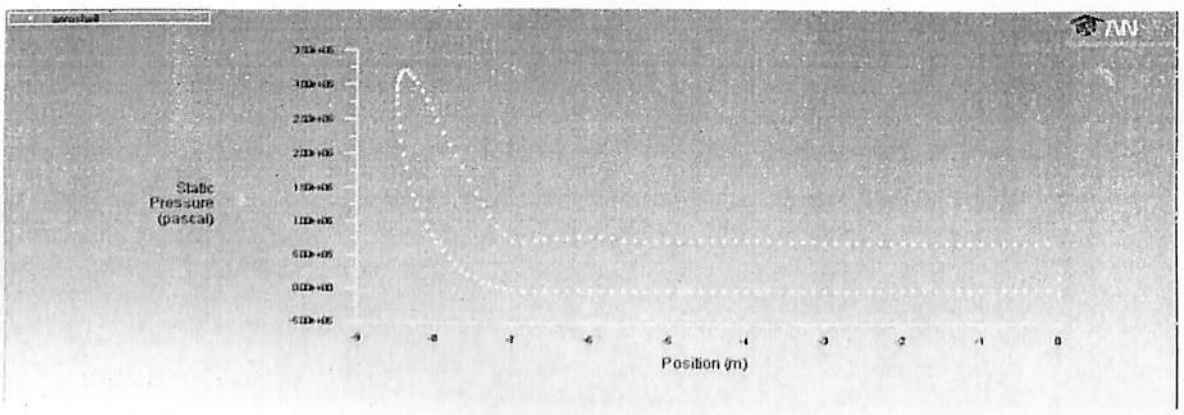

Figure 6.6: Static Pressure Plot (AOA 20 Degree)

- The Static pressure on the front part of the plate is maximum because of it being the stagnation point (zero velocity).
- Static pressure decreases rapidly on the curved part of the plate (with greater rate at upper curved part).
- Static pressure decreases fairly on upper and lower surface of the plate (with greater value at lower portion of the plate).

- Temperature rises substantially behind the Normal shock portion (in front of the stagnation point).
- Temperature re rises fairly behind the oblique shock portion (in front of the curved part).
- Temperature rises slightly as we move progressively on the lower part of the plate and is roughly constant on the upper edge.

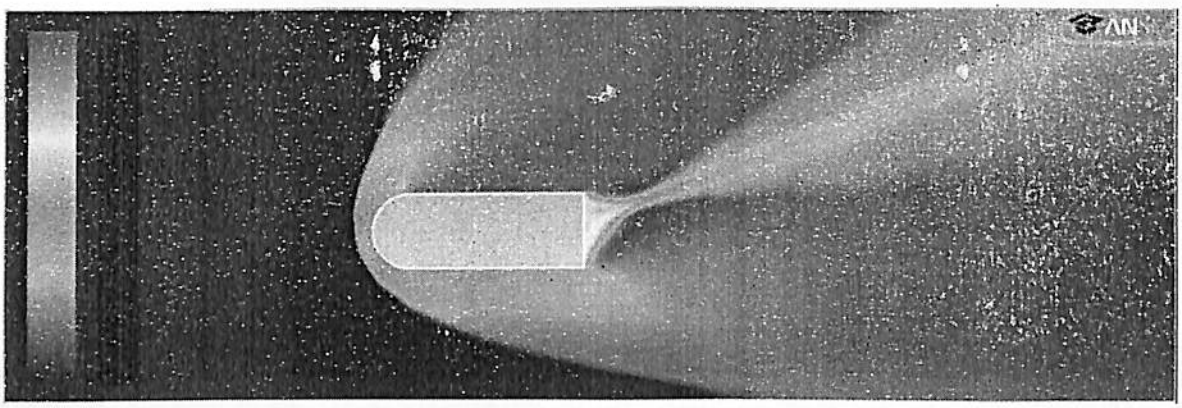

Figure 6.7: Static Temperature Contour (AOA 20 Degree)

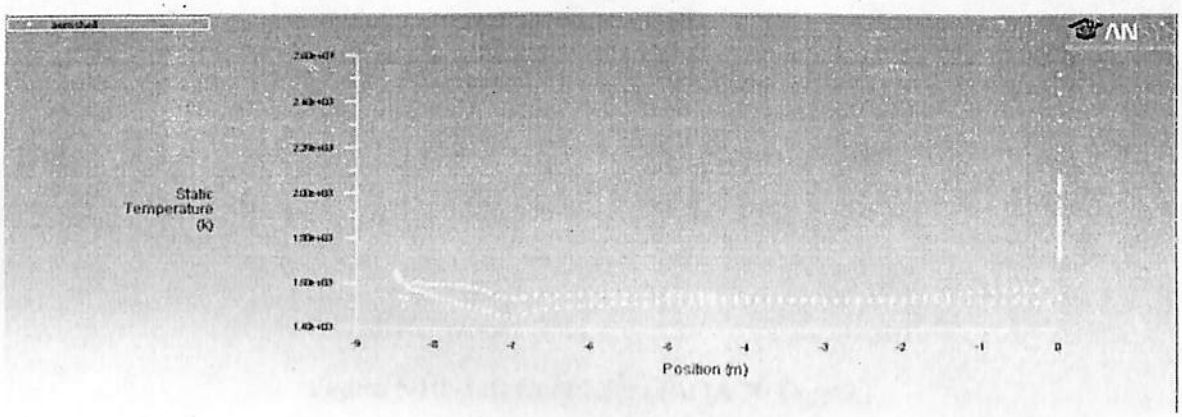

Figure 6.8: Static Temperature Plot (AOA 20 Degree)

- Static temperature on the front part of the plate is maximum because of it being the stagnation point (zero velocity).
- Static temperature decreases fairly on the curved part of the plate (with greater rate at upper curved part).
- Static temperature decreases fairly on upper and lower surface of the plate
- Static temperature is maximum at the end of the plate

- Drag coefficient was observed and plotted and found to be around 3:7.

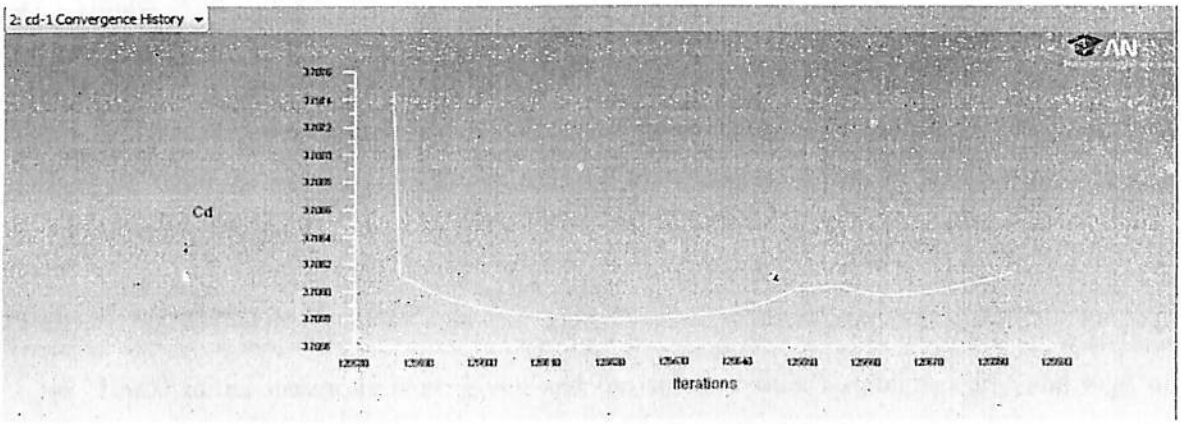

Figure 6.9: Drag Coefficient (AOA 20 Degree)

- Lift coefficient was observed and plotted and found to be around 3.9.

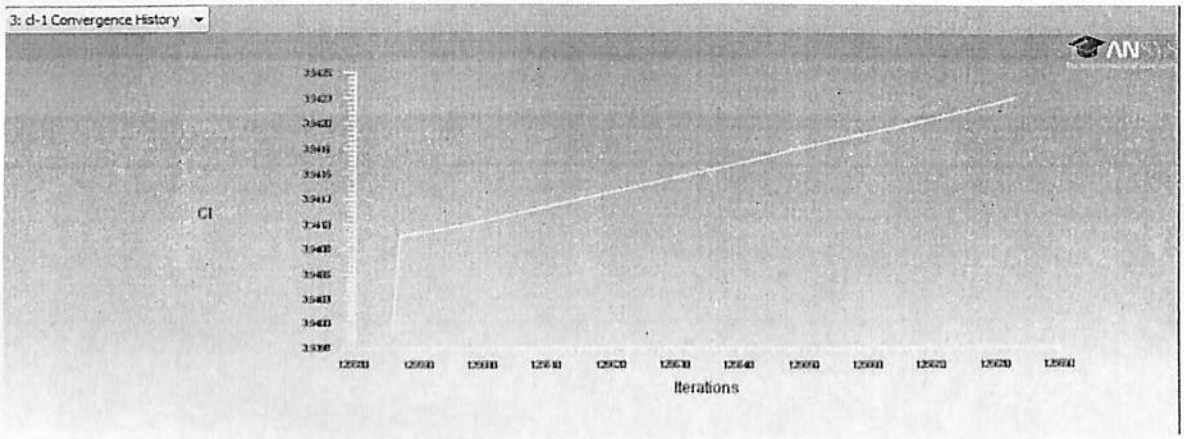

Figure 6.10: Lift Coefficient (AOA 30 Degree)

6.1.2 Problem Setup (Angle Of Attack=30 Degree): CFD Analysis of Hypersonic flow over a 2D Cylinder with dimensions 7m in length and 3m in diameter. Free Stream Mach no is 5. Ambient Temperature is 270.68 K.

Step 1, 2, 3 and step 4 remain the same as the meshed geometry and ambient conditions remains unchanged. Only the angle of attack was changed to 30 degree in step 4. The problem setup in the fluent was unchanged.

6.1.2.1 Result Analysis and Plots:

- 10000 initial iterations were given and the solution didn't stabilize early and kept on fluctuating so additional iterations were given and after about 174000 iterations the results were plotted.
- The continuity and Energy equations stabilized at 1e-2 but didn't converge below 1e-2.
- The X velocity and Y velocity equations kept on oscillating between 1e-2 and 1e-3 but didn't converged below 1e-6.

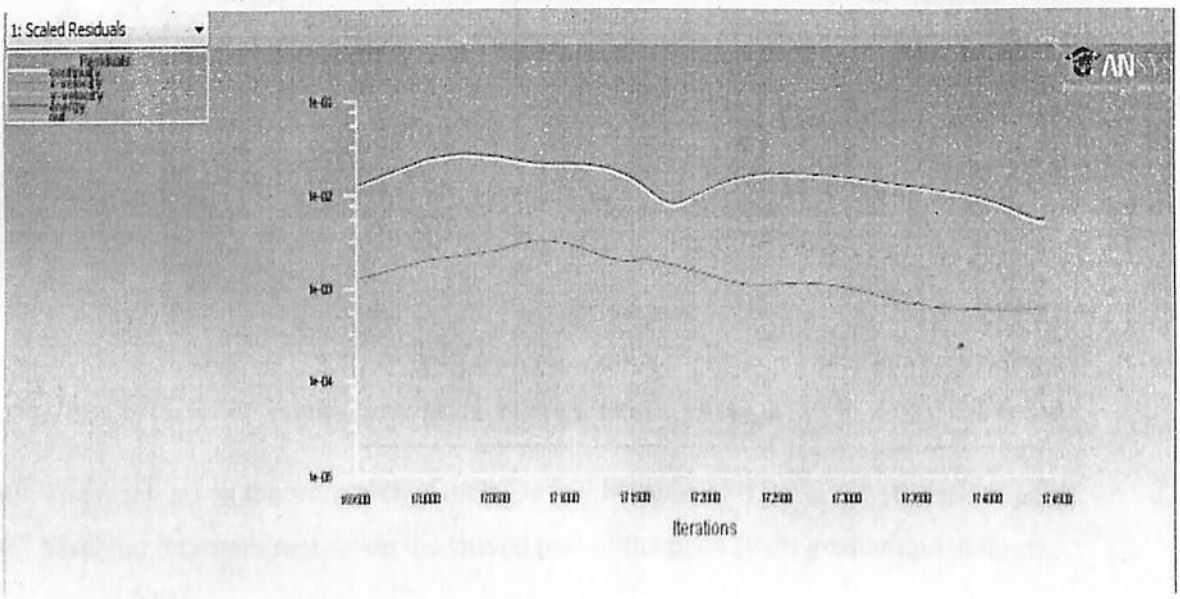

Figure 6.11: Iterations (AOA 30 Degree)

- Mach no decreases substantially behind the Normal shock (<1) just in front of the stagnation point, which is slightly lower than the previous case.
- Mach no decreases fairly behind the oblique Shock (>1 in front of curved part).
- There was a Expansion wave formation at the end of the plate and sudden decrease in mach no at the end of plate.

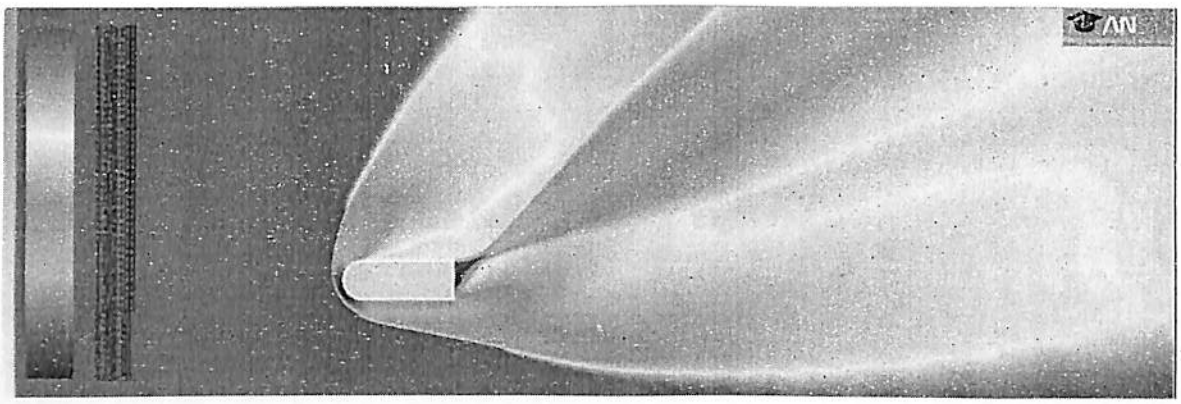

Figure 6.12: Mach No Contour (AOA 30 Degree)

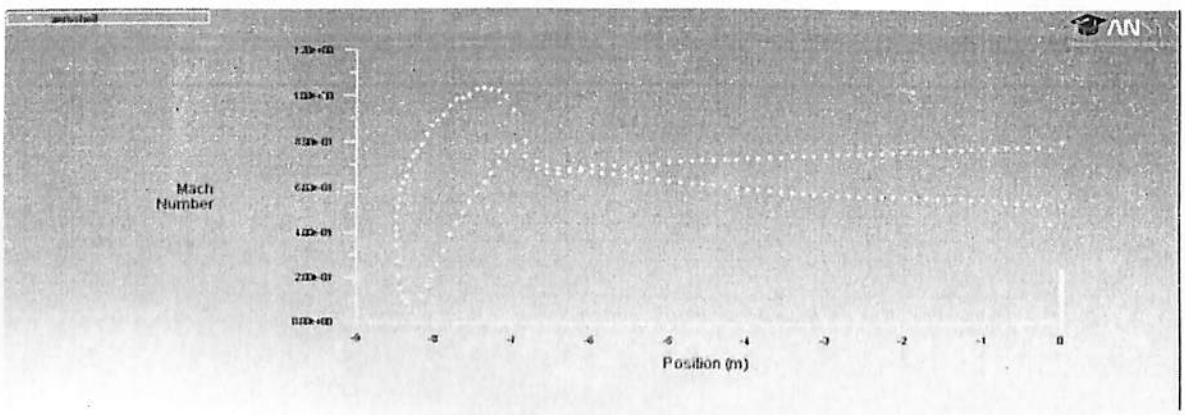

Figure 6.13: Mach No Plot (AOA 30 Degree)

- The mach no on the front part of the plate is 0 because of it being the stagnation point.
- Mach no increases rapidly on the curved part of the plate (with greater rate at upper curved part).
- Mach no increases rapidly on upper surface of the plate and fairly on the lower surface of the plate.

- Static pressure rises substantially behind the Normal shock portion (in front of the stagnation point).
- Static pressure rises fairly behind the oblique shock portion (in front of the curved part).
- Static pressure rises slightly as we move progressively on the lower part of the plate and is roughly constant on the upper edge.

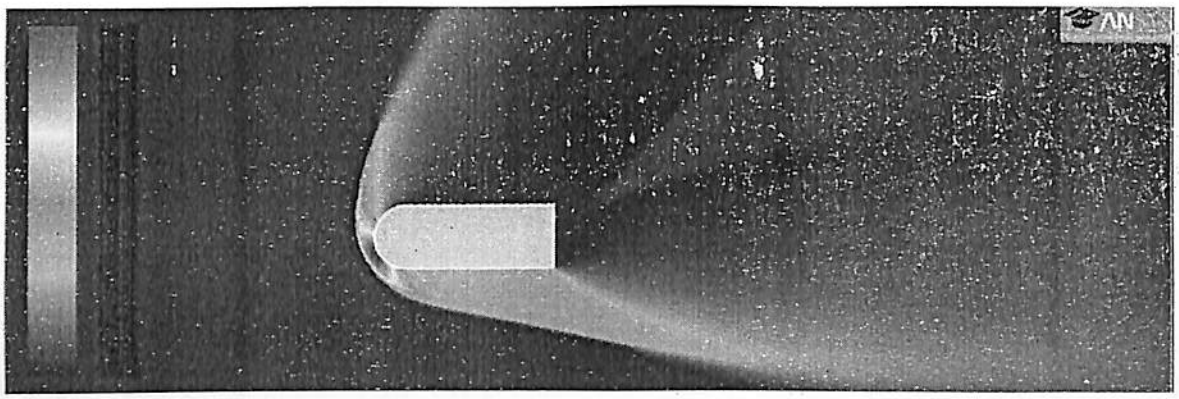

Figure 6.14: Static Pressure Contour (AOA 30 Degree)

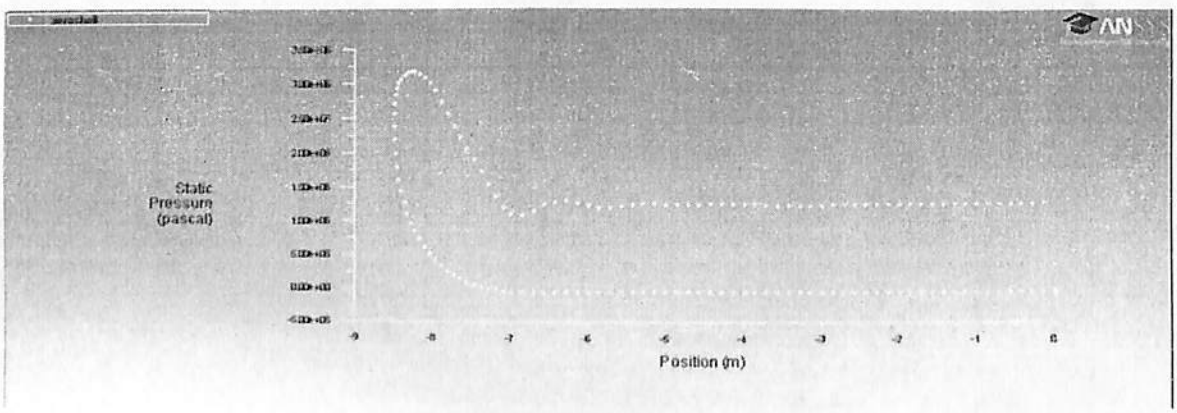

Figure 6.15: Static Pressure Plot (AOA 30 Degree)

- The Static pressure on the front part of the plate is maximum because of it being the stagnation point (zero velocity).
- Static pressure decreases rapidly on the curved part of the plate (with slower rate at lower curved part because of high angle of attack).
- Static pressure is constant on lower and upper surface of the plate (with greater value at lower portion of the plate).

- Temperature rises substantially behind the Normal shock portion (in front of the stagnation point).
- Temperature re rises fairly behind the oblique shock portion (in front of the curved part).
- Temperature remains constant as we move progressively towards the end of the plate and is less on the upper edge.

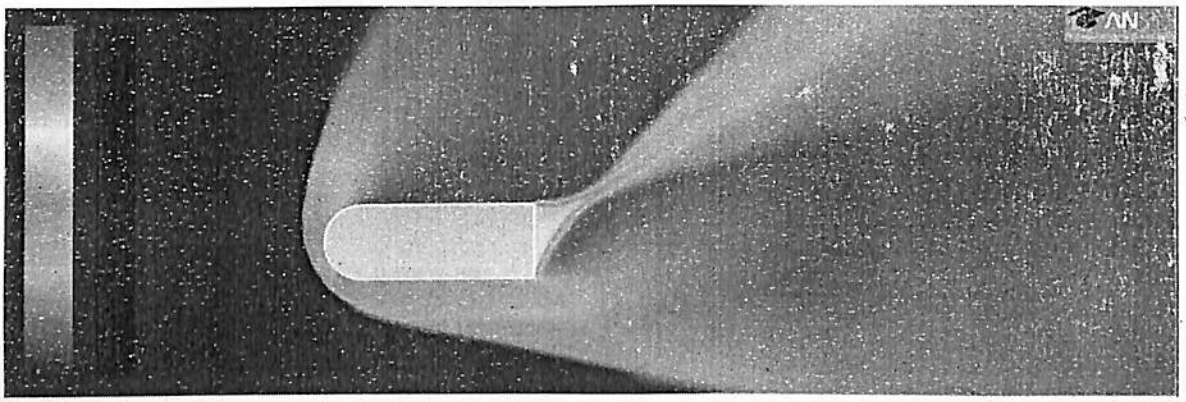

Figure 6.16: Static Temperature Contour (AOA 30 Degree)

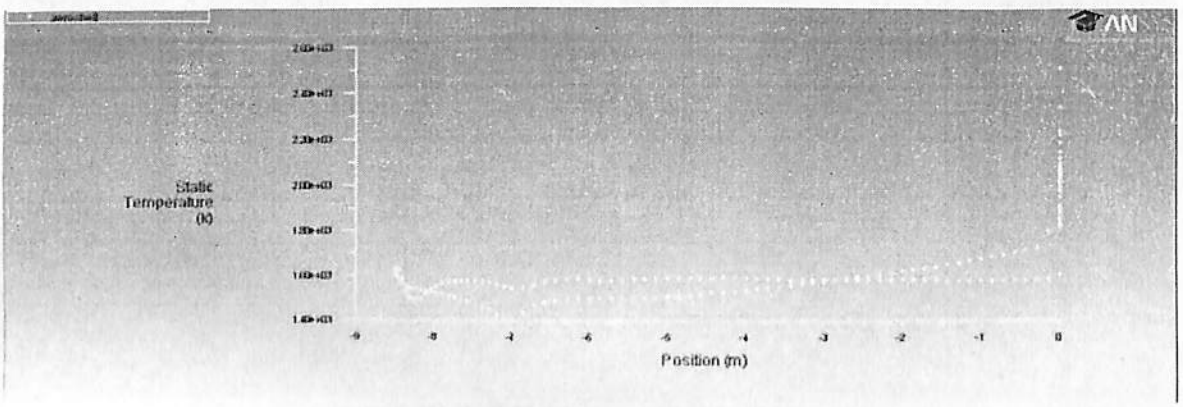

Figure 6.17: Static Temperature Contour (AOA 30 Degree)

- Static temperature on the front part of the plate is maximum because of it being the stagnation point (zero velocity). Static temperature decreases fairly on the curved part of the plate (with greater rate at upper curved part).Static temperature decreases fairly on upper and lower surface of the plate
- Static temperature is maximum at the end of the plate due to the formation of the expansion waves.

- Drag coefficient was observed and plotted and found to be around 3.4.

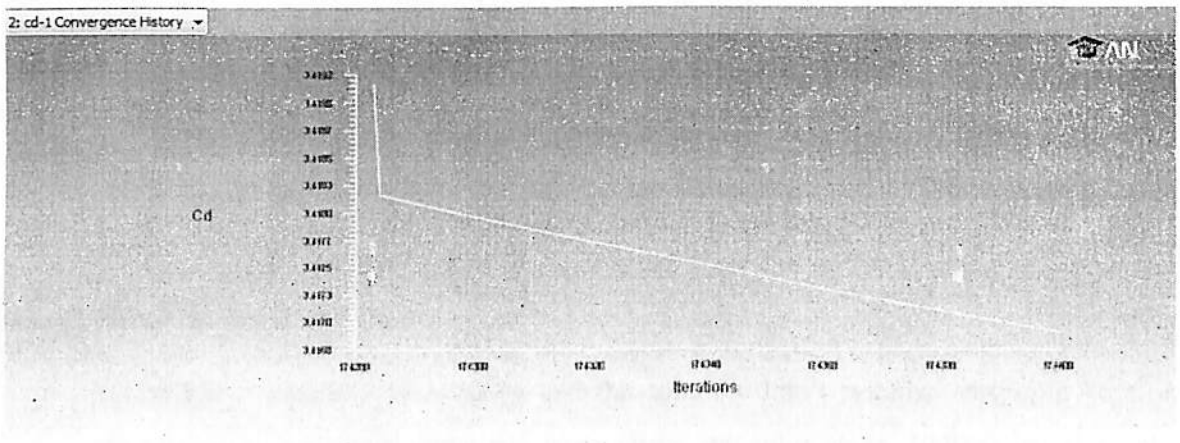

Figure 6.18: Drag Coefficient (AOA 30 Degree)

- Lift coefficient was observed and plotted and found to be around 6.6.

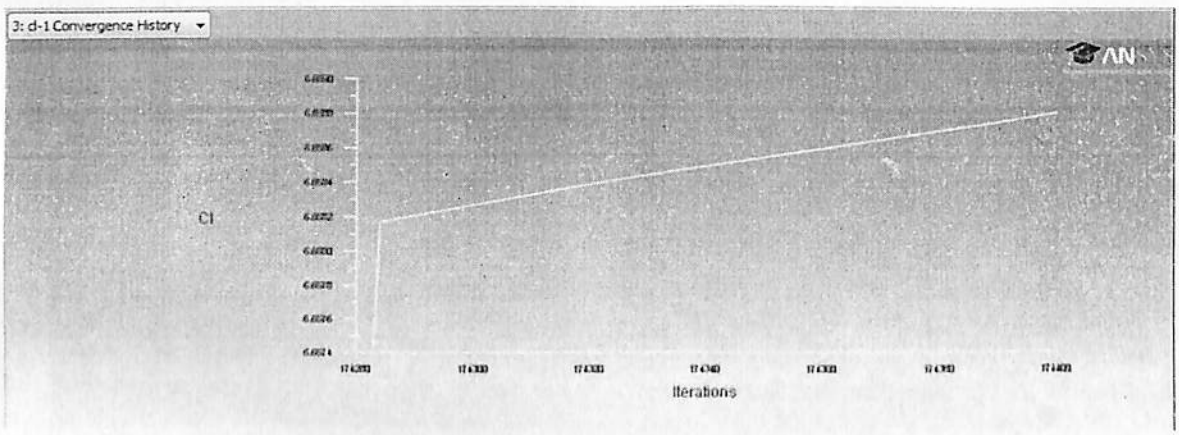

Figure 6.19: Lift Coefficient (AOA 40 Degree)

6.1.3 Problem Setup (Angle Of Attack=40 Degree): CFD Analysis of Hypersonic flow over a 2D Cylinder with dimensions 7m in length and 3m in diameter. Free Stream Mach no is 5. Ambient Temperature is 270.68 K.

Step 1, 2, 3 and step 4 remain the same as the meshed geometry and ambient conditions remains unchanged. Only the angle of attack was changed to 40 degree in step 4. The problem setup in the fluent was unchanged.

6.1.3.1 Result Analysis and Plots:

- 10000 initial iterations were given and the solution didn't stabilize early and kept on fluctuating so additional iterations were given and after about 174000 iterations the results were plotted.
- The continuity and Energy equations stabilized at 1e-2 but didn't converge below 1e-2.
- The X velocity and Y velocity equations kept on oscillating between 1e-2 and 1e-3 but didn't converged below 1e-6.

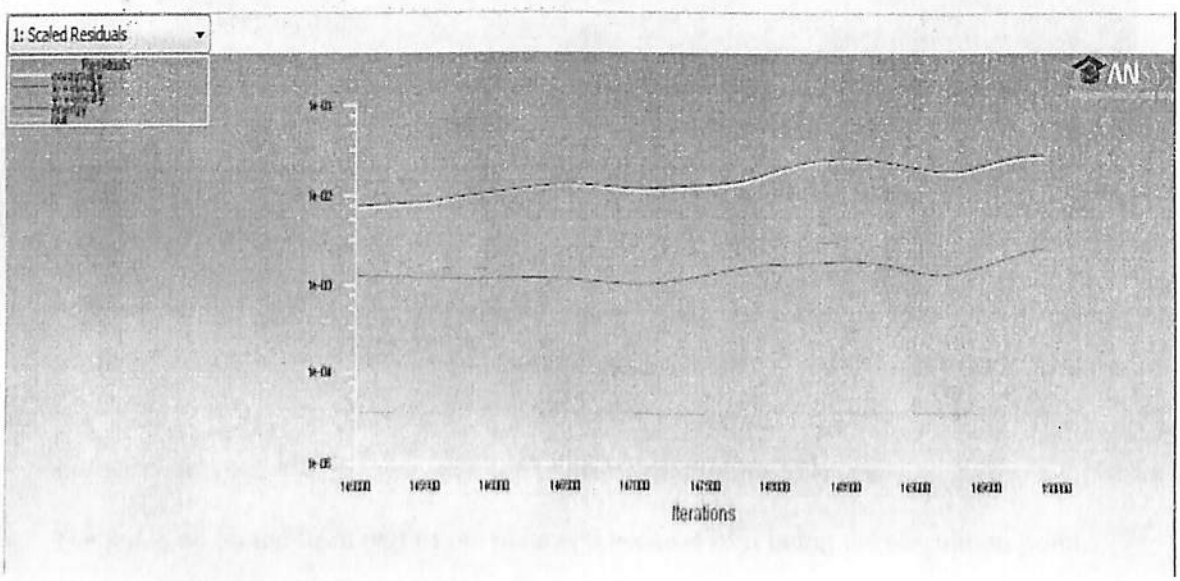

Figure 6.20: Iterations (AOA 40 Degree)

- Mach no decreases substantially behind the Normal shock (<1) just in front of the stagnation point, much lower than the 20 degree AOA.
- Mach no decreases fairly behind the oblique Shock (>1 in front of curved part).
- There was a Expansion wave formation at the rear end of the upper plate and sudden decrease in mach no at the end of plate.

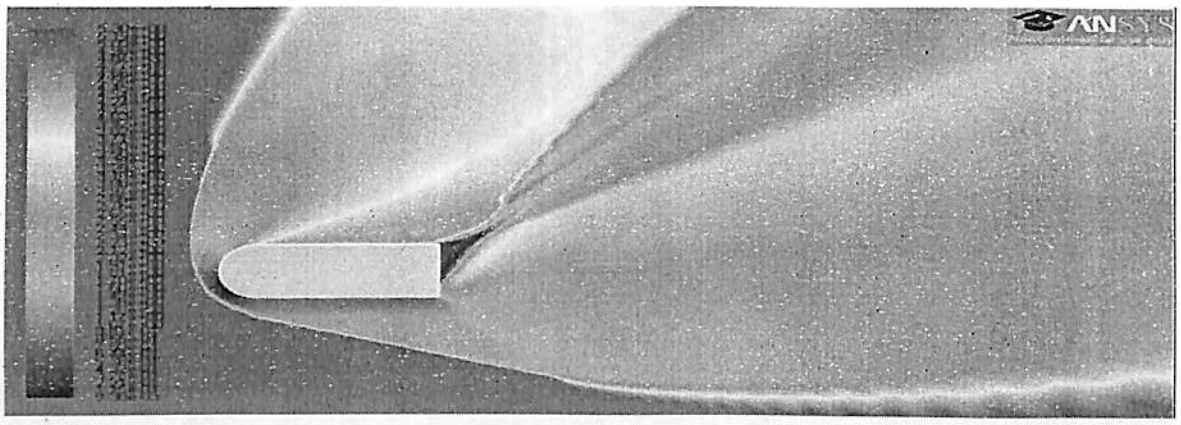

Figure 6.21: Mach No Contour (AOA 40 Degree)

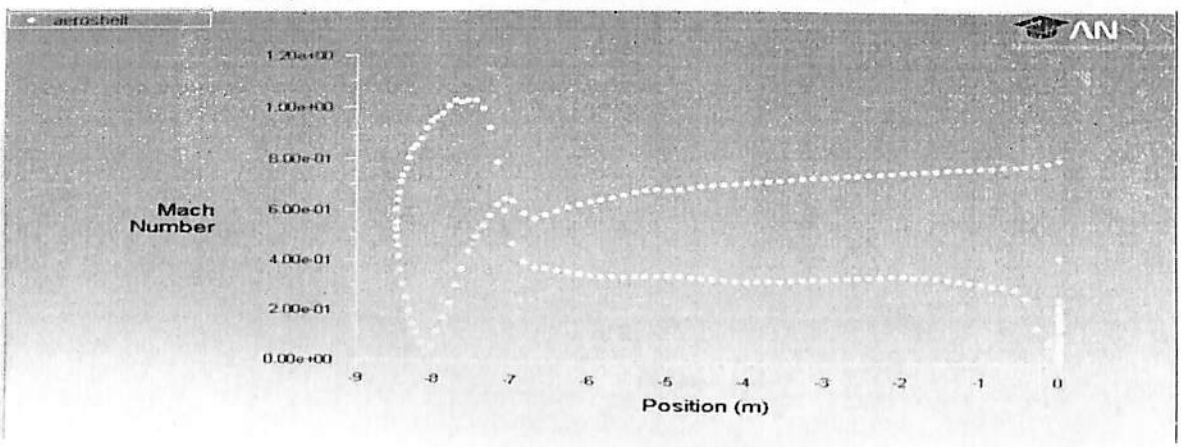

Figure 6.22: Mach No Plot (AOA 40 Degree)

- The mach no on the front part of the plate is 0 because of it being the stagnation point.
- Mach no increases rapidly on the curved part of the plate (with greater rate at upper curved part).
- Mach no increases on upper surface of the plate and fairly decreases on the lower surface of the plate.

- Static pressure rises substantially behind the Normal shock portion in front of the stagnation point, much lower in this case.
- Static pressure rises fairly behind the oblique shock portion (in front of the curved part).
- Static pressure is fairly constant along the lower part of the plate and the upper part but more on the lower part.

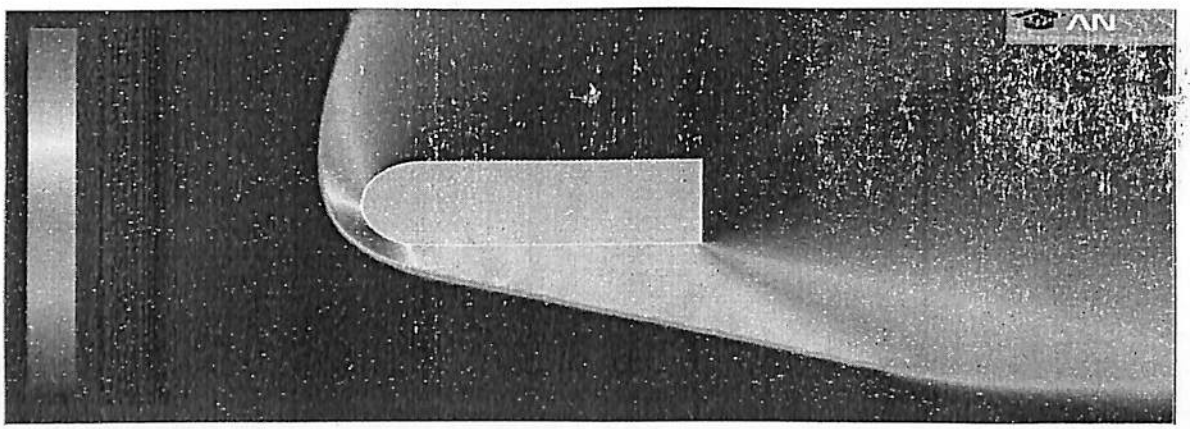

Figure 6.23: Static Pressure Contour (AOA 40 Degree)

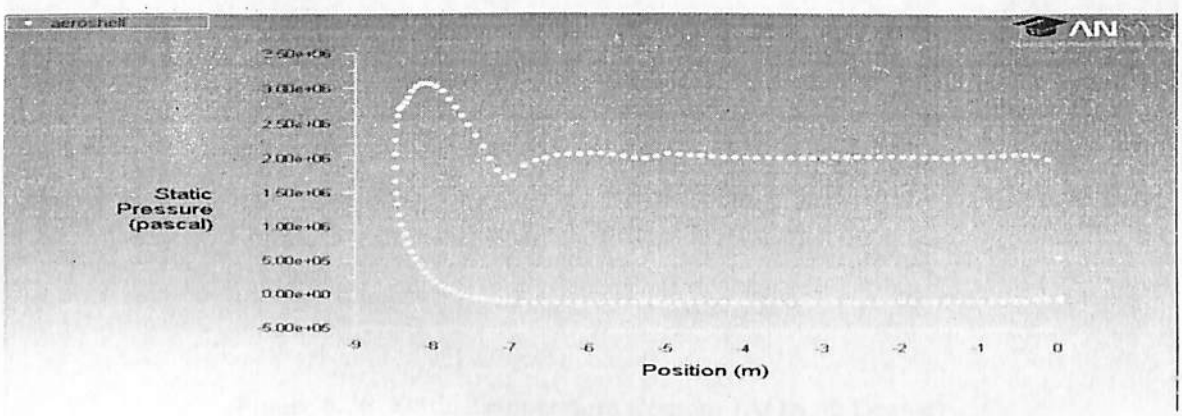

Figure 6.24: Static Pressure Plot (AOA 40 Degree)

- The Static pressure on the front part of the plate is maximum because of it being the stagnation point, much lower in this case.
- Static pressure decreases rapidly on the curved part of the plate (with slower rate at lower curved part because of high angle of attack).
- Static pressure is constant on lower and upper surface of the plate (with greater value at lower portion of the plate).

- Temperature rises substantially behind the Normal shock portion (in front of the stagnation point, much lower in this case).
- Temperature re rises fairly behind the oblique shock portion (in front of the curved part).
- Temperature remains constant as we move progressively towards the end of the plate and is less on the upper edge.

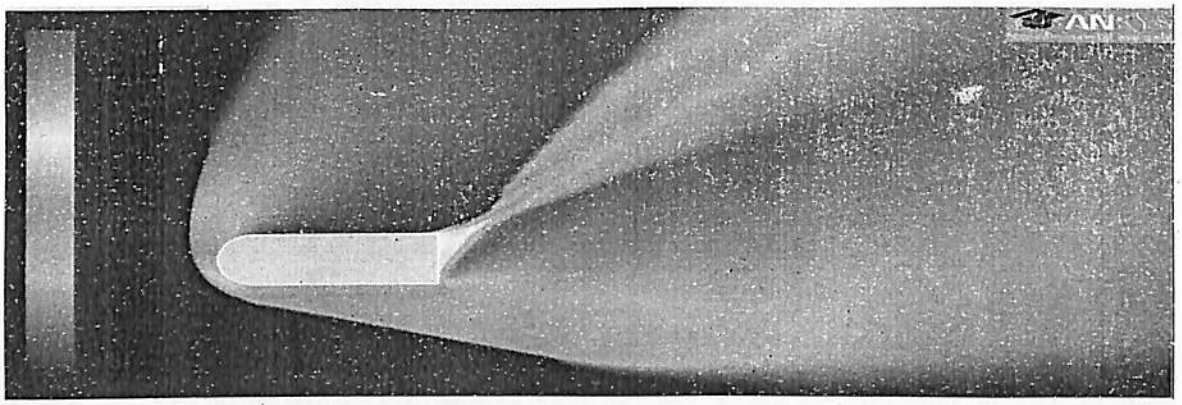

Figure 6.25: Static Temperature Contour (AOA 40 Degree)

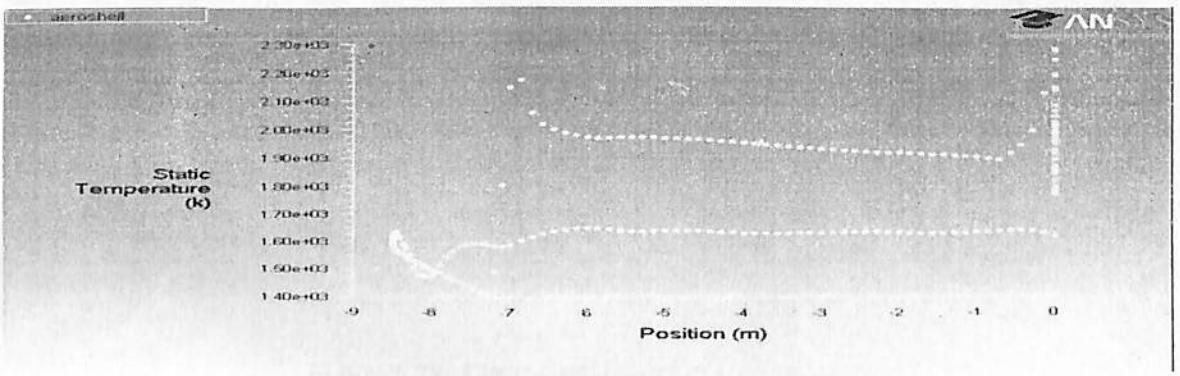

Figure 6.26: Static Temperature Contour (AOA 40 Degree)

- Static temperature is maximum at the end of lower arc because of it being the stagnation point, much lower in this case.
- Static temperature decreases fairly on the curved part of the plate (with greater rate at upper curved part).Static temperature decreases fairly on upper and lower surface of the plate
- Static temperature is maximum at the end of the plate due to the formation of the expansion waves.

- Drag coefficient was observed and plotted and found to be around 3.1.

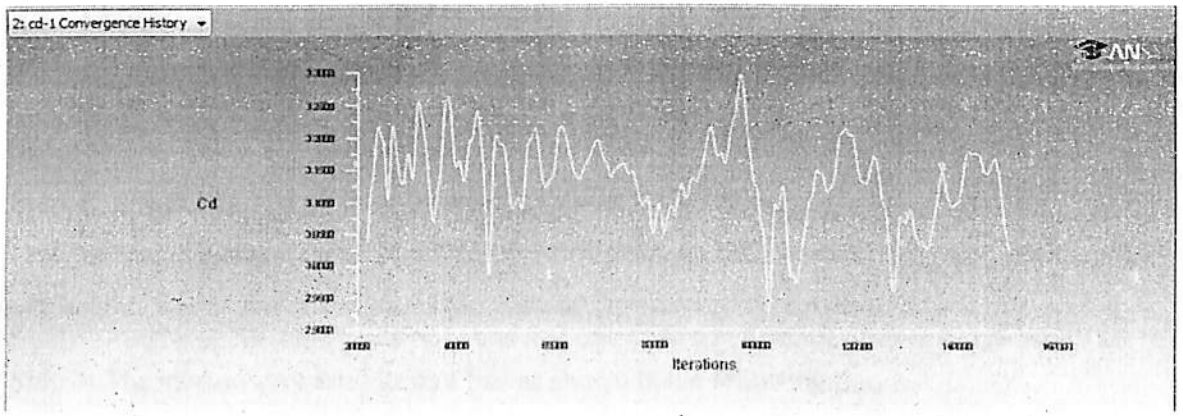

Figure 6.27: Drag Coefficient (AOA 40 Degree)

- Lift coefficient was observed and plotted and found to be around 10.

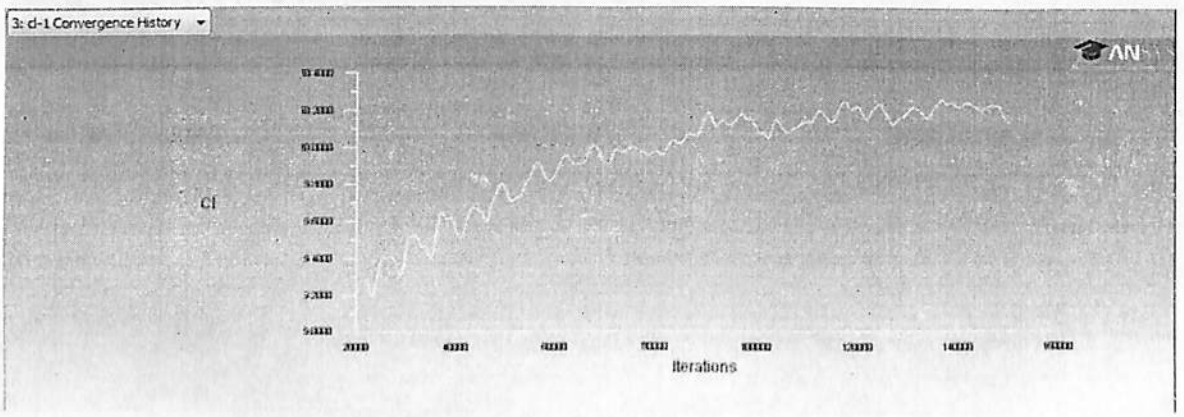

Figure 6.28: Lift Coefficient (AOA 40 Degree)

6.2 2D Cylinder (With Cavity)

6.2.1.1 Problem Setup (Angle Of Attack=20 Degree): CFD Analysis of Hypersonic flow over a 2D Cylinder with dimensions 7m in length and 3m in diameter. The cavity was 0.05 times diameter (0.05D). Free Stream Mach no is 5. Ambient Temperature is 270.68 K.

Step 1: The 2D curved plate of 7m in length and 3m in diameter was created in Ansys ICEM. Farfield was assumed to start 25.5m ahead of the plate and 85m behind the plate. It extended up to a height of 85m above and below the plate as shown in the figure given below.

Step 2: The meshed geometry looked like as shown in the following figure

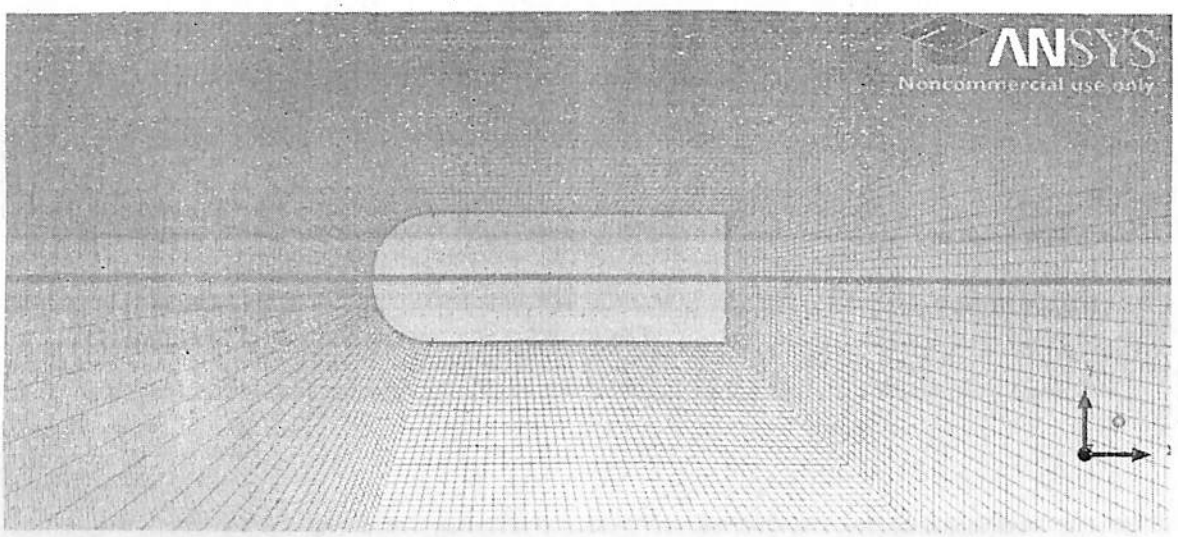

Figure 6.29: Meshed Geometry

Step3: Wall Y+ Estimation:

- Under the conditions specified the Reynolds's number was calculated and the flow turned out to be turbulent.
- Wall Y+ was estimated using an wall Y+ calculator online.
- It was specified as 2.1e-4 and the growth factor (b/a) of 1.2 was taken, with 20 rows.

Step 4: Problem Setup in Ansys Fluent 14:

- In the solver menu Coupled solver was selected and 2D was selected in Space.
- The Viscous model was taken as Spalarat Allmaras (1 eqn).
- Under the materials option the density of air was taken as ideal gas.
- Under the materials option the Cp was taken as piecewise polynomial.
- Viscosity was taken as Sutherland relation.
- The operating pressure was defined 0.
- Farfield values were set as Mach no=5 and gauge pressure was taken as 79.799 pa.
- Temperature was set as 270.69 K.
- Angle of attack was defined as 20 degree in the boundary conditions.
- Monitors of Cd and Cl were also set to compare the various values.
- The solution was initialized and residuals were set to 1e-6.

6.2.1.2 Result Analysis and Plots:

- 10000 initial iterations were given and the solution didn't stabilize early and kept on fluctuating so additional iterations were given.
- The continuity and Energy equations stabilized at 1e-2 but didn't converge below 1e-2.

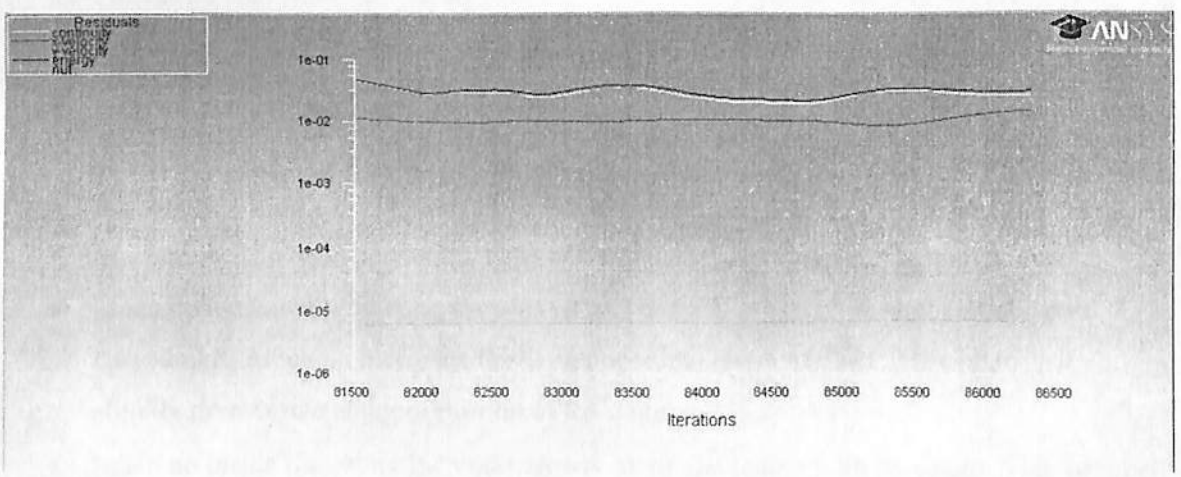

Figure 6.30: Iterations (Cavity At 20 Degree AOA)

- Mach no decreases substantially behind the Normal shock portion (<1) and decreases fairly behind the oblique Shock (>1)
- The flow leaving the cavity has very high velocity (greater than the ambient velocity).

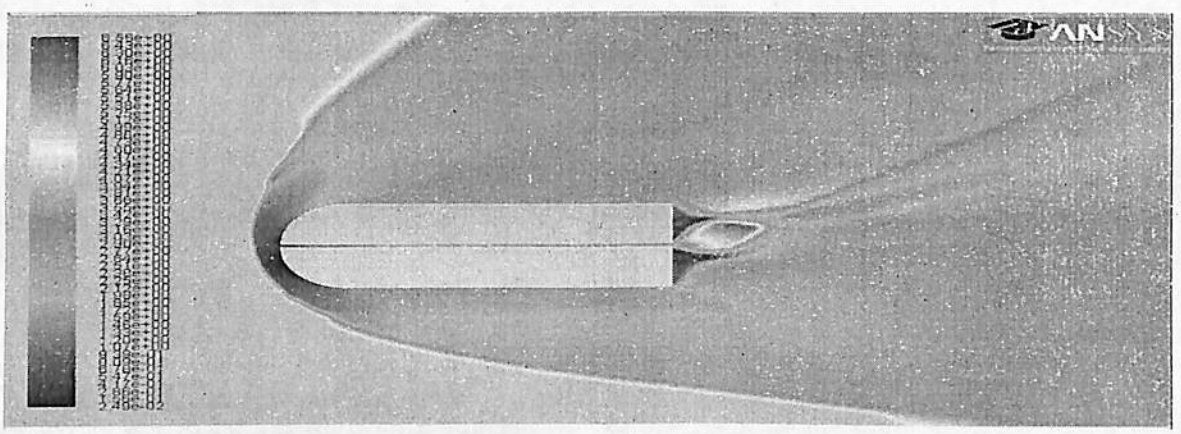

Figure 6.31: Mach No Contour (Cavity At 20 Degree AOA)

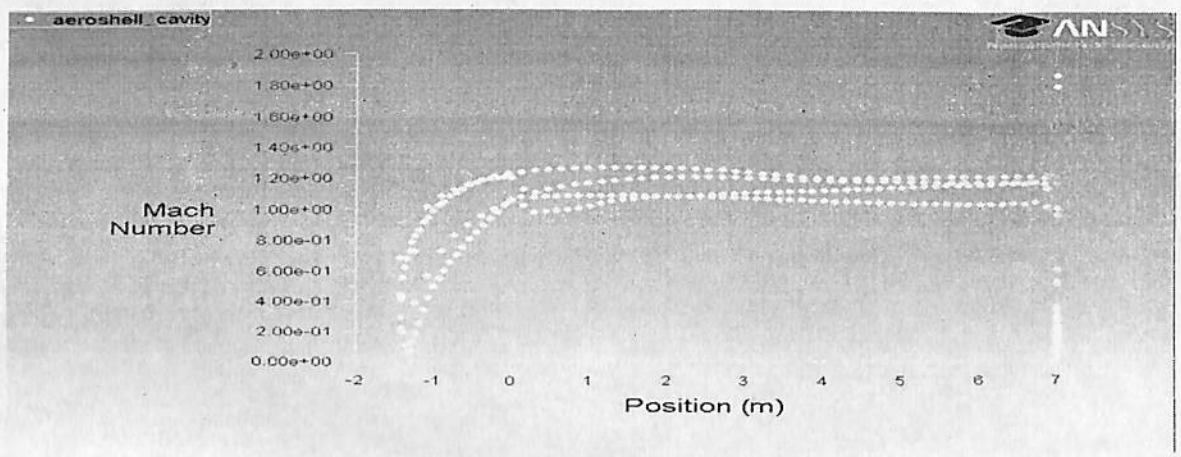

Figure 6.32: Mach No Plot(Cavity At 20 Degree AOA)

- Mach no on the front part of the plate is 0 because of it being the stagnation point.
- Mach no increases rapidly on the curved part of the plate (with greater rate at upper curved part).Mach no increases fairly on upper and lower surface of the plate (with slightly greater rate at upper portion of the plate).
- Mach no inside the cavity increases slowly along the length with its values lying between the values of upper and lower surface of the plate.

- Static pressure rises substantially behind the Normal shock portion; static pressure rises fairly behind the oblique shock portion (in front of the curved part).
- Static pressure rises slightly as we move progressively on the lower part of the plate and is roughly constant on the upper edge.
- Static pressure is maximum at the front cavity and decreases along the length.

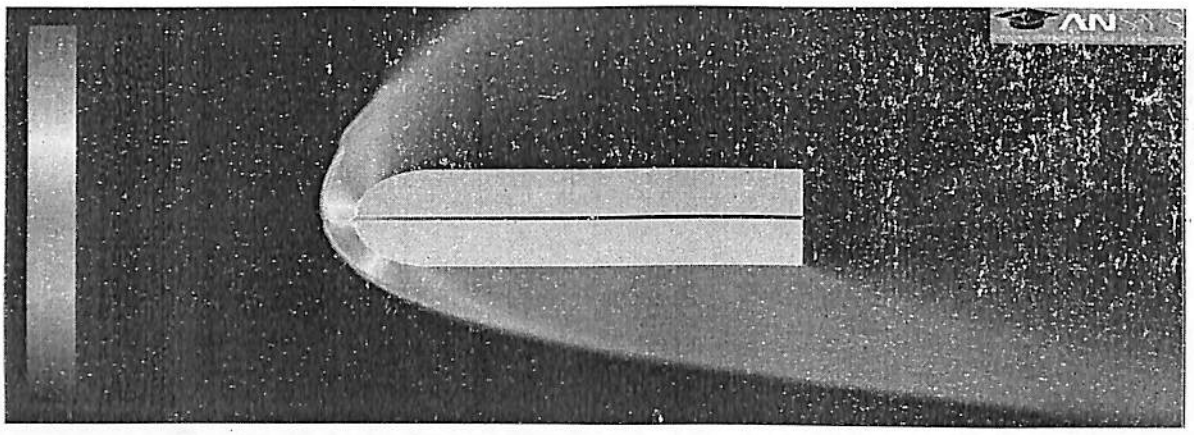

Figure 6.33: Static Pressure Contour (Cavity At 20 Degree AOA)

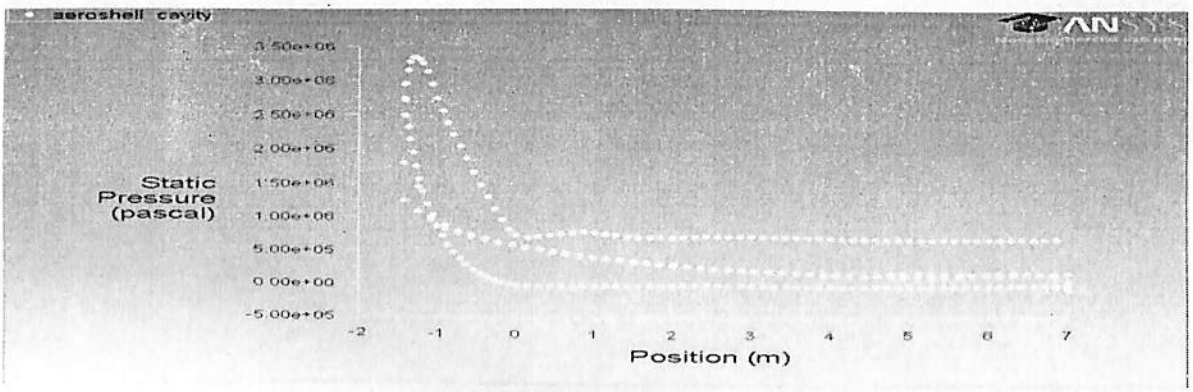

Figure 6.34: Static Pressure Plot (Cavity At 20 Degree AOA)

- The Static pressure on the front part of the plate is maximum because of it being the stagnation point (zero velocity).
- Static pressure decreases rapidly on the curved part of the plate (with greater rate at upper curved part).Static pressure is roughly constant on upper and lower surface of the plate (with greater value at lower portion of the plate).
- Static pressure is maximum at the front cavity and decreases along the length.

- Temperature rises substantially behind the Normal shock portion (in front of the stagnation point).Temperature re rises fairly behind the oblique shock portion (in front of the curved part).
- Temperature decreases as we move along the plate on lower and upper edge.
- Temperature along the cavity is fairly constant

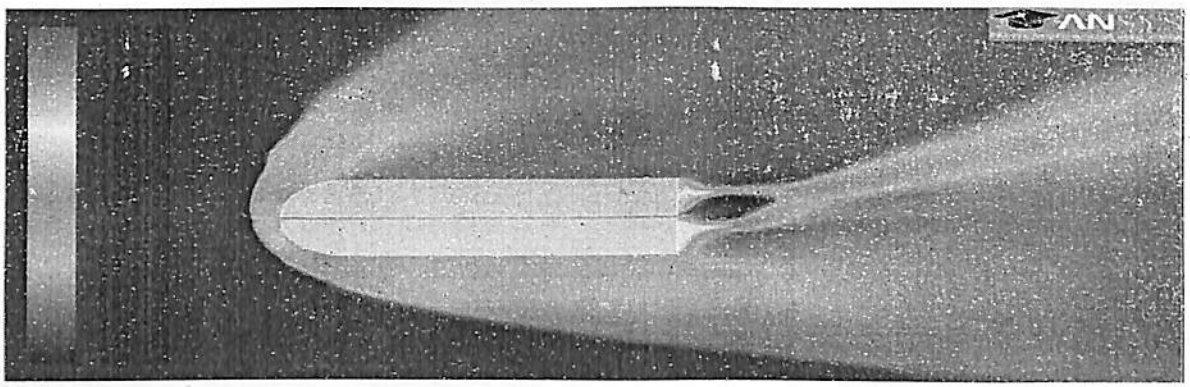

Figure 6.35: Static Temperature Contour (Cavity At 20 Degree AOA)

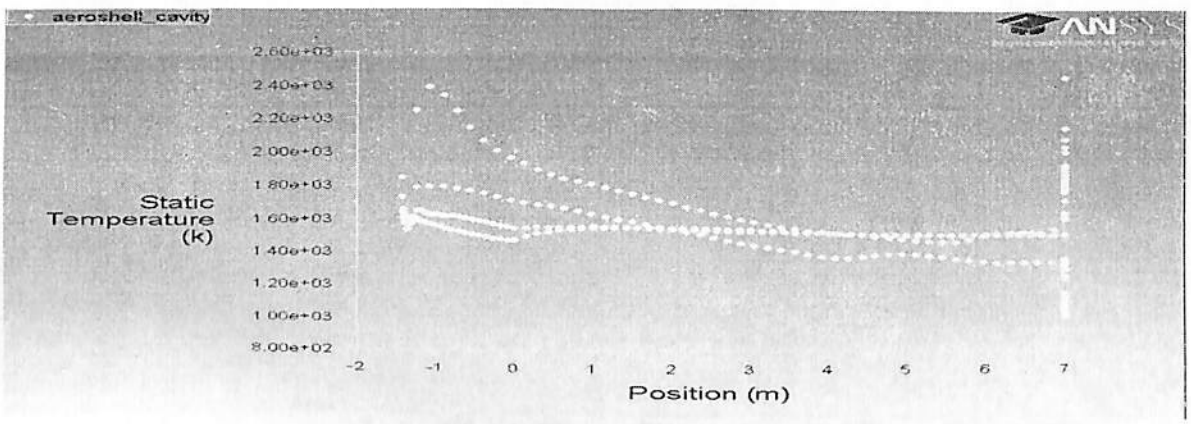

Figure 6.36: Static Temperature Plot (Cavity At 20 Degree AOA)

- Static temperature on the front part of the plate is maximum because of it being the stagnation point (zero velocity).Static temperature increases on the curved part of the plate (with greater rate at lower curved part).
- Static temperature decreases fairly on upper and lower surface of the plate.
- Static temperature is maximum at the end of the plate
- Static temperature first decreases then is fairly constant along the cavity.

- Drag coefficient was observed and plotted and found to be around 3.6.

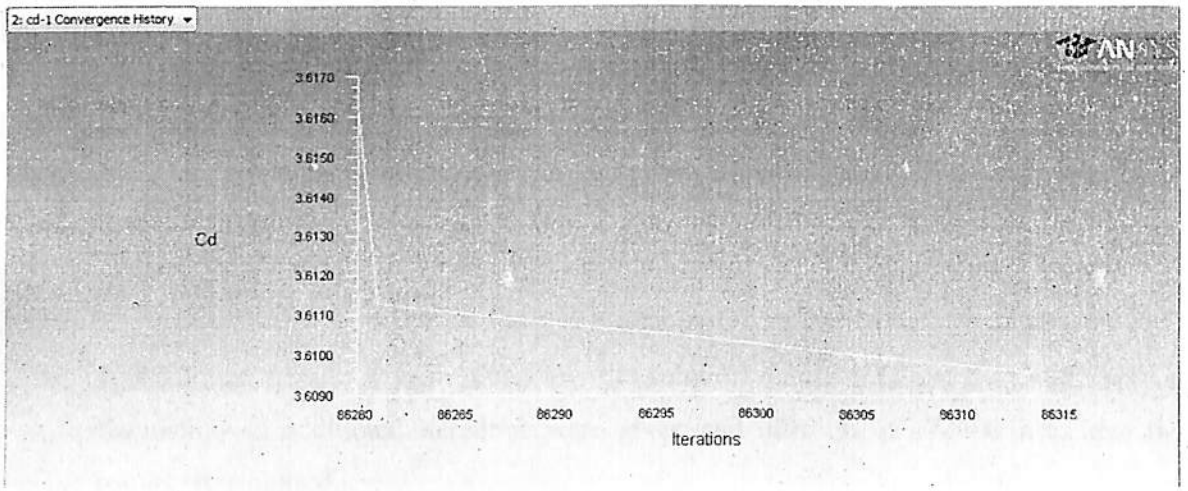

Figure 6.37: Drag Coefficient (Cavity At 20 Degree AOA)

- Lift coefficient was observed and plotted and found to be around 3.9.

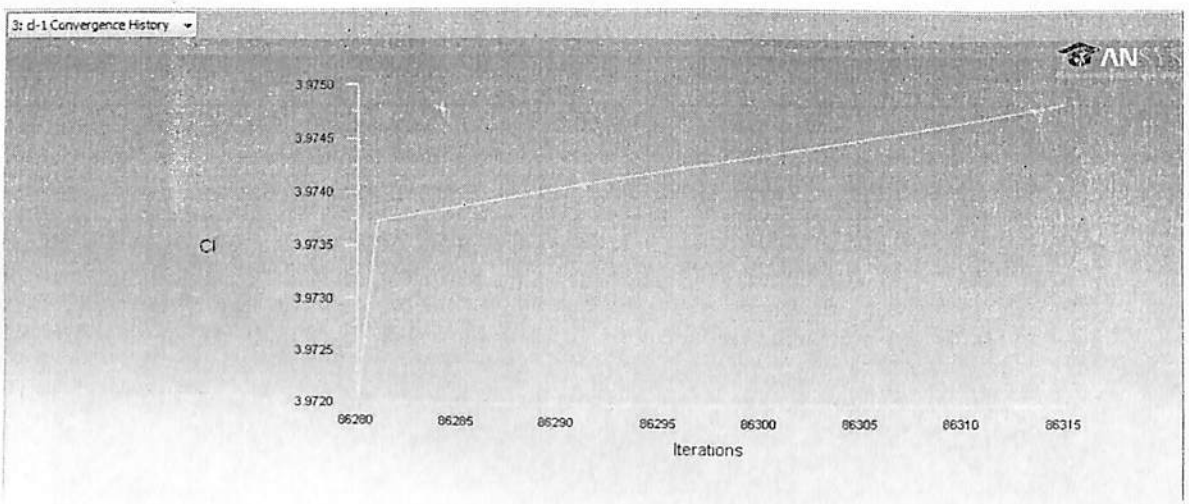

Figure 6.38: Lift Coefficient (Cavity At 20 Degree AOA)

6.2.2 Problem Setup (Angle Of Attack=30 Degree): CFD Analysis of Hypersonic flow over a 2D Cylinder with dimensions 7m in length and 3m in diameter. The cavity was 0.05 times diameter (0.05D). Free Stream Mach no is 5. Ambient Temperature is 270.68 K.

Step 1, 2, 3 and step 4 remain the same as the meshed geometry and ambient conditions remains unchanged. Only the angle of attack was changed to 30 degree in step 4. The problem setup in the fluent was unchanged.

6.2.2.1 Result Analysis and Plots:

- 10000 initial iterations were given and the solution didn't stabilize early and kept on fluctuating so additional iterations were given and after about 174000 iterations the results were plotted.
- The continuity and Energy equations stabilized at 1e-2 but didn't converge below 1e-2.
- The X velocity and Y velocity equations kept on oscillating between 1e-2 and 1e-3 but didn't converged below 1e-6.

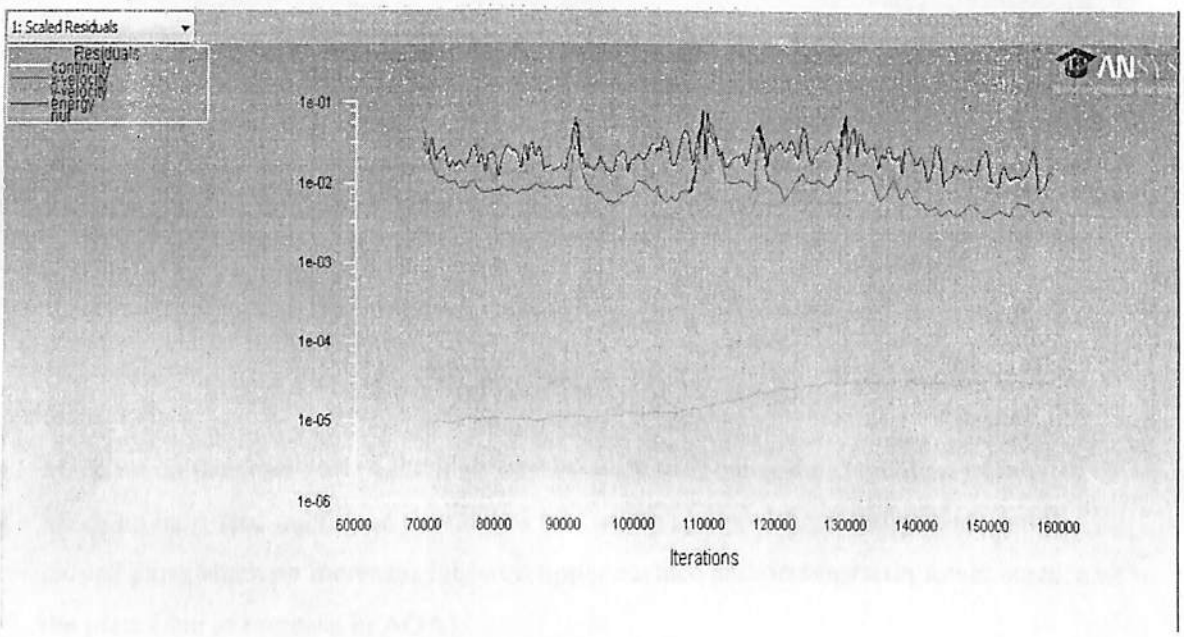

Figure 6.39: Iterations (Cavity At 30 Degree AOA)

- Mach no decreases substantially behind the Normal shock portion (<1) and decreases fairly behind the oblique Shock (>1). Stagnation point is lower than in previous case.
- The flow leaving the cavity has very high velocity (greater than the ambient velocity).

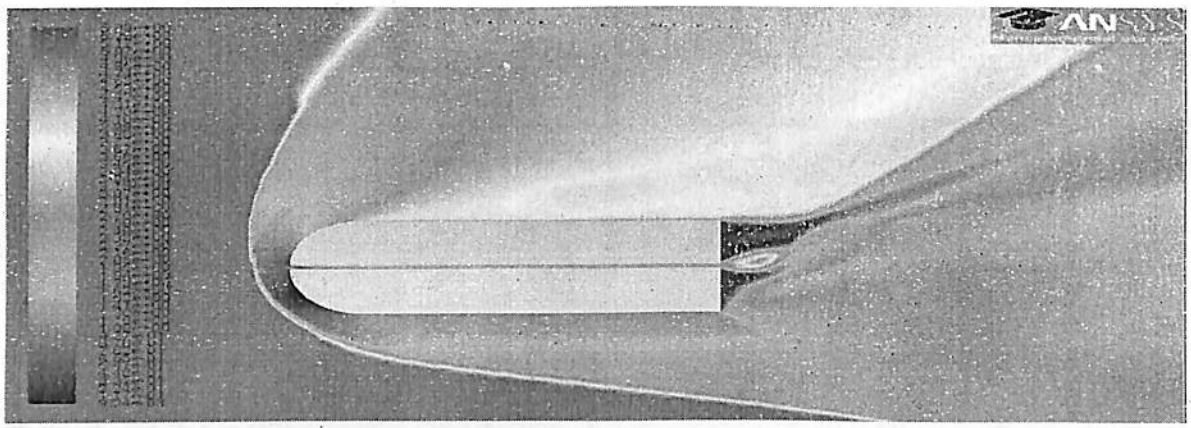

Figure 6.40: Mach No Contour (Cavity At 30 Degree AOA)

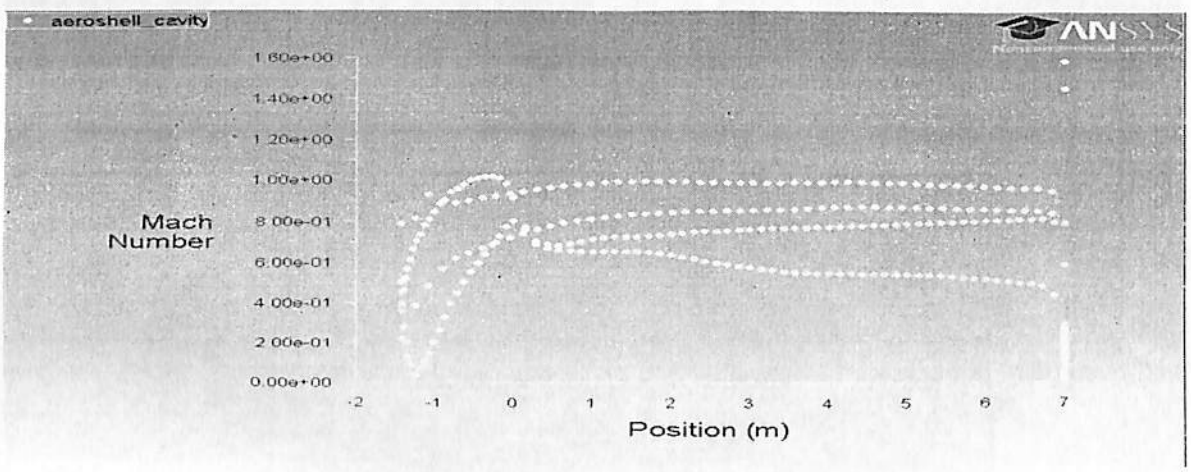

Figure 6.41: Mach No Plot (Cavity At 30 Degree AOA)

- Mach no on the front part of the plate is 0 because of it being the stagnation point.
- Mach no increases rapidly on the curved part of the plate (with greater rate at upper curved part).Mach no increases fairly on upper surface and decreases on lower surface of the plate (due to increase in AOA).
- Mach no inside the cavity increases slowly along the length with its values lying well within the values of upper and lower surface of the plate.
- Mach no of the flow leaving the cavity is higher than ambient mach no.

- Static pressure rises substantially behind the Normal shock portion, static pressure rises fairly behind the oblique shock portion (in front of the curved part).
- Static pressure is constant along the length on upper and lower surfaces(more on lower surface).
- Static pressure is maximum at the front cavity and decreases along the length.

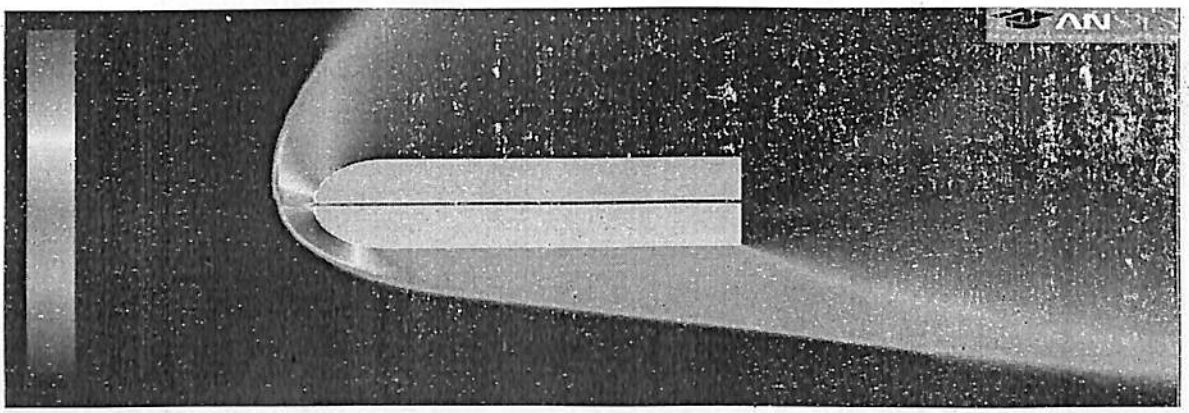

Figure 6.42: Static Pressure Contour (Cavity At 30 Degree AOA)

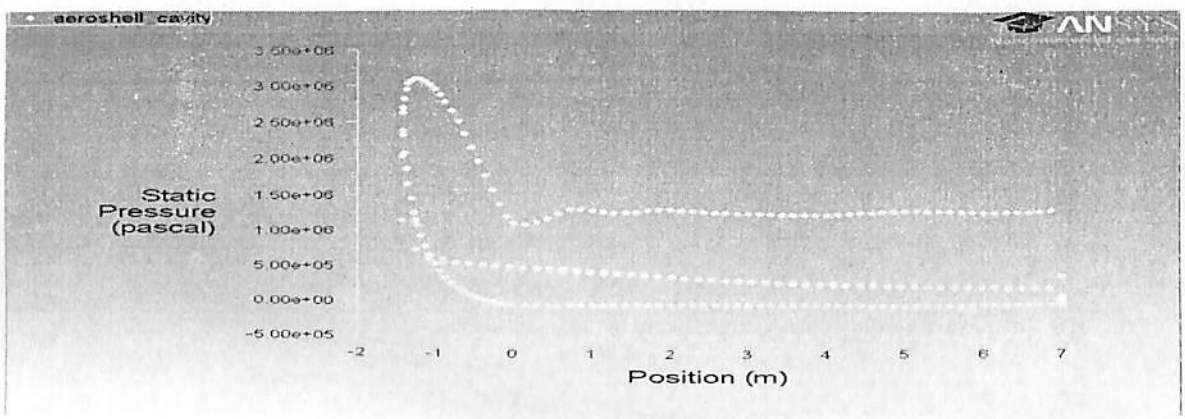

Figure 6.43: Static Pressure Plot (Cavity At 30 Degree AOA)

- The Static pressure on the front part of the plate is maximum because of it being the stagnation point, lower than previous case.
- Static pressure decreases rapidly on the curved part of the plate (with greater rate at upper curved part).Static pressure is roughly constant on upper and lower surface of the plate (with greater value at lower portion of the plate).
- Static pressure is maximum at the front cavity and decreases along the length.

- Temperature rises substantially behind the Normal shock portion (in front of the stagnation point).Temperature re rises fairly behind the oblique shock portion (in front of the curved part).
- Temperature decreases as we move along the plate on lower and upper edge.
- Temperature along the cavity is increasing and is maximum at the end of plate due to formation of expansion waves.

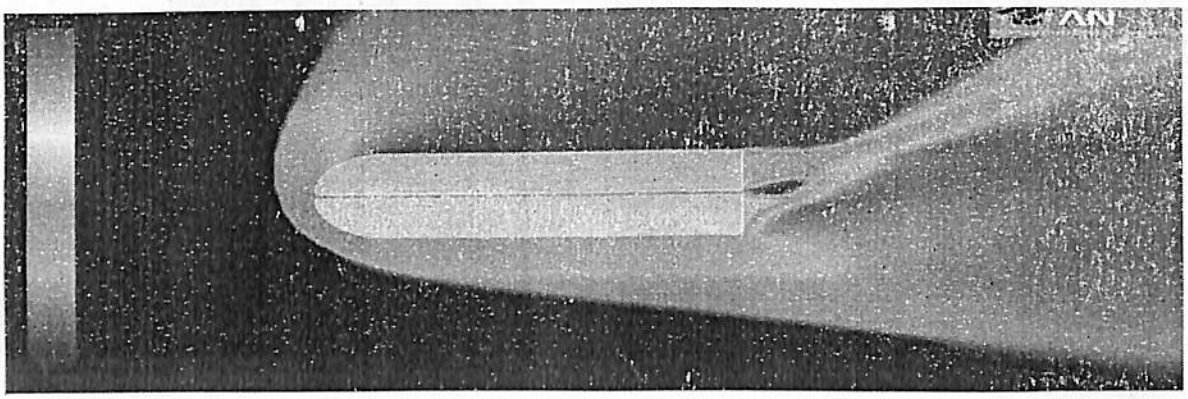

Figure 6.44: Static Temperature Contour (Cavity At 30 Degree AOA)

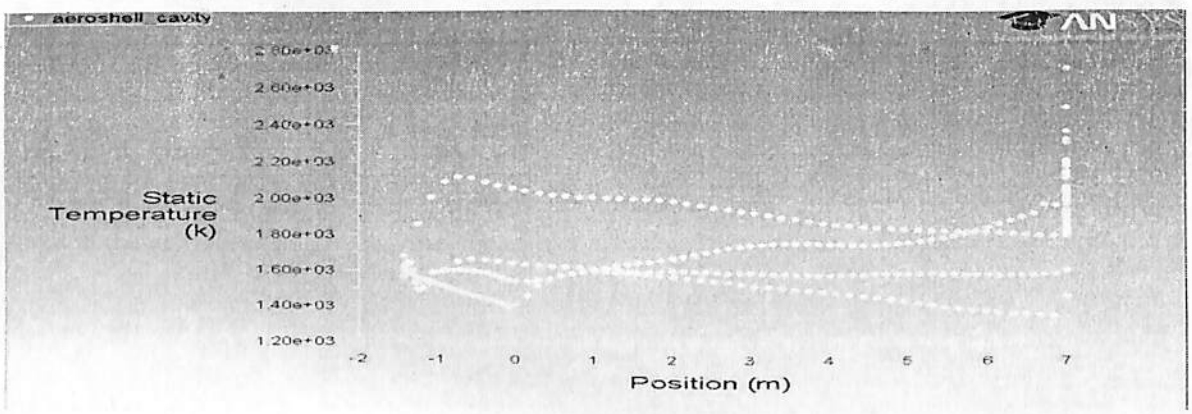

Figure 6.45: Static Temperature Contour (Cavity At 30 Degree AOA)

- Static temperature on the front part of the plate is maximum because of it being the stagnation point (zero velocity).Static temperature increases on the curved part of the plate (with greater rate at lower curved part).Static temperature decreases fairly on upper and lower surface of the plate. Static temperature is maximum at the end of the plate
- Static temperature first decreases then increases fairly along the cavity.

- Drag coefficient was observed and plotted and found to be around 3.3.

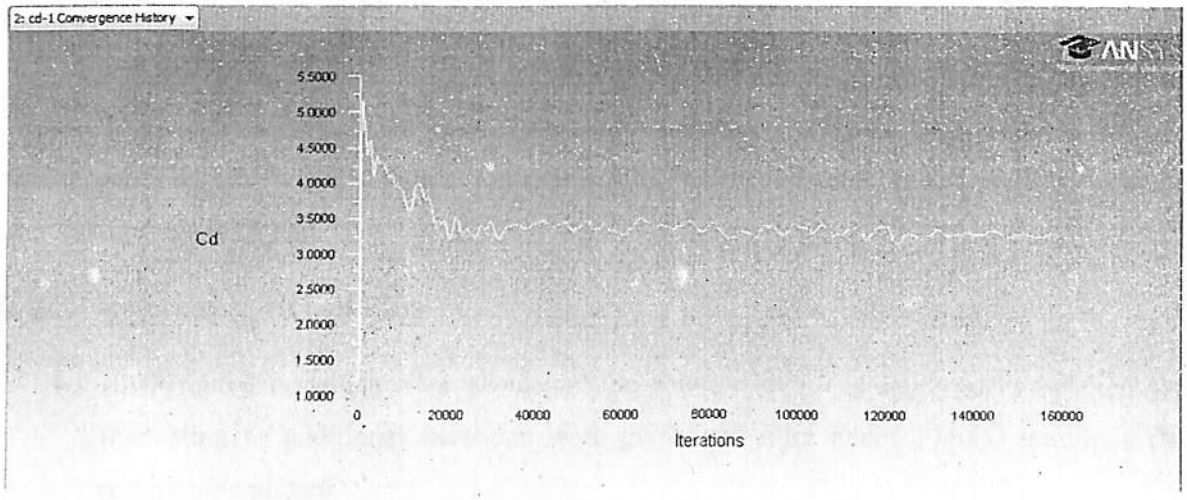

Figure 6.46: Drag Coefficient (Cavity At 30 Degree AOA)

- Lift coefficient was observed and plotted and found to be around 6.

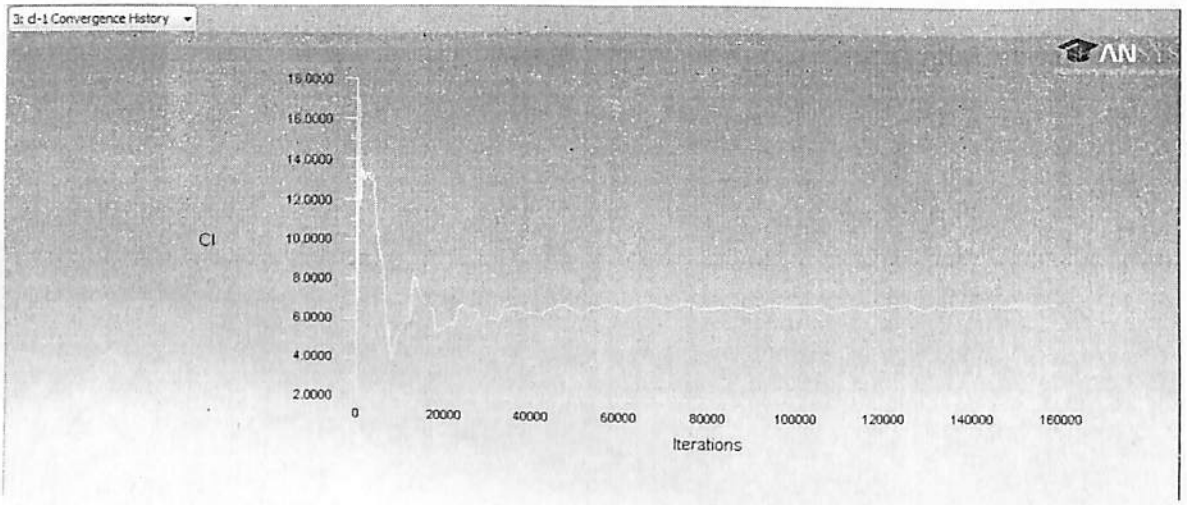

Figure 6.47: Lift Coefficient (Cavity At 30 Degree AOA)

6.2.3 Problem Setup (Angle Of Attack=40 Degree): CFD Analysis of Hypersonic flow over a 2D Cylinder with dimensions 7m in length and 3m in diameter. The cavity was 0.05 times diameter (0.05D). Free Stream Mach no is 5. Ambient Temperature is 270.68 K.

Step 1, 2, 3 and step 4 remain the same as the meshed geometry and ambient conditions remains unchanged. Only the angle of attack was changed to 30 degree in step 4. The problem setup in the fluent was unchanged.

6.2.3.1 Result Analysis and Plots:

- 10000 initial iterations were given and the solution didn't stabilize early and kept on fluctuating so additional iterations were given and after about 174000 iterations the results were plotted.
- The continuity and Energy equations stabilized at 1e-2 but didn't converge below 1e-2.
- The X velocity and Y velocity equations kept on oscillating between 1e-2 and 1e-3 but didn't converged below 1e-6.

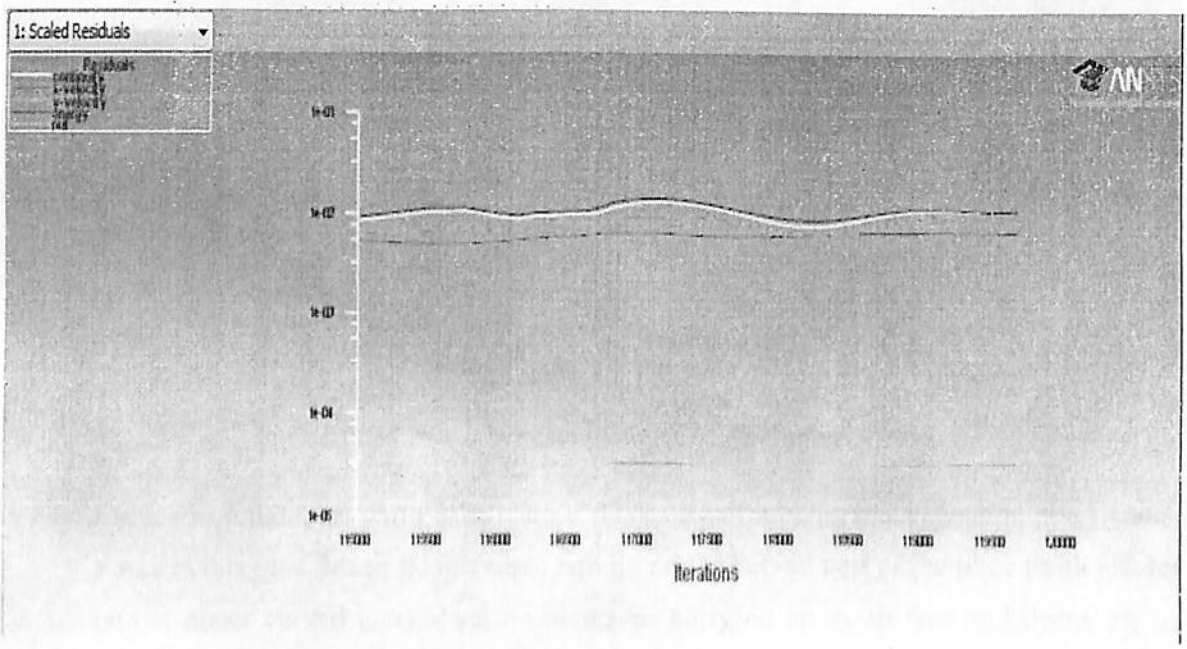

Figure 6.48: Iterations (Cavity At 40 Degree AOA)

- Mach no decreases substantially behind the Normal shock portion (<1) and decreases fairly behind the oblique Shock (>1). Stagnation point is lower than in previous case.
- The mach no on the upper plate is more than lower surface because of flow seperation.
- The velocity of the flow leaving the cavity is less than the ambient velocity, unlike previous cases.

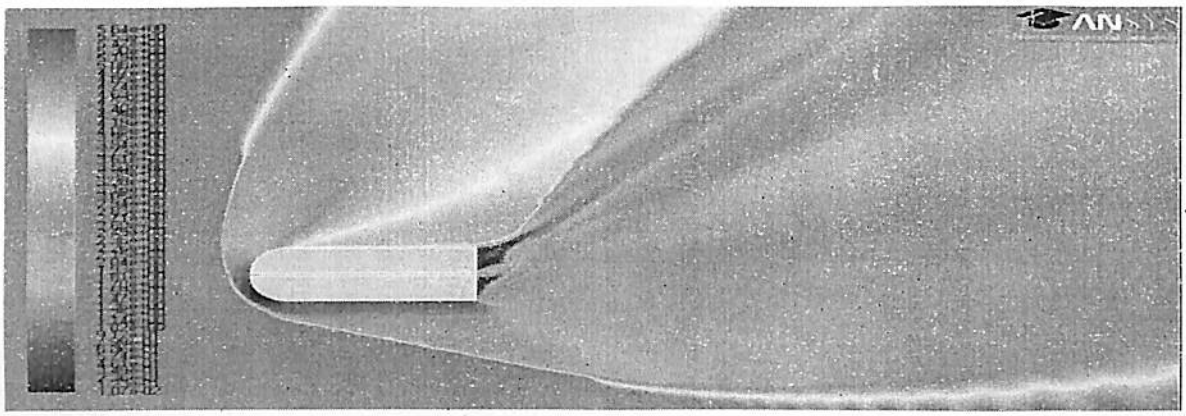

Figure 6.49: Mach No Contour (Cavity At 40 Degree AOA)

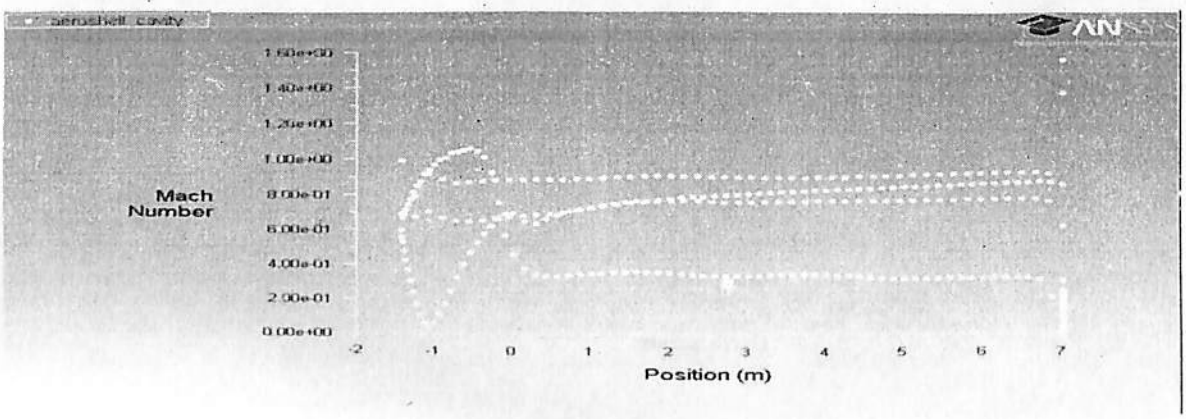

Figure 6.50: Mach No Plot (Cavity At 40 Degree AOA)

- Mach no on the front part of the plate is 0 because of it being the stagnation point, much lower in this case. Mach no increases rapidly on the curved part of the plate (with greater rate at upper curved part).Mach no increases fairly on upper surface and decreases on lower surface of the plate (due to increase in AOA).
- Mach no inside the cavity increases slowly along the length with its values lying well within the values of upper and lower surface of the plate.

- Static pressure rises substantially behind the Normal shock portion, static pressure rises fairly behind the oblique shock portion (in front of the curved part).
- Stagnation point is much lower in this case.
- Static pressure is constant along the length on upper and lower surfaces(more on lower surface).Static pressure is maximum at the front cavity and is constant along the length.

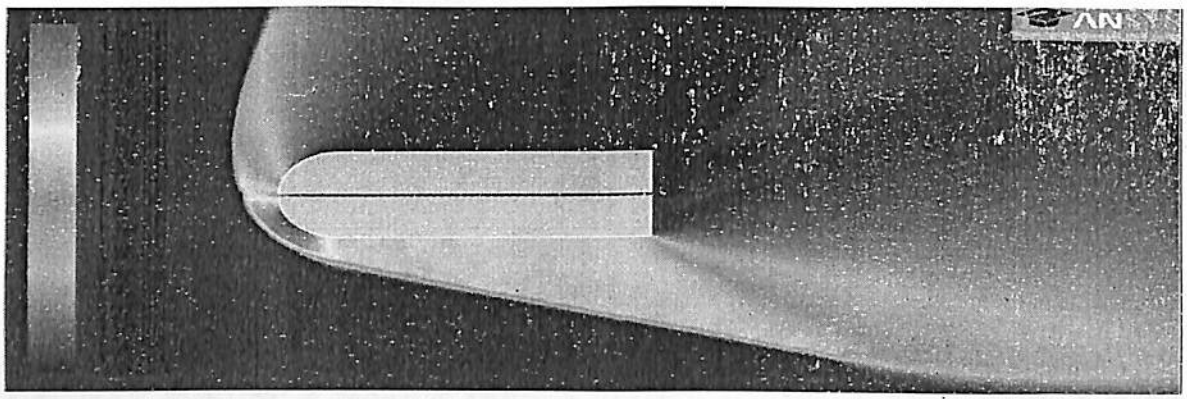

Figure 6.51: Static Pressure Contour (Cavity At 40 Degree AOA)

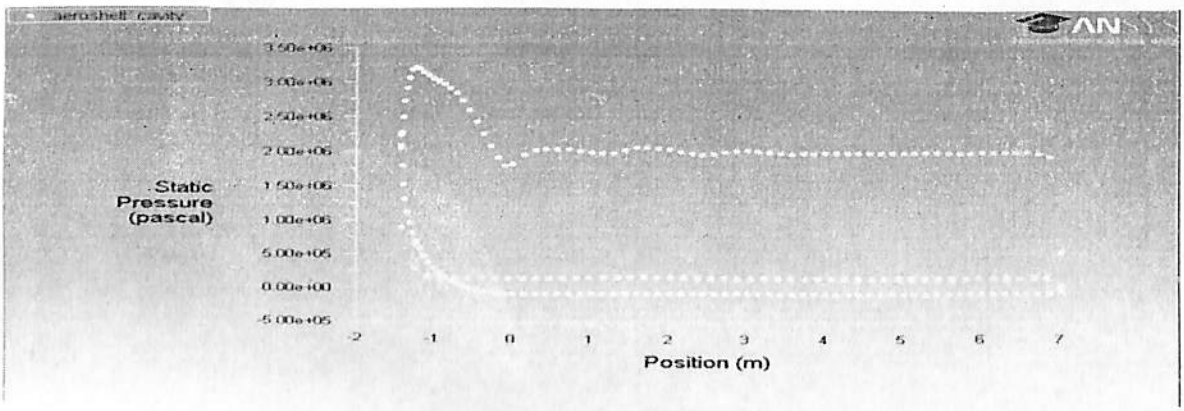

Figure 6.52: Static Pressure Plot (Cavity At 40 Degree AOA)

- The Static pressure on the front part of the plate is maximum because of it being the stagnation point, much lower in this case.
- Static pressure decreases rapidly on the curved part of the plate (with greater rate at upper curved part).Static pressure is roughly constant on upper and lower surface of the plate (with greater value at lower portion of the plate).
- Static pressure is maximum at the front cavity and constant along the length.

- Temperature rises substantially behind the Normal shock portion (in front of the stagnation point).Temperature re rises fairly behind the oblique shock portion (in front of the curved part).
- Temperature decreases as we move along the plate on lower and upper edge.
- Temperature along the cavity is increasing and is maximum at the end of plate due to formation of expansion waves.

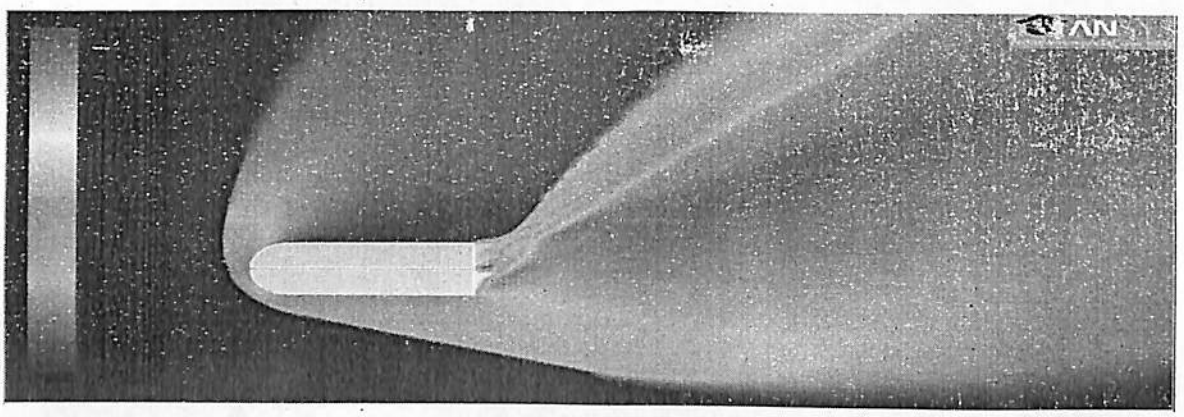

Figure 6.53: Static Temperature Contour (Cavity At 40 Degree AOA)

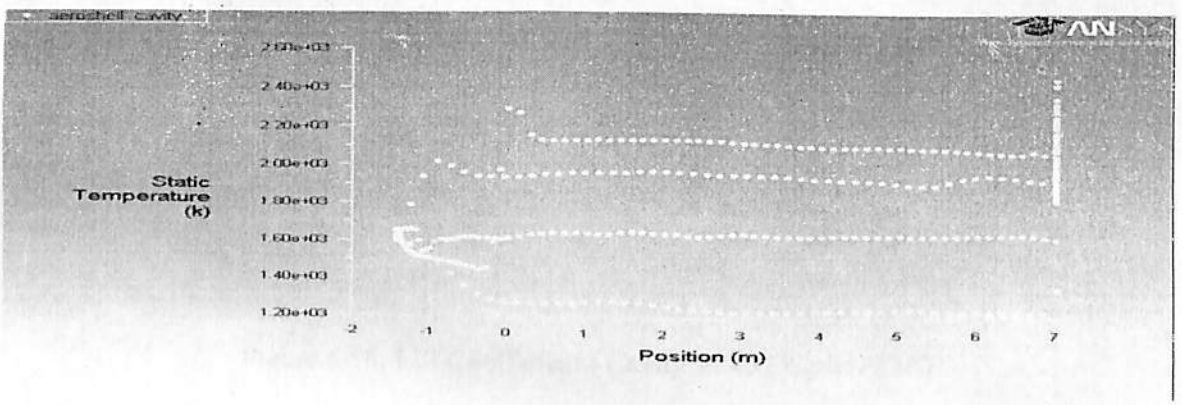

Figure 6.54: Static Temperature Contour (Cavity At 40 Degree AOA)

- Static temperature on the front part of the plate is maximum because of it being the stagnation point (zero velocity).Static temperature increases on the curved part of the plate (with greater rate at lower curved part).Static temperature decreases fairly on upper and lower surface of the plate. Static temperature is maximum at the end of the plate
- Static temperature first decreases then increases fairly along the cavity.

- Drag coefficient was observed and plotted and found to be around 3.

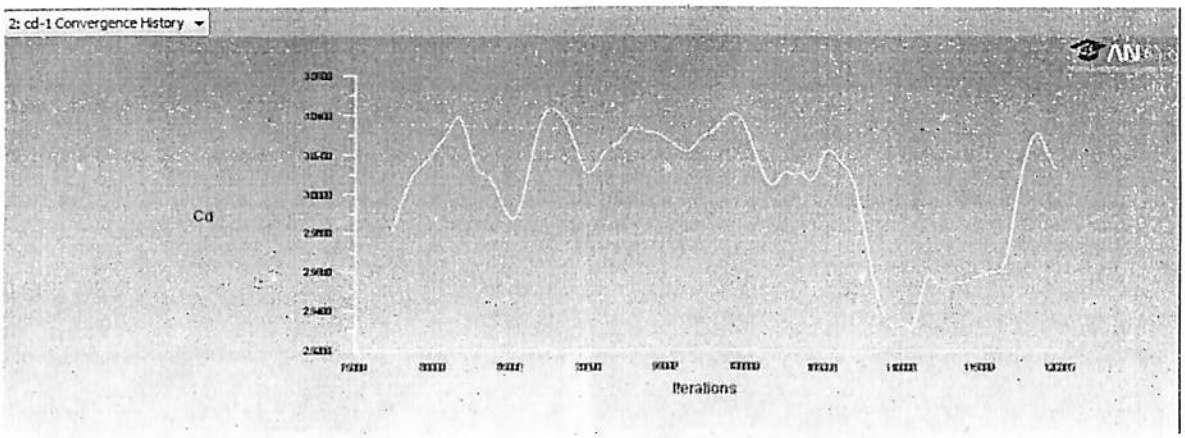

Figure 6.55: Drag Coefficient (Cavity At 40 Degree AOA)

- Lift coefficient was observed and plotted and found to be around 10.

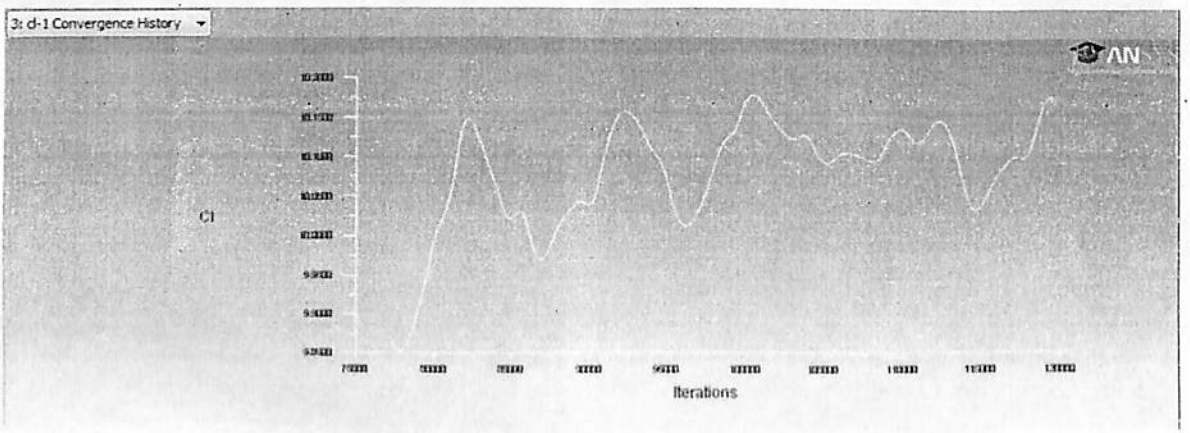

Figure 6.56: Lift Coefficient (Cavity At 40 Degree AOA)

Chapter 7

Conclusions

7.1 Comparison between 2D Cylinder (without cavity) and 2D Cylinder (with cavity)

7.1.1 Angle of Attack 20 Degree: Various parameters such as mach no, pressure, temperature and heat flux were compared to determine which geometry was best suited for the hypersonic flow.

7.1.1.1 Mach Number Comparison:

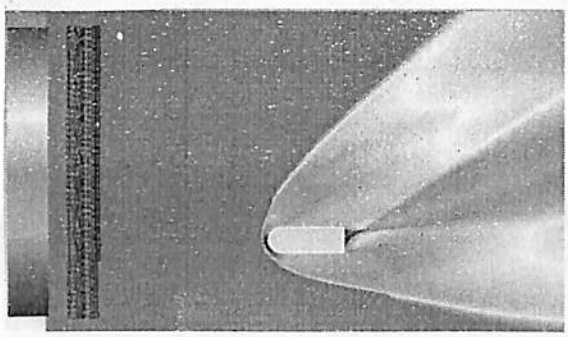

Figure 7.1 Mach no. (AOA 20 degree)

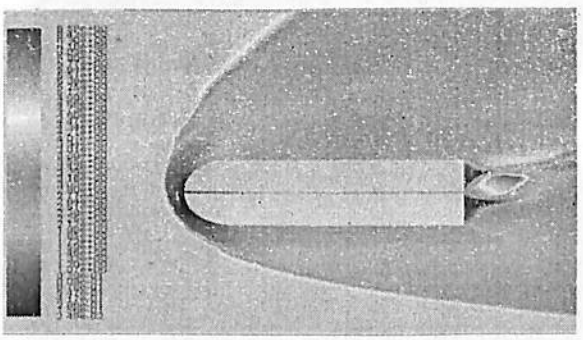

Figure 7.2 Mach no. (AOA 20 degree)

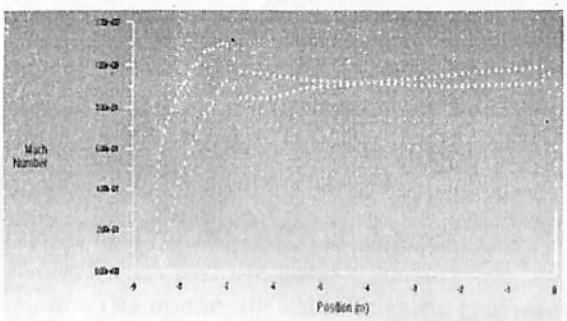

Figure 7.3 Mach no. (AOA 20 degree)

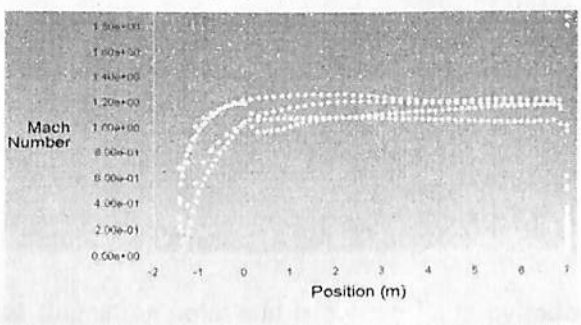

Figure 7.4 Mach no. (AOA 20 degree)

- The maximum mach no is 1.2 in cylinder (with cavity) and 1.1 in cylinder (without cavity).
- Along the length of the cylinder the mach no follows a similar trend in both geometries.
- Mach no varies b/w 0.8 to 0.9 in case of cylinder and 1.05 to 1.2 in case of cavity(upper surface having greater values in both the geometries).
- Mach no is increased (>5) at the end of the cylinder (with cavity) as the cavity acts like a nozzle and flow through it is accelerated.

7.1.1.2 Static Pressure Comparison:

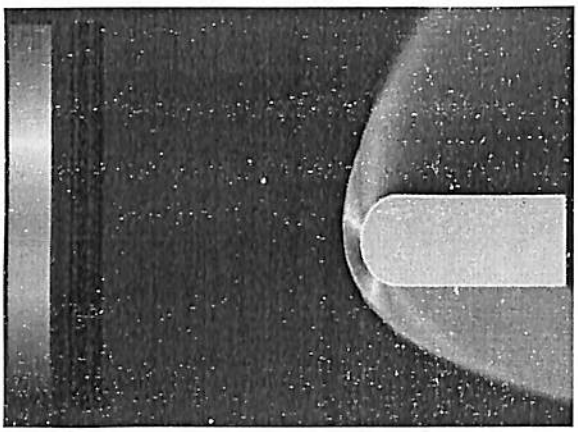

Figure 7.5 Pressure (AOA 20 degree)

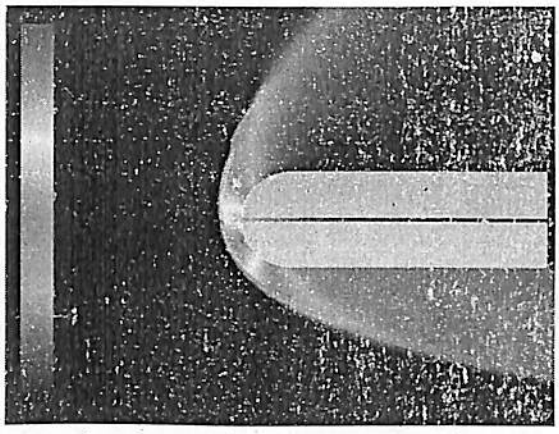

Figure 7.6 Pressure (AOA 20 degree)

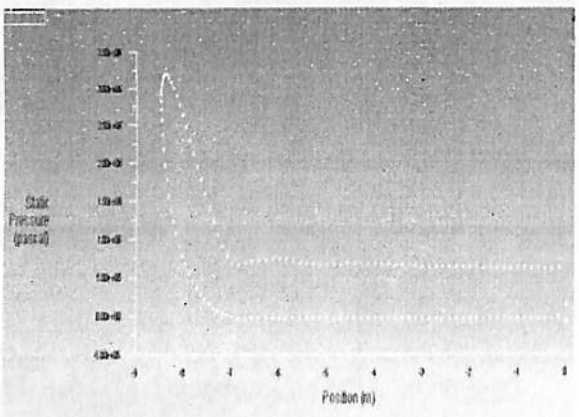

Figure 7.7 Pressure (AOA 20 degree)

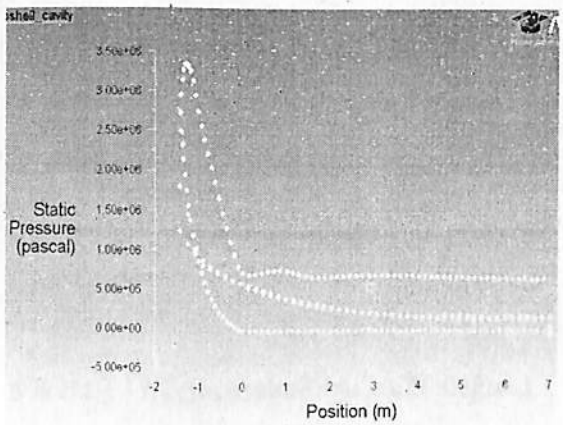

Figure 7.8 Pressure (AOA 20 degree)

- The maximum value of static pressure is at stagnation point and is 3.4e+6 Pa in cylinder (with cavity) and 3.25e+6 Pa in cylinder (without cavity).
- The upper curved surface experiences greater decrease of pressure than lower curved surface in both the geometries. Along the length of the cylinder the pressure remains roughly constant on both lower and upper surfaces in both the geometries.
- Pressure on upper surface is 0 and on lower surface is7.5e+5 pa in both cases.
- The pressure inside the cavity gradually decreases and its value is well within the upper and lower surface pressure values.

7.1.1.3 Static Temperature Comparison:

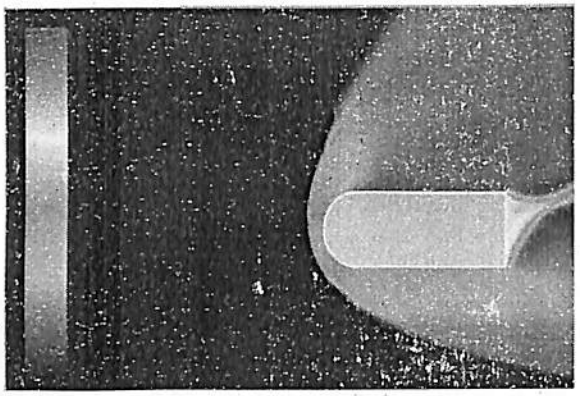

Figure 7.9 Temperature (AOA 20 degree)

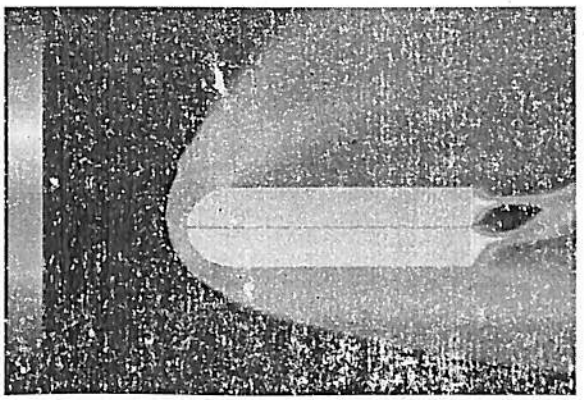

Figure 7.10 Temperature (AOA 20 degree)

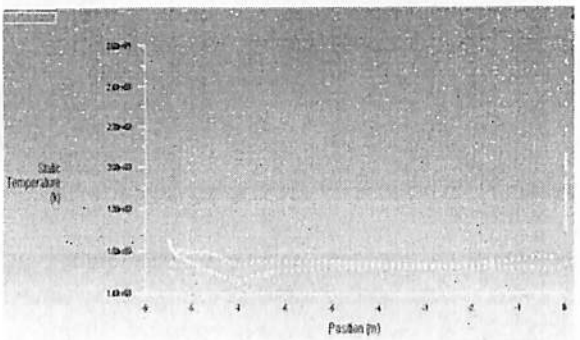

Figure 7.11 Temperature (AOA 20 degree)

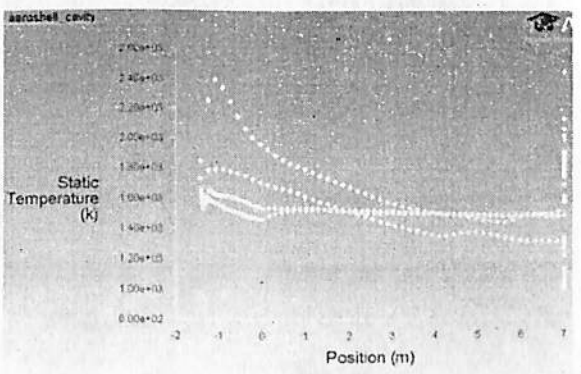

Figure 7.12 Temperature (AOA 20 degree)

- The maximum value of static temperature is at stagnation point and is 2.4e+3 K in cavity and 1.6e+3 K in cylinder (without cavity).
- The upper curved surface experiences greater decrease of temperature than lower curved surface in flat cylinder.
- Temperature first increases then decreases on the curved part in cavity (with greater rate at lower curved part).
- In cylinder (without cavity) temperature remains roughly constant on upper surface and increases gradually on lower surface.(with temperature on lower cylinder first lesser than on upper surface at beginning of cylinder and increasing thereafter)
- In cylinder (with cavity) the temperature remains roughly constant on upper surface and increases gradually on lower surface.(with temperature on lower cylinder greater than that on upper surface at beginning of cylinder)
- The temperature inside the cavity is max at stagnation point and gradually decreases inside the curved part and along the length.

7.1.1.4 Total Energy Comparison:

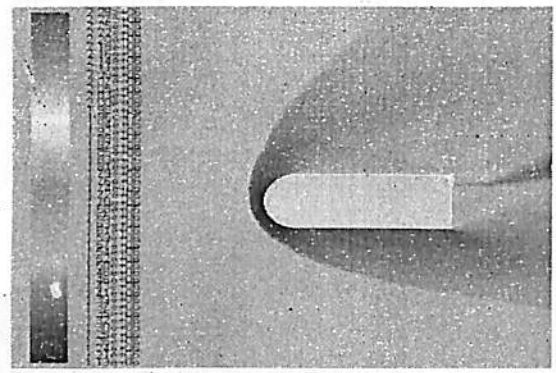

Figure 7.13 Total Energy (AOA 20 degree)

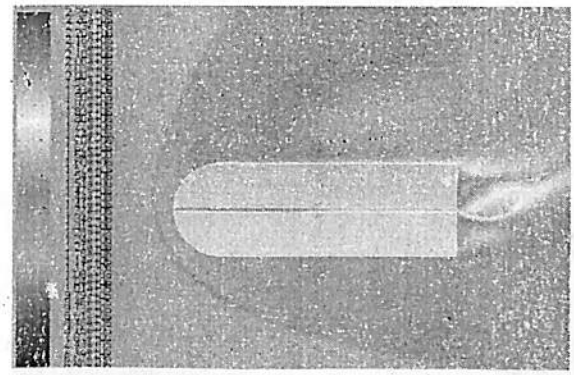

Figure 7.14 Total Energy (AOA 20 degree)

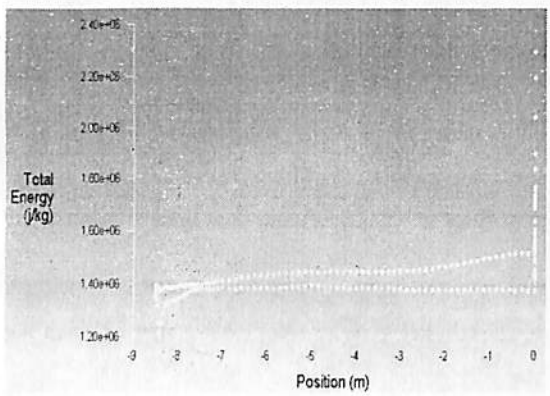

Figure 7.15 Total Energy (AOA 20 degree)

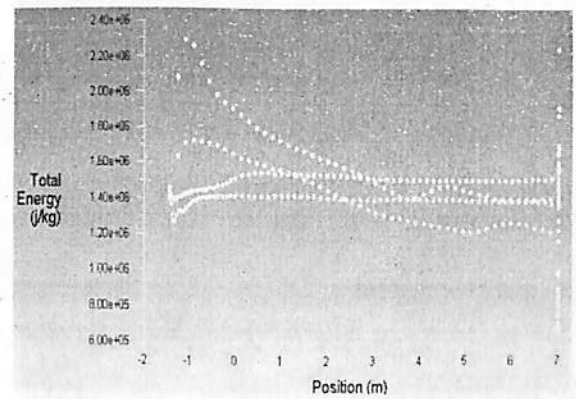

Figure 7.16 Total Energy (AOA 20 degree)

- Minimum total energy is at stagnation point with a value of 1.2e+6 J/Kg at flat cylinder (without cavity) and 1.2e+6 J/Kg at cavity.
- The total energy increases along the curved part with greater rate at upper in both the geometries.
- Total energy is fairly constant along the length in both the geometries(the upper part shows slight increase in energy towards the end in case of cylinder without cavity).
- The total energy inside the cavity first increases and then decreases inside the curved part of cylinder and its value decreases along the length.
- It increases substantially at the end of the cylinder with a maximum value 2.30e+6 J/Kg in both cases.

7.1.2 Angle of Attack 30 Degree: Various parameters such as mach no, pressure, temperature and heat flux were compared to determine which geometry was best suited for the hypersonic flow.

7.1.2.1 Mach Number Comparison:

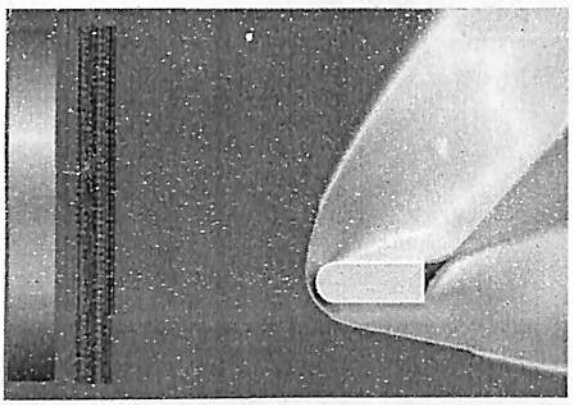

Figure 7.17 Mach no. (AOA 30 degree)

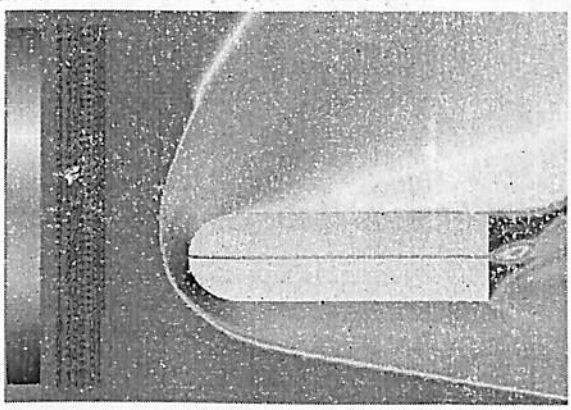

Figure 7.18 Mach no. (AOA 30 degree)

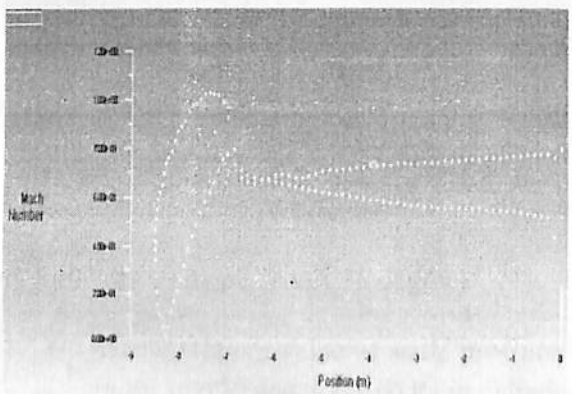

Figure 7.19 Mach no. (AOA 30 degree)

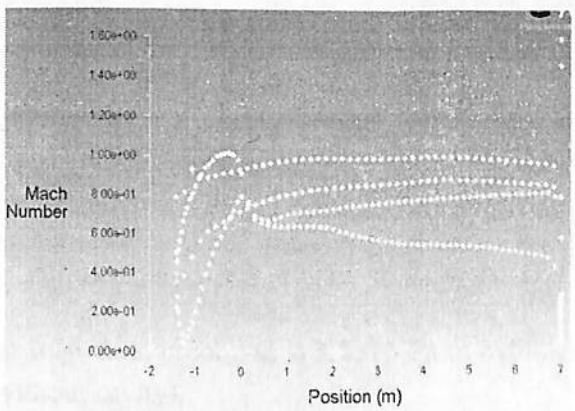

Figure 7.20 Mach no. (AOA 30 degree)

- The maximum mach no is 1 in cylinder (with cavity) and 1.05 in cylinder (without cavity).
- Along the length of the cylinder the mach no follows a similar trend in both geometries.
- Mach no varies b/w 0.4 to 0.8 in case of flat cylinder and 0.5 to 0.8 in case of cavity(upper surface having greater values in both the geometries).
- Mach no is increased (>5) at the end of the cylinder with cavity as the cavity acts like a nozzle and flow through it is accelerated.

7.1.2.2 Static Pressure Comparison:

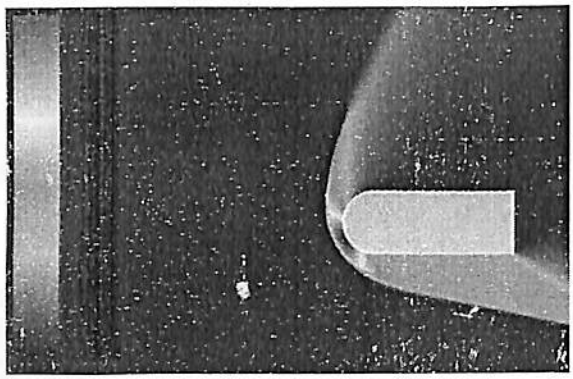

Figure 7.21 Pressure (AOA 30 degree)

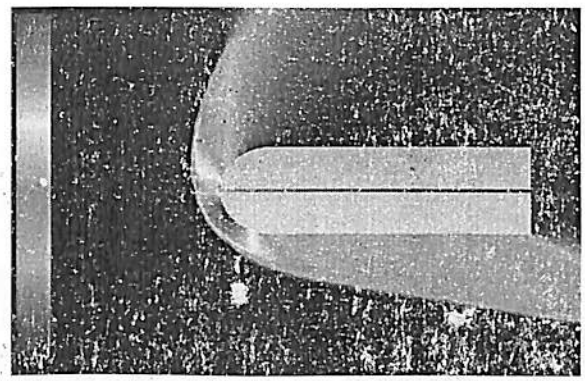

Figure 7.22 Pressure (AOA 30 degree)

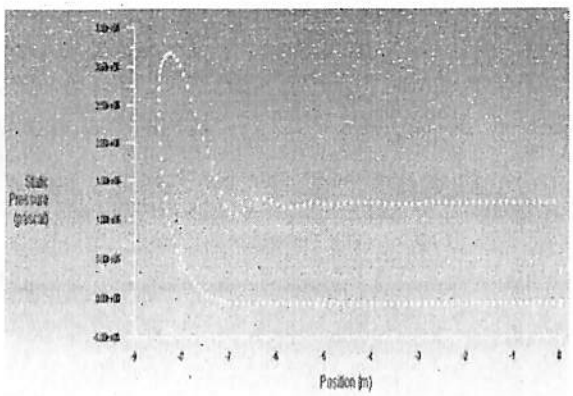

Figure 7.23 Pressure (AOA 30 degree)

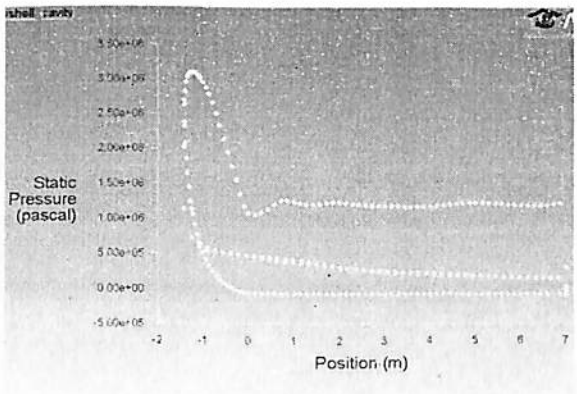

Figure 7.24 Pressure (AOA 30 degree)

- The maximum value of static pressure is at stagnation point and is 3.1e+6 Pa in cylinder (with cavity) and 3.25e+6 Pa in cylinder (without cavity).
- The upper curved surface experiences greater decrease of pressure than lower curved surface in both the geometries. Along the length of the cylinder the pressure remains roughly constant on both lower and upper surfaces in both the geometries.
- Pressure on upper surface is 0 and on lower surface is1.2e+6 pa in both cases.
- The pressure inside the cavity gradually decreases and its value is well within the upper and lower surface pressure values.

7.1.2.3 Static Temperature Comparison:

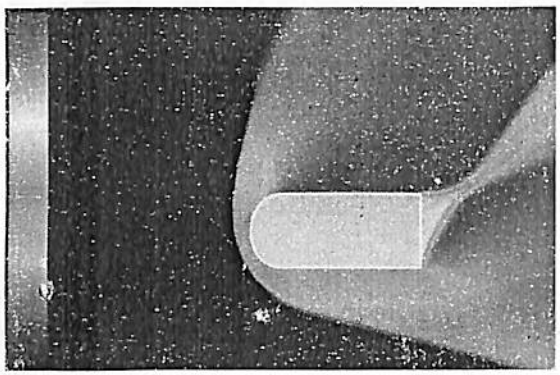

Figure 7.25 Temperature (AOA 30 degree)

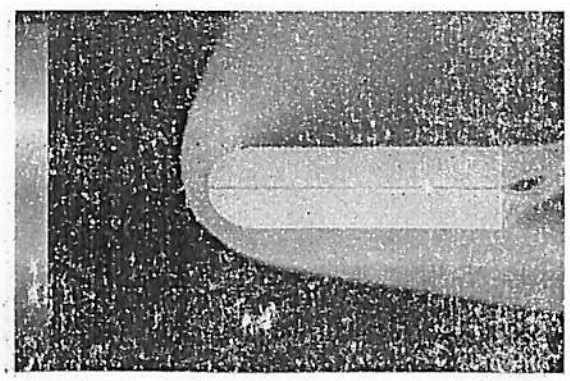

Figure 7.26 Temperature (AOA 30 degree)

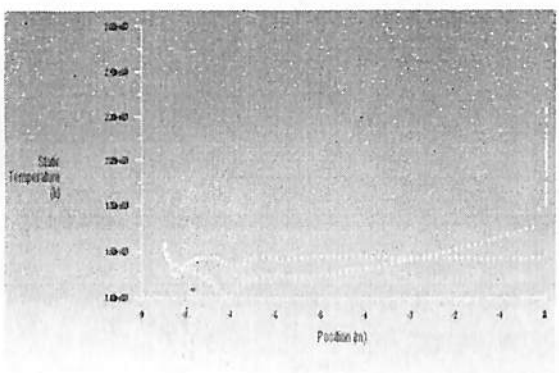

Figure 7.27 Temperature (AOA 30 degree)

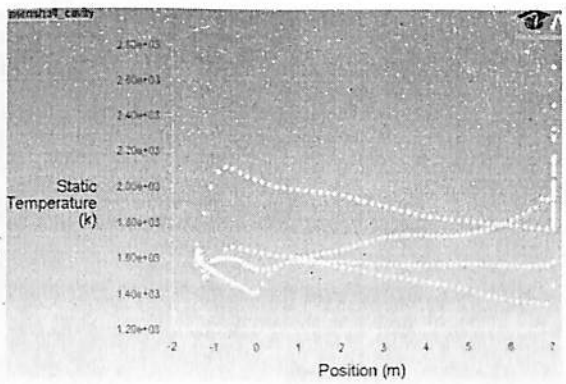

Figure 7.28Temperature (AOA 30 degree)

- The maximum value of static temperature is at stagnation point and is 2.1e+3 K in cylinder (with cavity) and 1.6e+3 K in cylinder (without cavity).
- The upper curved surface experiences greater decrease of temperature than lower curved surface in flat cylinder.
- Temperature first increases then decreases on the curved part in cavity.(with greater rate at lower curved part)
- In cylinder (without cavity) temperature remains roughly constant on upper surface and increases gradually on lower surface.(with temperature on lower cylinder first lesser than on upper surface at beginning of cylinder and increasing thereafter)
- In cylinder (with cavity) the temperature remains roughly constant on upper surface and increases gradually on lower surface.(with temperature on lower cylinder greater than that on upper surface at beginning of cylinder)
- The temperature inside the cavity is max at stagnation point and gradually decreases inside the curved part and along the length.

7.1.2.4 Total Energy Comparison:

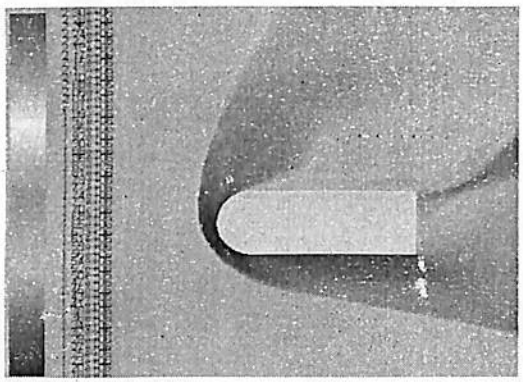

Figure 7.29 Total Energy (AOA 30 degree)

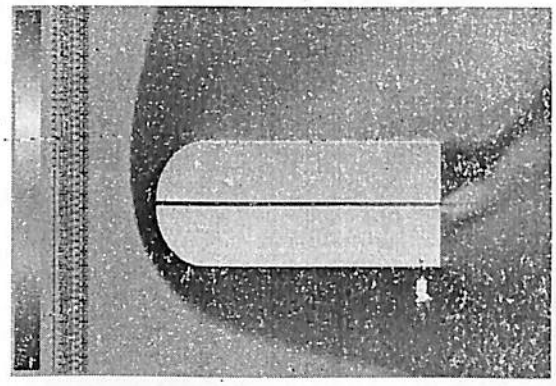

Figure 7.30 Total Energy (AOA 30 degree)

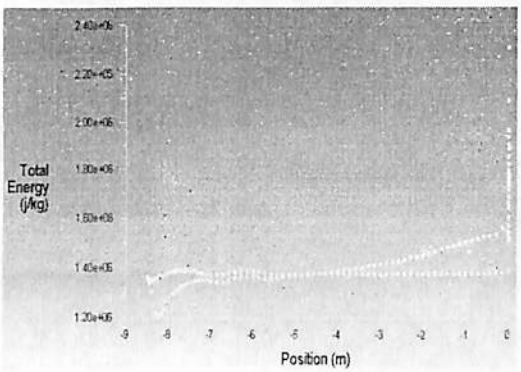

Figure 7.31 Total Energy (AOA 30 degree)

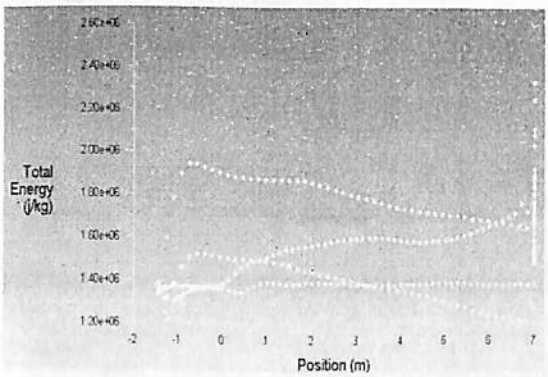

Figure 7.32 Total Energy (AOA 30 degree)

- Minimum total energy is at stagnation point with a value of 1.2e+6 J/Kg at flat cylinder (without cavity) and 2.30e+6 J/Kg at cavity.
- The total energy increases along the curved part with greater rate at upper in both the geometries.
- Total energy is fairly constant along the length on the lower surface in both the geometries.
- On the upper surface energy is gradually increasing along the length (at a greater rate in cylinder with cavity).
- The total energy inside the cavity first increases and then decreases inside the curved part of cylinder and its value decreases along the length.
- It increases substantially at the end of the cylinder with a maximum value 2.30e+6 J/Kg in both cases.

7.1.3 Angle of Attack 40 Degree: Various parameters such as mach no, pressure, temperature and heat flux were compared to determine which geometry was best suited for the hypersonic flow.

7.1.3.1 Mach Number Comparison:

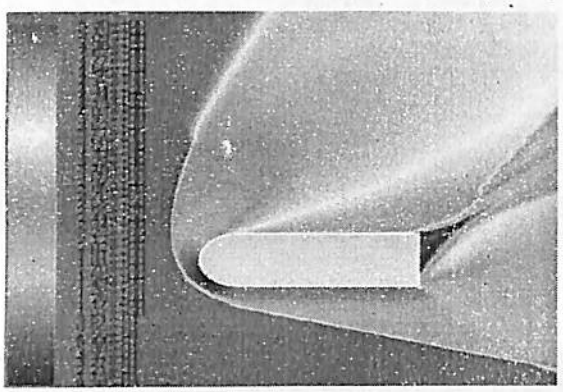

Figure 7.33 Mach no. (AOA 40 degree)

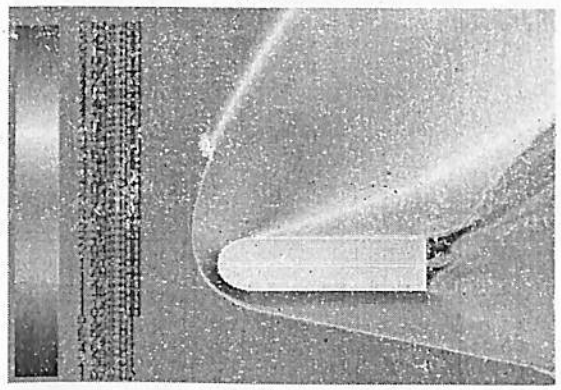

Figure 7.34 Mach no.(AOA 40 degree)

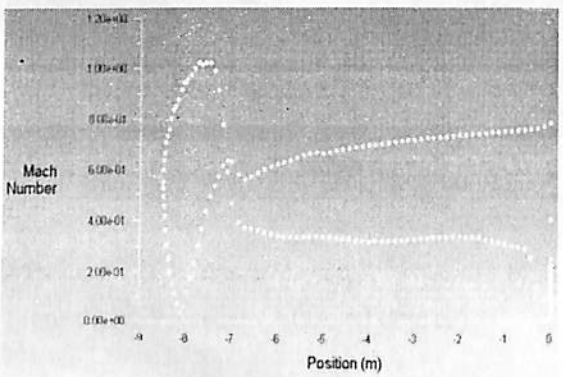

Figure 7.35 Mach no. (AOA 40 degree)

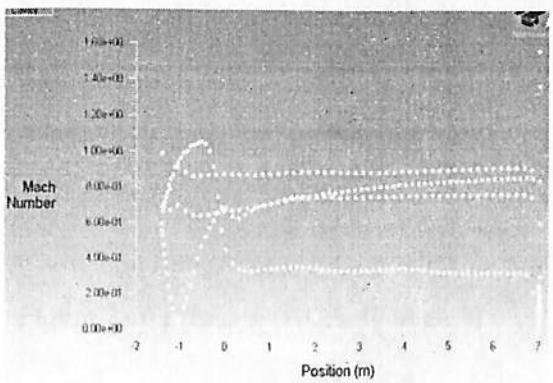

Figure 7.36 Mach no. (AOA 40 degree)

- The maximum mach no at stagnation point is about 1 in case of cylinder (with cavity) and 1.1 in case of cylinder (without cavity).
- Along the length of the cylinder the mach no follows a similar trend in both geometries; it increases fairly on upper surface and decreases on lower surface.
- Mach no varies b/w 0.6 to 0.9 in case of cylinder (with cavity) and remains constant on both lower and upper surfaces of the cavity.
- Flow passing through the nozzle has a lesser mach no as compared to the case where flow was 20 degree because of the increase in angle of attack.

7.1.3.2 Static Pressure Comparison:

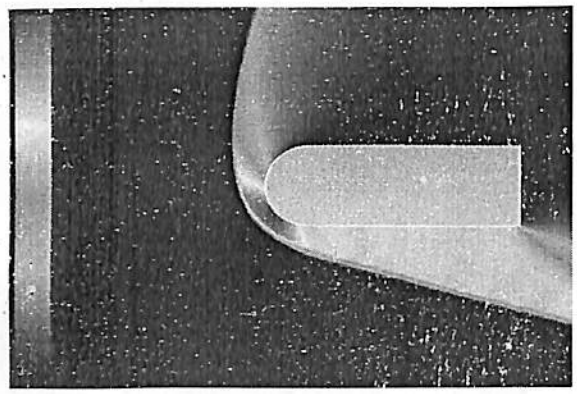

Figure 7.37 Pressure (AOA 40 degree)

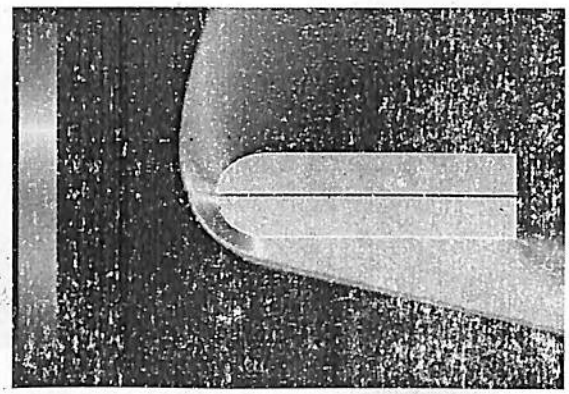

Figure 7.38 Pressure (AOA 40 degree)

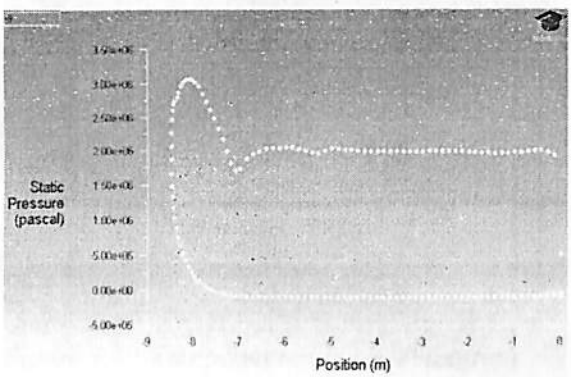

Figure 7.39 Pressure (AOA 40 degree)

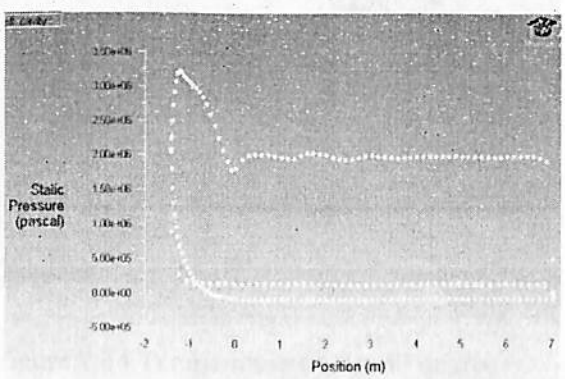

Figure 7.40 Pressure (AOA 40 degree)

- The maximum value of static pressure is at stagnation point and is 3.25e+6 Pa in cylinder (with cavity) and 3.00e+6 Pa in cylinder (without cavity).
- The upper curved surface experiences greater decrease of pressure than lower curved surface in both the geometries. Along the length of the cylinder the pressure remains roughly constant on both lower and upper surfaces in both the geometries.
- Pressure on upper surface is 0 and on lower surface is 2.0e+6 pa in both cases.
- The pressure inside the cavity remains constant and its value is well within the upper and lower surface pressure values (closer to the lower surface).

7.1.3.3 Static Temperature Comparison:

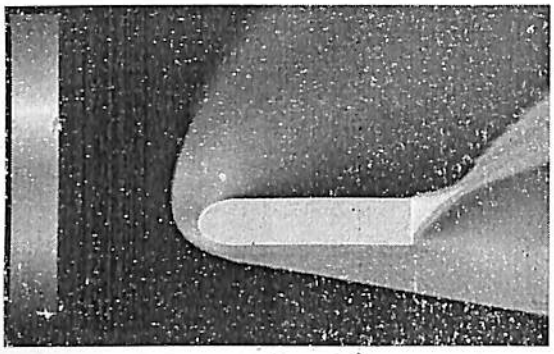

Figure 7.41 Temperature (AOA 40 degree)

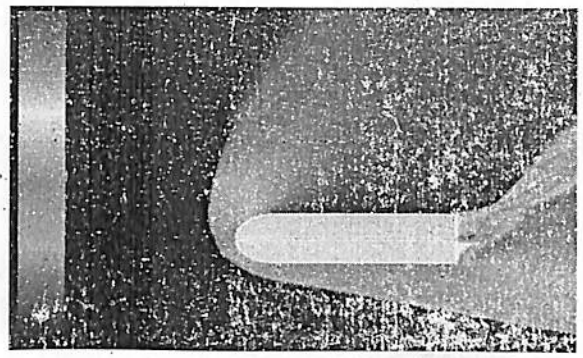

Figure 7.42 Temperature (AOA 40 degree)

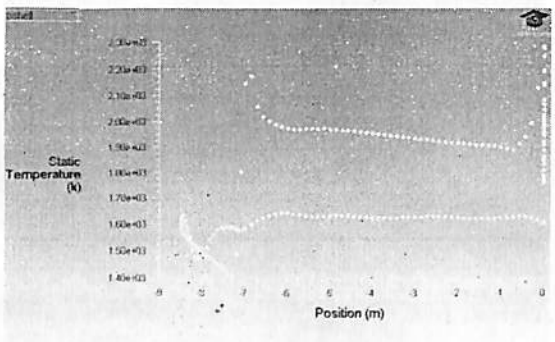

Figure 7.43 Temperature (AOA 40 degree)

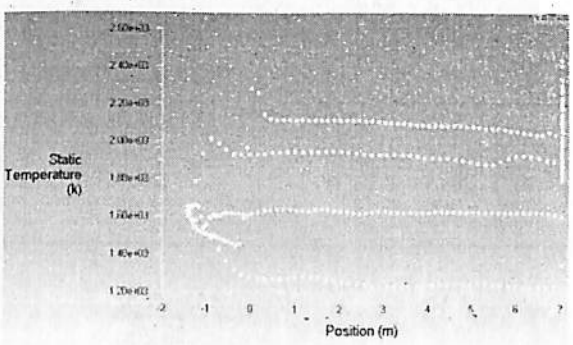

Figure 7.44 Temperature (AOA 40 degree)

- The maximum value of static temperature is at stagnation point and is 2.3e+3 K in cavity and 2.15e+3 K in flat cylinder.
- The upper curved surface experiences greater decrease of temperature than lower curved surface in cylinder (without cavity).
- Temperature first decreases then increases on the lower curved part in cylinder (without cavity).
- Along the length of the cylinder the temperature remains roughly constant on lower surface with value of 1.6e+3 K in both geometries.
- Along the length of the cylinder the temperature decreases gradually on upper surface in both the geometries.
- The temperature inside the cavity gradually decreases inside the curved part and its value is roughly constant along the length.

7.1.3.4 Total Energy Comparison:

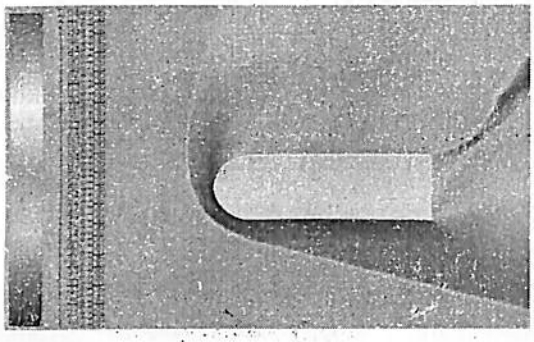

Figure 7.45 Total Energy (AOA 40 degree)

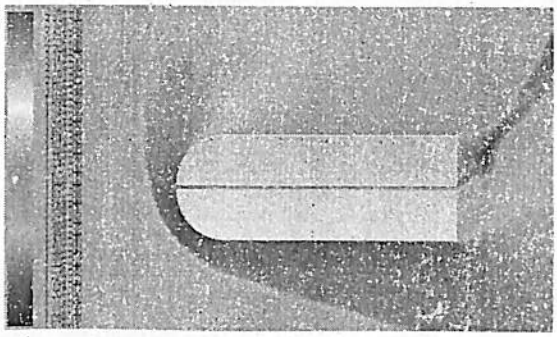

Figure 7.46 Total Energy (AOA 40 degree)

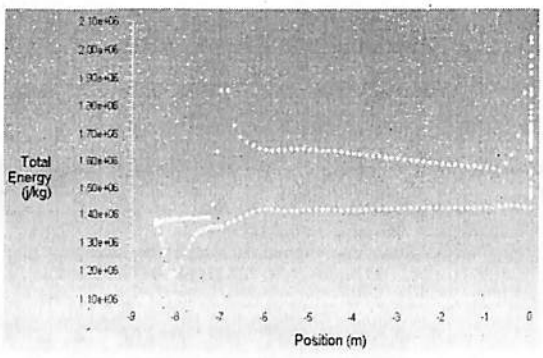

Figure 7.47 Total Energy (AOA 40 degree)

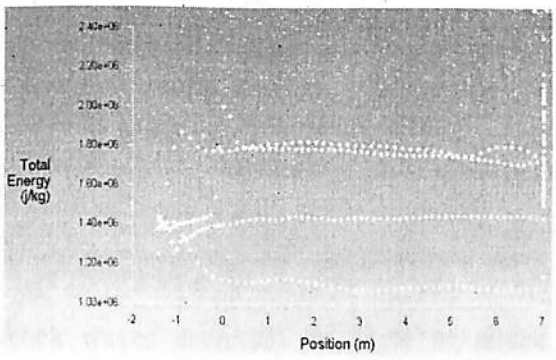

Figure 7.48 Total Energy (AOA 40 degree)

- Minimum total energy is at stagnation point with a value of 1.2e+6 J/Kg in case of both the geometries.
- The total energy first decreases then increases along the lower curved part and then remains constant along the length with value 0f 1.4e+6 J/Kg on lower surface in both the geometries.
- Total energy is fairly constant on the upper curves part and decreases gradually along the length on upper surface in both the geometries.
- The total energy on the upper part of cavity first increases and then decreases along the length very slowly.
- The total energy on the lower part of cavity keeps on decreasing along the length.

7.2 Final Conclusion: The results of 2D cylinder with cavity and 2D cylinder without cavity were compared on various parameters like Mach no, static pressure, static temperature, and total energy.

7.2.1 Mach no:

- Maximum value of mach no. behind the shock waves decreases as angle of attack is increases from 20 degree to 30 degree in both geometries.
- Mach no is almost constant when angle is increased to 40 degree in both geometries.
- The flow through the cavity is accelerated at the end for it acts as a nozzle. The velocity of flow is decreased as angle is increased to 40 degree.

7.2.2 Pressure:

- Maximum static pressure behind the shock waves decreases as angle of attack is increases from 20 degree to 30 degree in both geometries.
- Pressure decreases when angle is increased to 40 degree in both geometries.
- Inside the cavity pressure decreases at 20 degree AOA, the rate of decrease is lowered at 30 degree AOA and pressure is almost constant inside cavity at 40 degree AOA.

7.2.3 Temperature:

- Maximum Temperature behind the shock waves decreases as angle of attack is increases from 20 degree to 30 degree in both geometries.
- Temperature decreases when angle is increased to 40 degree in both geometries.
- Inside the cavity temperature follows a similar profile at 20 and 30 degree AOA (decreasing along the length). It is constant inside the cavity at 40 degree AOA.

7.2.3 Total Energy:

- Energy also shows the same pattern of variation, it is more at the leading edge of cavity at all 3 angles of attack (substantially more than cylinder without cavity).
- This result shows that more heat is concentrated on the leading edges of cavity and these points will be heated the most and heat concentration inside the cavity will be more than on surface.
- This shows that the geometry with cavity is a better choice for hypersonic space capsule as there will be less disintegration of the geometry due to heat as the heat resisting tiles could be easily removed once their purpose is served.
- As a result the same space capsule could be used repeatedly saving considerable amount of money, labor, precious time and resources.

References

1) Charles-Henri Brunaeu, August 1990. Computation of Hypersonic Flow around a Blunt Body.
2) Dr. Ugur Guven, Sandeepan Goswami, N Pawan Kumar, Applications of CFD,Gambit and Fluent.
3) Ernst Heinrich Herschel, 2004. Basics of Aerothermodynamics
4) http://nptel.iitm.ac.in/courses/101103003/43, NPTEL, Aerospace engineering, Hypersonic flows
5) John D Anderson Jr. 2011, Fundamentals of Aerodynamics, Tata McGraw Hill.
6) John Argyris, Ioannis St. Doltsinis, Heinz Friz and Jurgen Urban, October 1990. An exploration of chemically reacting viscous hypersonic flow.
7) Mc. Clinton, R.C., 2001: High Speed/ Hypersonic Aircraft Propulsion Technology Development, James City
8) Lewis, Mark J., 2003: The Promise of Hypersonic Flight, Institute of Bristol & Philadelphia, December.
9) Tsuchiya, T. & Mori, T., 2005: Optimal Design of Two stage to orbit Spaceplanes with air breathing engines, University of Tokyo, Tokyo.
10) Vincent Morio , Franck Cazaurang , Philippe Vernis, June 2006, Flatness-based hypersonic reentry guidance of a lifting-body vehicle.
11) Zeutzius, M., Setoguchi, T., Terao, K. & Miyanishi, H., 2000: Propulsion System for Hypersonic Spaceplanes, Saga University, Japan.